RF and GIS: Field Strength Prediction for Frequencies between 900 MHz and 28 GHz.

Paige Marie Baldassaro

Thesis submitted to the Faculty of
Virginia Polytechnic Institute and State University
in partial fulfillment of the requirements for the degree of

MASTER of SCIENCE
in
GEOGRAPHY

Dr. Lawrence Carstensen
Dr. Charles Bostian
Dr. Dennis Sweeney

August 15, 2001
Blacksburg, Virginia
Key words: GIS, RF, LMDS, Line-of-Sight Prediction, Signal Strength Prediction, Diffraction, Path Loss

RF and GIS: Field Strength Prediction for Frequencies between 900 MHz and 28 GHz.

Paige Marie Baldassaro

(Abstract)

This thesis presents a model to predict signal strength for frequencies between 902 MHz and 28 GHz. The model approximates diffraction using the knife-edge concept and equations proposed by Lee (1985). LOS pathways are calculated using the Bresenham algorithm and the corresponding elevations are obtained from a 30m DEM base map. The base map was generated by the procedure outlined in Rose (2001) and includes building elevations. The effect of Fresnel zones on prediction accuracy is considered. The effect of interpolating elevations along the Bresenham line is also considered. An Inverse Distance Weighting algorithm was used to interpolate the elevations.

The accuracy of the model was evaluated using received signal strength data compiled from studies conducted at 902 MHz, 24.12 GHz and 27.525 GHz. In addition to the compiled data, data was also collected for this study at 2.4 GHz. 257 receiver locations were evaluated; 70 samples were Line-of-Sight. The study area incorporates the Virginia Polytechnic Institute and State University campus.

Incorporating Fresnel zones, Interpolating elevations and calculating double blockages do not have an effect on the program's overall ability to predict signal strength. However, for obstructed pathways, it is not adequate to simply use path loss as an estimate of signal strength. Accurate estimates of diffraction gain are crucial for obstructed pathways. In addition, examination of the standard deviation for the data sets indicates that the model is independent of frequency. The average error across the frequencies is positively correlated with frequency, indicating that the model predicts signal strength better for higher frequencies. The smaller wavelengths associated with the higher frequencies require a more directional antenna and are therefore less sensitive to multipath interference. In addition, the smaller wavelengths are less able to diffract around buildings and terrain features.

To John.
Forever

Acknowledgements

I would sincerely like to thank my committee members for giving me the opportunity to work with such a wonderful committed group of researchers. This past year has proven to be a remarkable journey. I am glad to be able to end my career as a student on such a positive note. I will never forget you.

To my fellow students, I am grateful for the brief time that we have spent together. As usual, I have learned far more than I expected because of you and will cherish the knowledge as much as the memories. Keep in touch!

To my friends, you never cease to amaze me. More importantly, you never cease to honor me with your presence and loyalty. I can only hope I have been able to return the favor.

To my family, without you, I would have nothing. Without you, I would be nothing. Without you, I would go nowhere. Thank you.

To John, you never cease to surprise me. You are my rock. You are a part of my world. You are timeless.

Table of Contents

List of Figures

List of Tables

List of Appendices

Chapter 1. Introduction

In 1897, Guglielmo Marconi introduced wireless communications to the world by providing continuous radio contact with ships sailing the English Channel (Rappaport, 1996). Since then, wireless communication has developed into a multibillion-dollar industry. Most of the industry's explosive growth was fueled by dramatic changes in technology, consumer base and by an unprecedented information explosion that began in the 1980's (Figure 1). There are very few inventions in the 20th century whose growth in popularity rivals that of mobile communications - one aspect of the wireless communication industry (Figure 2). Furthermore, with the introduction of geolocation services and increased data and multimedia capabilities, the wireless industry in the 21st century is poised to become a serious competitor of traditional wireline phone systems (Bi et al., 2001).

Network design for mobile communications is based on the cellular concept. This concept was developed and introduced by Bell Laboratories in the 1960's and 1970's (MacDonald, 1979). Its emergence was a result of the need to serve a growing consumer base in urban areas with limited available spectrum. The basic unit of the cellular concept is the hexagonal cell. It represents the theoretical area that will receive a signal transmitted from a tower located in its center. This hexagonal cell is also referred to as a communication viewshed or a commshed. The hexagonal shape was adopted merely for ease of design and geometric fit. The cellular concept is quite simple. A transmitter tower is located in the center of cell A, and transmits at frequency A. Adjacent cells would transmit at different frequencies enabling towers to "hand off" the mobile signal as a subscriber moves out of the area of one cell and into the area of another cell (Figure 3a).

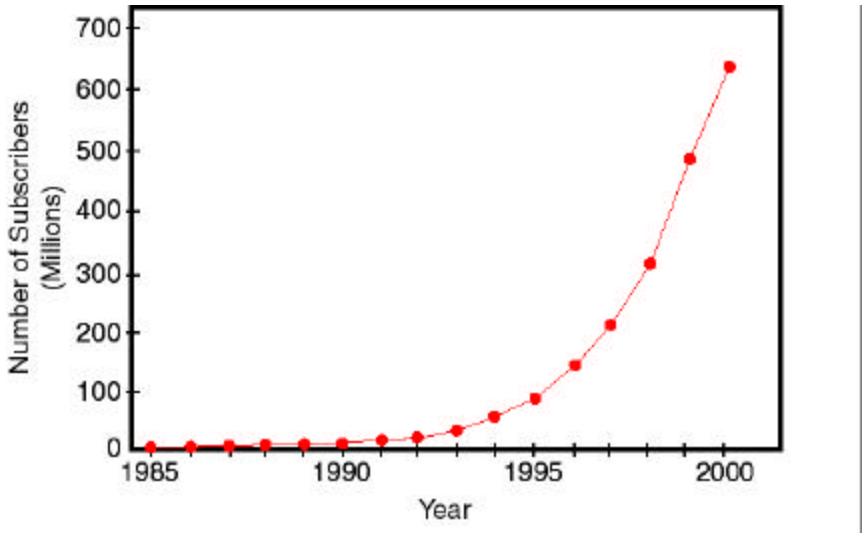

Figure 1: Graph illustrating subscriber growth in mobile communications (Bi et al., 2001).

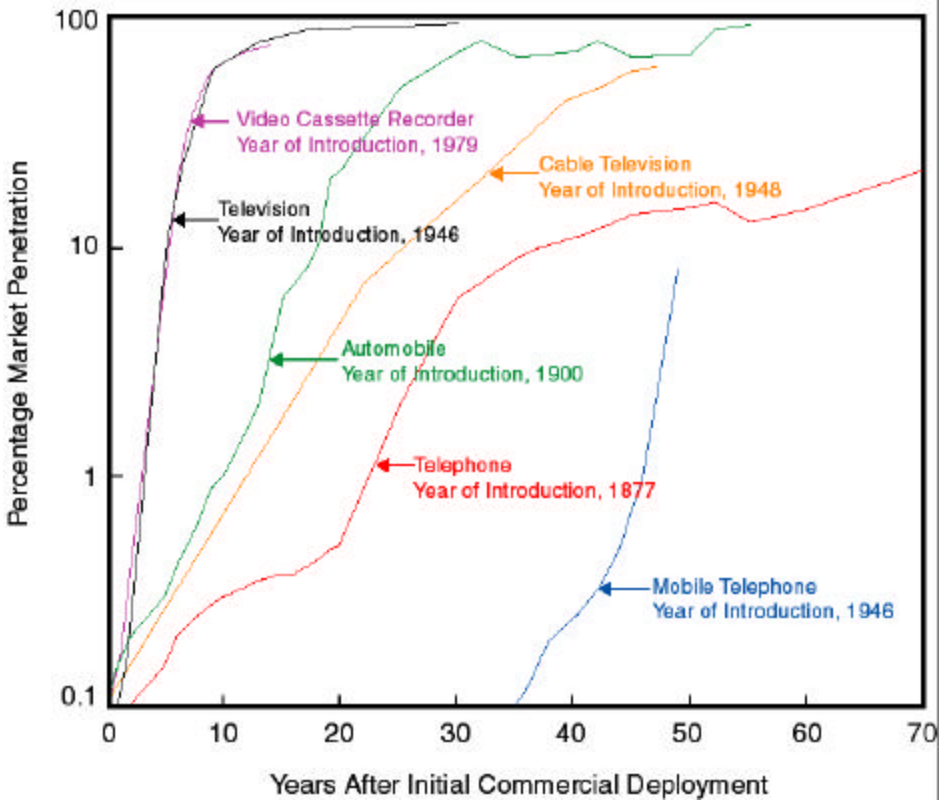

Figure 2: Graph illustrating the percentage market penetration of popular inventions of the 20th century (Rappaport, 1996).

In urban areas, the limiting factor of mobile communications is capacity, not coverage (Rappaport, 1996). As capacity increases, the cell resolution must also increase. However, the amount of available spectrum allocated for mobile communications is finite and limited. The idea of frequency reuse developed as a solution to this dilemma. The key to frequency reuse is to have *non-adjacent* cells transmitting at the same frequencies. The original network design consisted of supercells in which the spectrum was divided such that only a few towers transmitting over the entire available spectrum was necessary to provide adequate coverage to all subscribers. If this idea is implemented, supercells can be subdivided into macrocells and even into microcells as demand increases (Bölcskei et al., 2001). The amount of available spectrum never increases, and there is still the same number of divisions in the spectrum. However, more towers are transmitting over any particular division at shorter distances. Furthermore, since cells transmitting at the same frequency are not adjacent to each other, destructive interference between towers is eliminated (Figures 3a – 3c).

The basic cellular concept can also be applied to fixed wireless networks such as LMDS (Local Multipoint Distribution Service). However, the amount of spectrum available for fixed wireless networks is large enough that the idea of frequency reuse is currently irrelevant. There are two different configurations for fixed wireless networks: Point-to-Point and Point-to-Multipoint. In fixed wireless networks, a central station transmits to remote stations, which transmit to one (Point-to-Point) or more (Point-to-Multipoint) terminals or subscribers. If necessary, repeater towers are included between the central station and a remote station to extend the link or overcome terrain difficulties. In addition, repeater stations can also be utilized as remote stations. The central station is located at the public switched network or where the last fiber, or wireline, is available. The remote stations must be located close to their subscribers and at in the center of the cells that they serve. The repeater stations are usually located on top of a hill or building to support the hops over terrain where Line-of-Sight (LOS) links do not exist (Figure 4).

Identifying suitable locations for central, remote and repeater stations is a very time consuming and computationally intensive process; therefore, most site selection is done manually or using basic geometric models (Krzanowski and Raper, 1999). Algorithms exist to aid in the site selection process, but most of these do not easily incorporate spatial data. The site

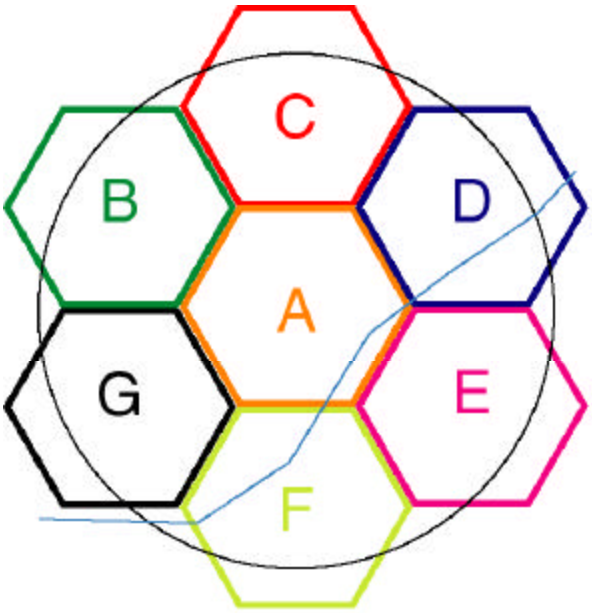

Figure 3a: Diagram illustrating the cellular concept (MacDonald 1979). The Black circle represents the commshed and the colored hexagons represent individual supercells that transmit at different frequencies. The Blue line represents a theoretical path that a cellular subscriber might take and the corresponding signal transference that would occur. Traveling from left to right, the signal would transfer from cell F (transmitting at frequency F) to cell A (transmitting at frequency A) and, finally, to cell D (transmitting at frequency D).

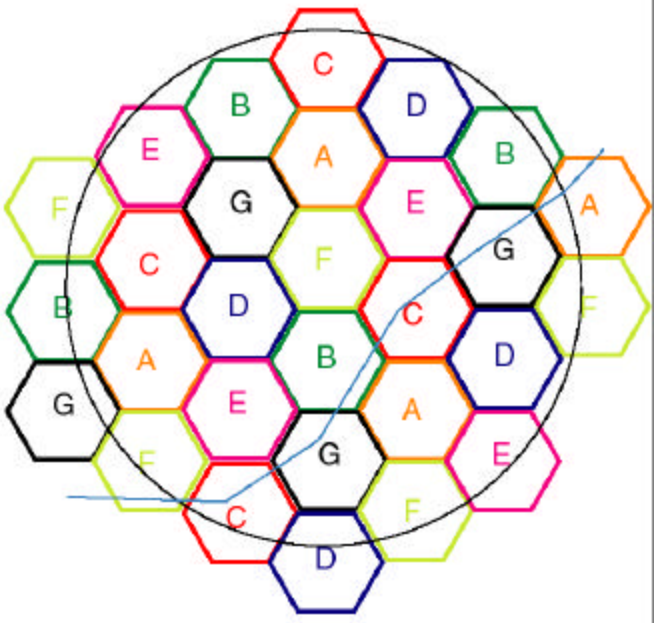

Figure 3b: Diagram illustrating the idea of frequency reuse and the macrocell structure. In this scenario, the subscriber will pass through cells C and G twice, though the distance between the cells, which are transmitting at the same frequency, will cause neither destructive interference with each other nor disruption of service. The cell size has been arbitrarily reduced by 50% as an analogy to an equivalent increase in subscriber growth.

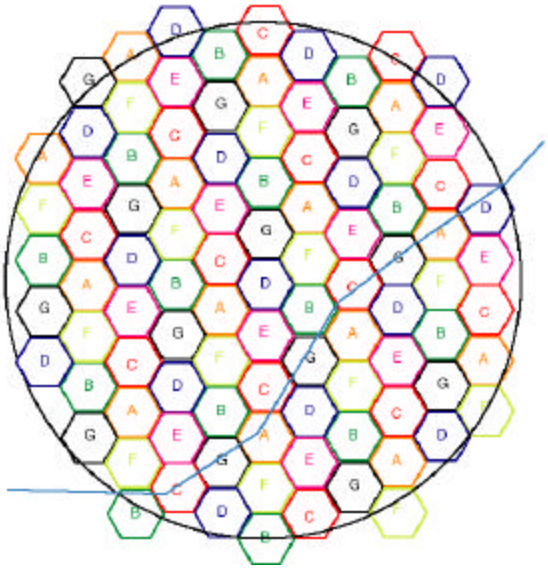

Figure 3c: Diagram illustrating the cellular concept and the idea of frequency reuse in a microcellular structure. Here, the cell size has been reduced again by 50%, but the Blue line still remains the same. Despite the tremendous growth indicated by the reduction in cell size, there is no need for more spectrum. Cells transmitting at similar frequencies still do not overlap.

selection process developed without the aid of GIS systems, even though the ability of GIS systems to process spatial data greatly enhances the efficiency of this process. Furthermore, limitations on the site selection process such as customer location, location of the public switched network, location of preexisting towers and location of power sources often make the use of complex algorithms unnecessary.

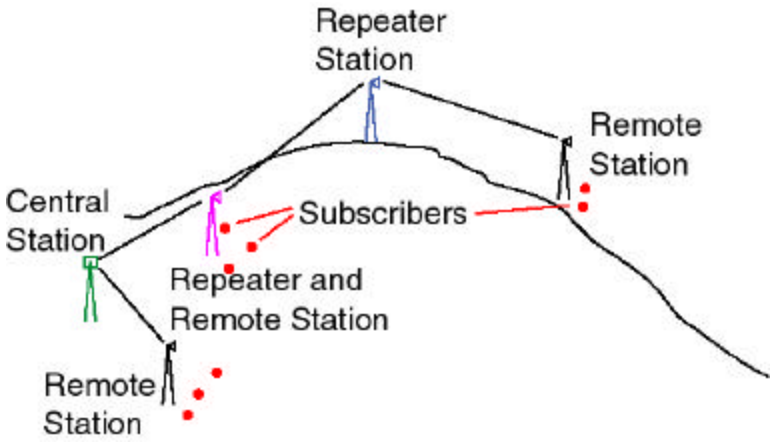

Figure 4: Diagram illustrating a simple fixed wireless network. The Green tower is the central station located near the public switched network. Black towers are remote stations. The Blue tower is a repeater station completing an LOS link over difficult terrain (in this case, a hill). The Purple tower is both a repeater station and a remote station. In this illustration, the Purple tower is overcoming distance. The red dots indicate where the links terminate, and the subscribers are located.

Link budgeting is one of the most important engineering steps in network design. Received signal power between stations and to subscribers needs to be calculated to determine the viability of the radio links (Sandrasegaran and Prag, 1999). One of the major limitations to accurate link budgeting is obtaining and incorporating detailed terrain information. Link budget calculations are critical to efficient network design because they determine antenna characteristics, signal fading and the need for additional equipment.

A variety of markets in the telecommunication industry such as rural communities and emergency response agencies are under-served by both the wireline and wireless industries. Rural areas are often not considered economically viable by the telecommunications industry due to the lack of preexisting capabilities and isolation of consumer base. However, the inherent characteristics of the wireless industry makes it uniquely capable of overcoming many of the obstacles present in serving rural environments. Some of those characteristics are lower startup

costs, efficient targeting of isolated consumer bases and quick deployment (Sandrasegaran and Prag, 1999). Still, many rural economies cannot afford the equipment or software essential to planning the network and developing and economically viable business case for wireless companies.

The cellular concept is also an appropriate description for rural environments. Quite often, there are isolated communities (cells) in rural areas located in valleys and on flood plains because the terrain in these locales is flat, easily accessible and conducive to community development. Local topography, which might inhibit wireline development, may be very advantageous for wireless networks. It can provide excellent sites for transmitting towers. However, simply placing the transmitting tower on the highest location may not provide the best coverage for the isolated communities. Access to site selection software that can predict signal strength would enable these isolated rural communities to determine the best site for a transmitter tower. Therefore, it is important that research be conducted that provides an accurate cost-effective signal strength prediction module on which broader site selection software can be developed. Finally, an efficiently developed deployment plan for a wireless system could then be used to develop the business case that would convince a wireless network company to invest in their particular area.

Emergency response systems apply in both rural and urban environments. Rural areas may not have the necessary wireline capabilities to support emergency-response teams. In contrast, urban environments have sufficient wireline capabilities, but they are often incapacitated after natural disasters such as hurricanes and earthquakes. For example, after the Loma Prieta, California, earthquake of October 17, 1989, dialtone delays up to 3 minutes were reported for the public switched network and congestion continued for 4 days. Furthermore, the emergency 911 system was significantly hampered by the congestion of the public switched network (Schiff et al., 1998). The ability to rapidly deploy a wireless network in areas of incapacitated or non-existing wireline capability almost makes the fixed wireless network a necessity for some emergency situations.

In disaster relief operations conducted by emergency response teams, field operators are sent out into the damaged area to conduct disaster assessment or aid in victim recovery

operations. It is critical that the field operators maintain contact with the remote station at all times to obtain and transmit information about ruptured gas lines, damaged power lines, trapped victims, etc. However, if critical communication systems such as the public switched network have been damaged by the disaster, then constant communication may not be possible. Emergency response systems are very cellular in nature. Field operators work in an area centered on a remote station. Therefore, a wireless network can be established to transmit from the remote station and provide the constant communication so vital in disaster relief operations.

The software developed in this research can help optimize the location of the central station or remote stations (if a larger coverage area is needed) in a disaster area. In addition, the simple and compact nature of the software would enable an emergency response team to respond to a disaster in a timely fashion. Furthermore, the software footprint is small enough that it can easily run on hand-held computers and laptops, enabling field operators to adjust their positions once in the field and establish better links to the base.

This research will expand upon the current geospatial research conducted by the Department of Geography and the Center for Wireless Telecommunications at Virginia Polytechnic Institute and State University. The purpose of this research is to develop a computer model to predict received signal strength. The model will incorporate terrain information as well as radio propagation equations for path loss, Fresnel clearance and diffraction gain. The intent of the model is to create software that is compact and easy to use in the field in emergency situations, less expensive than existing software packages, adaptable to specific needs and circumstances of rural environments and scalable as more research is conducted. The software was developed using the Visual Basic© programming language and ESRI's Map Objects© library.

Chapter 2. Previous Work

An almost overwhelming number and variety of propagation models can be found in the literature. Two factors contribute to this abundance of information. First, basic academic research continues to reveal the complex nature of diffraction and the crucial role that natural (I.e. hills and trees) and artificial (i.e. buildings and highway overpasses) terrain plays in efficient wireless network design. The publication of complex and sophisticated techniques to predict the field strength at a given receiver location in a commshed is a direct result of this basic research. Second, the sustained growth of the wireless communication industry keeps the demand for accurate models at the forefront of propagation research. Whereas this paper makes no attempt to examine thoroughly, explain or even understand all of the available documentation pertaining to diffraction, it is still necessary to provide the basic concepts on which the research is based.

Initial techniques to predict signal strength in shadowed regions relied heavily on classical Fresnel theory and the concept of single knife-edge diffraction (Schelleng et al., 1933; Bachynski, 1963). Single-knife edge diffraction is the simplest and most understood case of knife-edge diffraction (Figure 5). Calculations of knife-edge diffraction gain based on the Fresnel-Kirchoff diffraction parameter, v, can provide useful insight into the order or magnitude of diffraction loss (Figure 6; Rappaport, 1996). The lack of accuracy of approximation

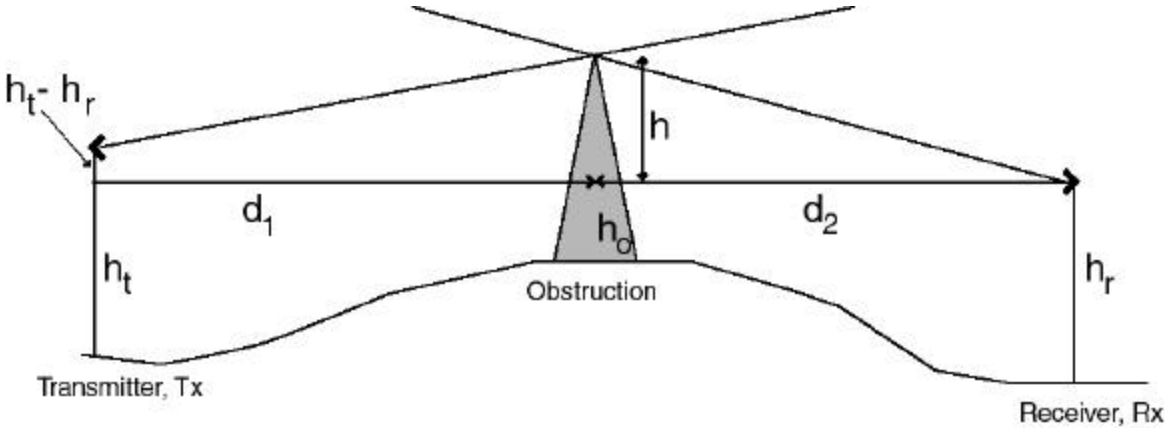

Figure 5: Single knife-edge geometry used in this research. The smaller height (in this case, h_r) is subtracted from the height of the obstruction (h_o) to obtain the height (h) needed to calculate diffraction gain. The height of the transmitter is h_t. The distances from the transmitter to the blockage and from the blockage to the receiver are d_1 and d_2, respectively.

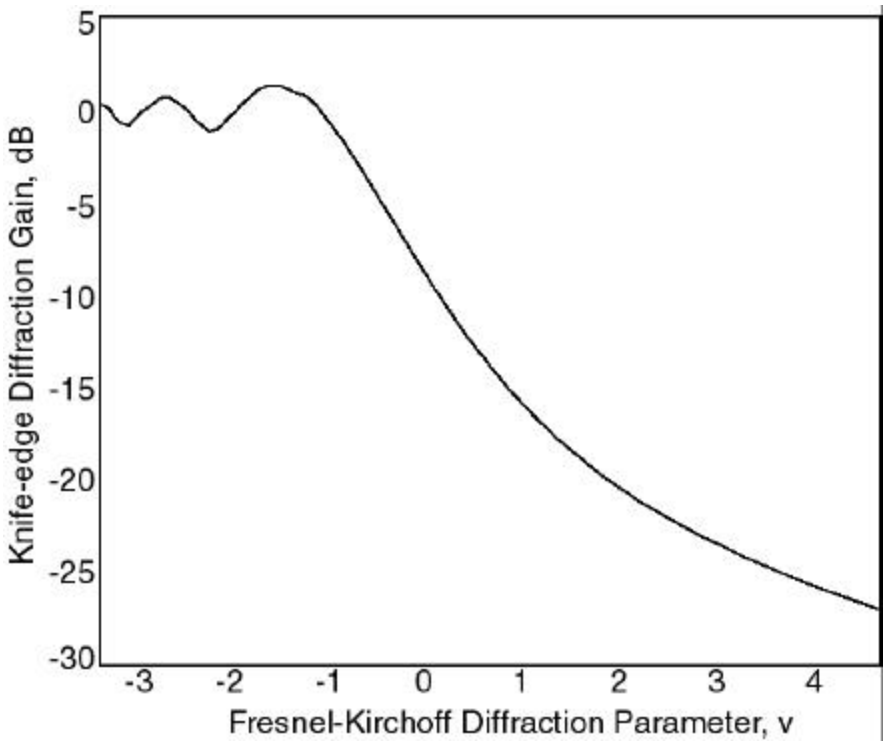

Figure 6: Knife-edge diffraction gain graphed as a function of the Fresnel-Kirchoff diffraction parameter (Rappaport, 1996).

techniques was a direct result of the single knife-edge concept not adequately describing obstacles found in natural environments. This knowledge prompted researchers to initially derive empirical correction factors. These correction factors were applied to the model to improve its overall accuracy. However, often the models still produced overly optimistic results (Rappaport, 1996).

Field tests of approximation techniques, which utilized the single knife-edge model, frequently encountered multiple obstructions. As a result of this, more sophisticated multiple knife-edge models emerged (Figures 7a – 7c). In addition to approximation techniques, real solutions for these models have been published. One example is an integral solution that was based on "a double application of Huyghens' Principle expressed in terms of simple Fresnel theory" published by Millington et al. (pg. 1, 1962). Huyghens was a Dutch scientist who first explained the phenomenon of diffraction. In 1963, Furutsu published a multiple residue series based on his own integrals developed a few years earlier (1957a, 1957b, 1959). More recently, Vogler (1982) derived a multiple integral solution that could be reduced to a series formulation

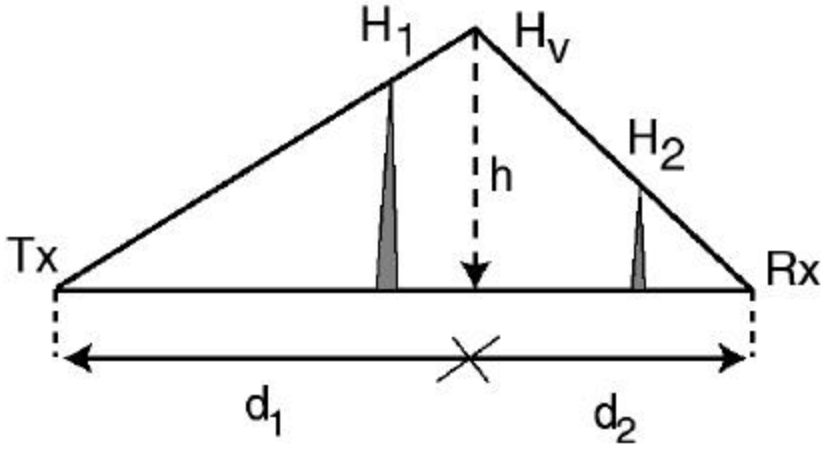

Figure 7a: Diagram illustrating the double knife-edge approximation technique developed by Bullington (1947) (Deygout, 1966).

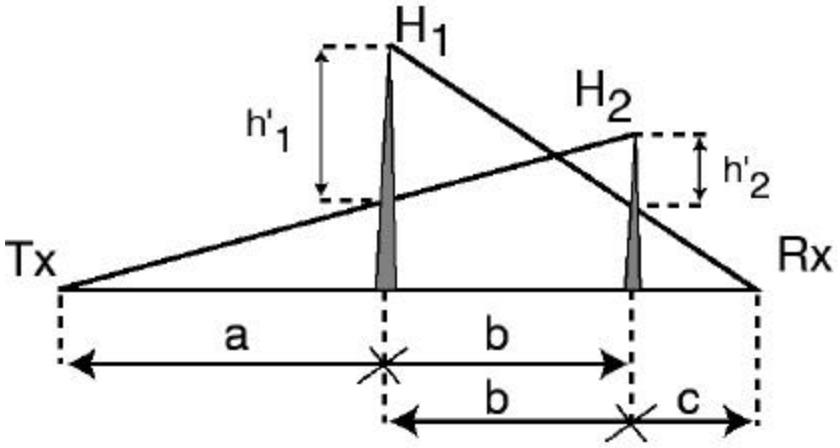

Figure 7b: Diagram illustrating the double knife-edge approximation technique developed by Epstein and Peterson (1953) (Deygout, 1966).

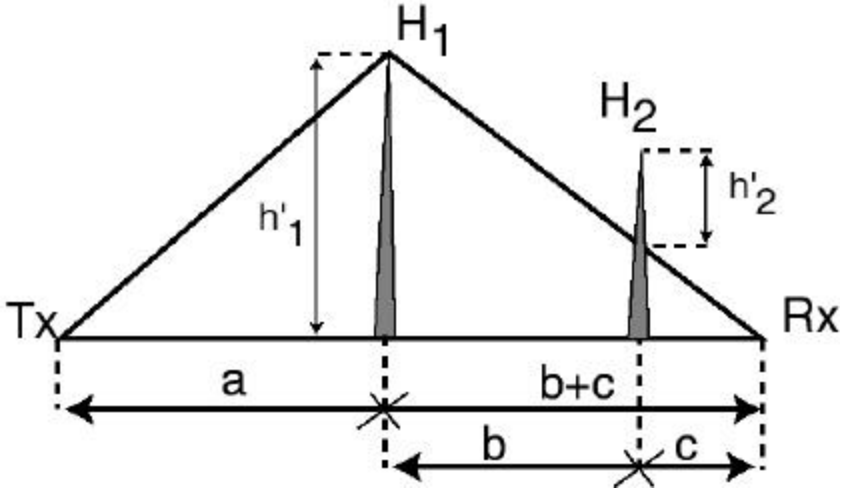

Figure 7c: Diagram illustrating the double knife-edge approximation technique developed by Deygout (1966).

amenable to computer programming. Despite the availability of these theoretical solutions to researchers, engineers and network designers, they are still not useful for wireless network planning. Their mathematical complexity and computational intensity inhibits their application to solve real-world wireless network design problems. Because of this, most research in signal propagation, including this research, centers on developing practical cost-effective solutions that accurately approximate field strength.

There are many approximation techniques that utilize the concept of knife-edge diffraction, all of which are more practical for application to real-world problems than are real solutions. A multiple knife-edge model is a more accurate predictor of received signal strength than a single knife-edge model, but it is also more complex and computationally intense. One example of a model based on the multiple knife-edge concept was published by Bullington (1947). It provided a geometric solution to multiple knife-edge diffraction (Figure 7a). He proposed that a single virtual knife-edge could be created from two obstructions. Signal attenuation would then be approximated using the virtual knife-edge and classical Fresnel solutions. He determined that this representation was within two or three decibels of results produced using the graphical integration techniques available at that time. One serious limitation to Bullington's model is that, for the solution to work, the virtual knife-edge must be positioned between the original knife-edges. Obstacles in natural environments do not often generate virtual obstructions that meet this exacting requirement.

Epstein and Peterson (1953) developed another multiple knife-edge approximation technique. This geometric model does not generate a single knife-edge. It calculates the contribution from each obstruction to overall diffraction loss using LOS paths that cross each other (Figure 7b). Whereas this model produced better results, both of the above-mentioned models have been considered optimistic and produce an overestimation up to ten decibels (Deygout, 1966). The final model to be discussed was published by Deygout (1966). This model determines the diffraction loss due to the main obstacle, then calculates addition attenuation for subsequent knife-edges based on the new LOS pathway between the primary knife-edge and receiver (Figure 7c).

Many obstructions in urban environments are not adequately described using the knife-edge concept. The tops of buildings can hardly be conceptualized as a knife-edge and the physical characteristics of signal propagating over rooftops are very different from signal propagating over knife-edges (Zhang and Lähteenmäki, 1999). Furthermore, many urban environments are microcellular. In microcellular environments, the distance covered is not always significantly larger than the height of the obstacles, a requirement in some knife-edge approximation techniques (Deygout 1966). Signal propagation in these environments is often more accurately characterized using the concept of ray tracing. Examples of some ray tracing models can be found in Ikegami et al. (1991), Zhang and Lähteenmäki (1999) and Erricolo and Uslenghi (*in pub*.). Ray tracing models are considered superior to knife-edge models because they use a more detailed description of the environment. Unfortunately, due to time constraints, comparison of results from ray tracing models to the knife-edge methods used in this research is left for future work.

In addition to obstructions, vegetation is a significant signal attenuator of high frequencies (~28-30 GHz). The small wavelengths (~1 cm) that are characteristic of these frequencies are easily absorbed by the water in vegetation. Little experimental work exists that thoroughly examines this effect. However, the research that has been conducted has found, among other things, that leaves can add approximately 10 dB to overall signal attenuation (Papazian et al., 1992; Schwering et al., 1988). In addition to the lack of experimental work, vegetation or land cover information in a format usable in network design models were unavailable or inaccessible. In recent times, the USGS has published on the Internet 1:250,000-scale land use/land cover data in digital form describing vegetation, water, natural surfaces and cultural features as a result of their National Mapping Program. Even more recently, 30-m resolution land cover maps have also been published online and are available by state (http:\\mapping.usgs.gov). A key stage in the future development of the geospatial project will be to incorporate land use/land cover information into the model.

As mentioned previously, this paper is part of the interdisciplinary geospatial research being conducted between the Department of Geography and the Center for Wireless Telecommunications. The overall goal is to develop a simple cost-effective method to accurately

predict signal strength for use in planning a wireless network in a rural area, or for an emergency response organization. Preliminary work for this project focused on examining the accuracy of ArcView's viewshed algorithm (Dodd, 2001). Signal strengths at various locations on and around the Virginia Tech campus were obtained for two frequencies, 902 MHz and 27.525 GHz. Locations were chosen to adequately represent both LOS and obstructed pathways. The results were compared to the viewshed created in ArcView to determine if the algorithm had accurately predicted the extent and coverage of the transmitting signal. The findings relevant to this research are:

- Building heights are important for accurate prediction of LOS signal coverage, and can significantly increase the accuracy of a viewshed (41% accurately predicted LOS pathways without buildings to 85% accurately predicted LOS pathways with buildings).

- ArcView's viewshed function is a more accurate predictor at LMDS (Local Multipoint Distribution Service) frequencies (27.525 GHz) compared to cellular telephone frequencies (902 MHz). The propagation characteristics of LMDS frequencies more closely resemble LOS than cellular frequencies. Cellular frequencies are more able to bend around objects, a characteristic that is not as easily modeled by LOS pathways.

The second research topic evolved directly from one of the findings of Dodd (2001): ten of the eleven receiver locations that were omitted from ArcView's viewshed (predicted out, but actually in) all resided within one cell of the border of the viewshed for the 30-meter resolution DEM. As a result, it was hypothesized that a higher resolution DEM would produce more accurate results. The experiment to determine the effect of DEM resolution on ArcView's viewshed accuracy was conducted at 24.12 GHz, a frequency that also displays LOS characteristics (Rose, 2001). The relevant results can be summarized as follows:

- When both rural and urban receiver locations were considered, there was no noteworthy increase in the number of points correctly predicted as unobstructed. However, discrete multivariate analysis indicated that there was a difference in the

error matrices of the 30-meter DEM with respect to the other higher resolution DEM's.

- When separating receiver locations into urban and rural environments, there was no change in the accuracy of predictions based on the DEM resolution. Discrete multivariate analysis indicated no difference in the error matrices. However, when building heights were included in the DEM, often the 30-meter DEM was considered a better predictor than the higher resolution DEM's.

The above-mentioned geospatial experiments were conducted using ArcView's viewshed algorithm. The algorithm generates a Boolean viewshed based on Line-of-Sight (LOS). Either the cell is within LOS of the observation point (value = 1) or the cell is not (value = 0). This basic information is inadequate for wireless network planning. It is more beneficial to have knowledge about the actual signal strength received, because links can be established in shadowed regions where there is no LOS. Alternatively, knowledge of established but weak links can aid the designer in decisions about hardware design or tower placement. This research addresses the issue of predicting signal strengths in shadowed regions. Based on the previous research endeavors (Dodd, 2001; Rose, 2001), a 30-meter DEM resolution was appropriate, if it included building heights. Computation time was another important factor in the decision of appropriate DEM resolution. The time it takes to run a 30-meter DEM is significantly shorter than a 1-meter resolution DEM (Figure 8), and time is very crucial in emergency response situations. The DEM used in this research was generated by the procedure outlined in Rose (2001).

In addition to academic publication of signal propagation models, GIS software companies have developed proprietary software packages with the ability to predict signal strength for a commshed and to incorporate many types of spatial data (ESRI's RF module and Map Info's Decibel Planner®). An independent comparison of the modules was not performed due to the difficulty of obtaining access to evaluation copies. In addition, very little academic information could be gathered about the algorithms utilized in the modules due to the proprietary nature of the software. Regardless, these software packages are expensive and complex and may not be as practical for the types of applications for which this research is being conducted.

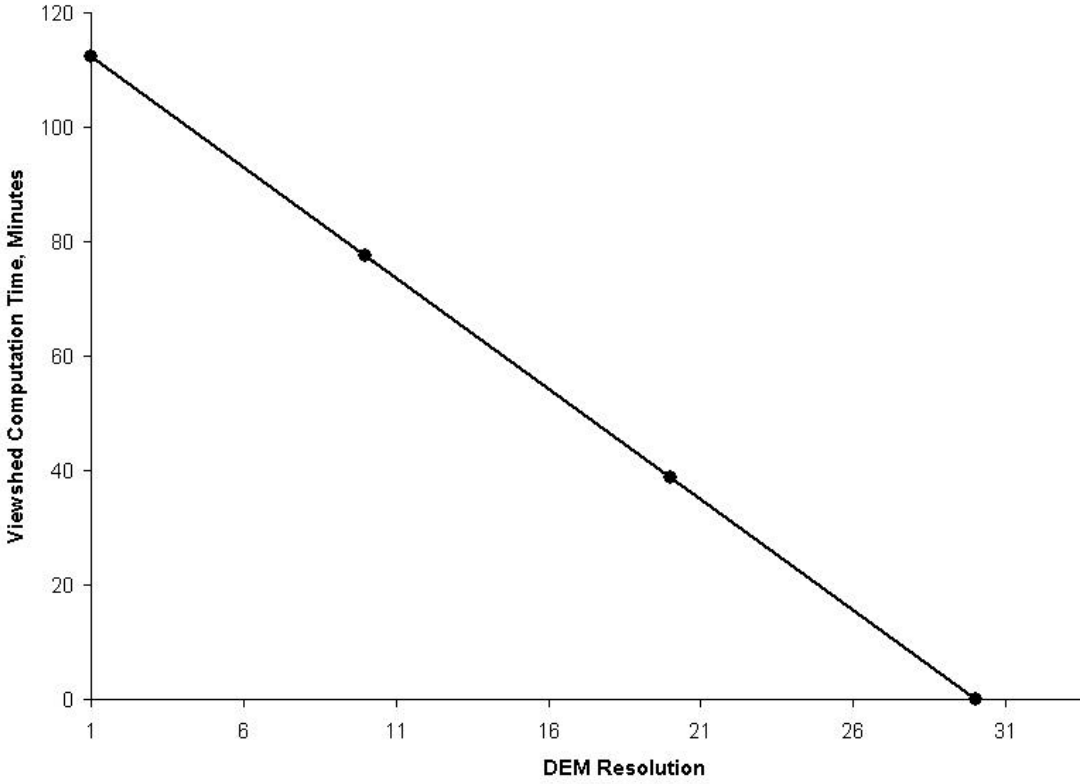

Figure 8: Graph illustrating the effect of DEM resolution on computation time for a 500-meter radius viewshed. Parameters for model used in this example were single blockage, without Fresnel zones or interpolating for a single transmitting tower.

Chapter 3. Data

The data used in this research consists of a DEM base map (Figure 9), topographic maps (Figure 10), measured received signal strength values for LOS and obstructed pathways (Appendix A) and predicted signal strength values for the same locations for each technique (Appendix B). The measured signal strength values were obtained from three independent sources: Dodd (2001, Appendix A.1), Rose (2001, Appendix A.2) and this study (Appendix A.3). The study area is Blacksburg, Virginia, and incorporates the Virginia Tech campus and the adjacent golf course. The size of the study area is approximately 1.7 km wide by 1.5 km long and it includes 257 sample receiver locations. The campus and golf course were chosen because they contain LOS and obstructed pathways.

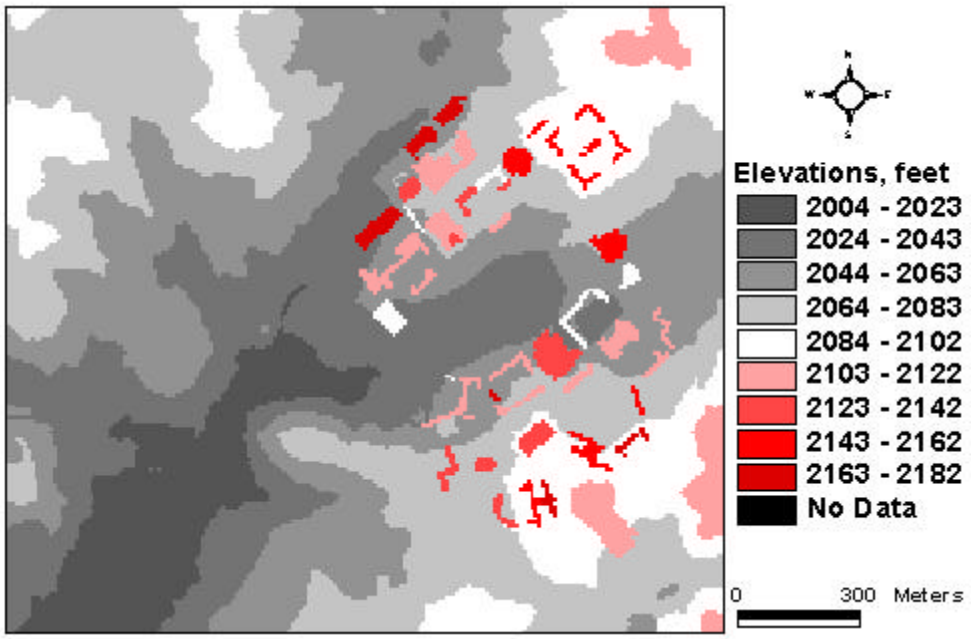

Figure 9: 30-meter DEM base map used in this study. Base map models the study area (Virginia Tech campus). The legend style was chosen to emphasize the building locations.

The DEM map is the base map for the model (Figure 9). The DEM is a model of the earth's surface. It is a gridded representation of surface elevations. The resolution of the DEM describes the size of the grids that are represented by a single elevation. As mentioned previously, prior research indicated that a 30-meter resolution DEM was appropriate, but that the map needed to include building heights. The coordinate system of the base map is Virginia State Plane – South Zone, NAD 83. Elevations and ground distances are measured in feet and converted to meters for signal strength calculations. The process used to generate the DEM is outlined in Rose (2001). Since building heights are included in the DEM, the model should predict LOS pathways with an accuracy greater than 84% (Dodd, 2001).

The topographic maps were downloaded from Virginia Tech's University Facilities Information Services' Aerial Mapping web page as AutoCad® DWG files and imported into ArcView (http://www.ufis.vt.edu/aerials.html, Figure 10). Nine map sections were needed to cover all of the receiver locations used in this study: C7-1a, C7-1b, C7-1c, C7-1d, C7-3a, C7-3b, C8-3c, D7-2b and D7-2d. Topographic maps are also elevation models of the earth's surface. However, topographic maps only contain elevation information at specific intervals (contour intervals). DEM's contain an elevation at every point, making it a better base map for the model. Despite the lack of elevation information contained within the topographic map, this particular set of maps contributed significantly to this research. The scale of the maps is 1": 50' (1 foot contour intervals); therefore, the resolution of the map is significantly higher than the DEM. In addition to high-resolution contour intervals, the map contains detailed cultural information as well. Locations of manholes, streetlights and individual trees are recorded in this map to an accuracy of one foot. Therefore, the accuracy of the receiver locations is greatly improved by comparing detailed field notes to the coordinates obtained from the Global Positioning System

Figure 10: Topographic map of study area with tower and receiver locations collected in this study.

(GPS) unit (to be discussed in detail later). The coordinate system for the maps is Virginia State Plane – South Zone, NAD 83, and the ground distances are measured in feet.

In addition to the data obtained from this research, measured signal strength data was compiled from previous research. One set was obtained from Dodd (2001) where the purpose was to examine the viability of using a Geographic Information System as a predictor for radio wave propagation (Appendix A.1). The data set included X-Y coordinates (decimal degrees), indication of LOS, nature of blockage if present and received signal strengths (dBm) for two frequencies (902 MHz and 27.525 GHz). The data were manually examined and points whose accuracy was in question or whose main blockage was vegetation were excluded. The coordinates were transformed from decimal degrees into Virginia State Plane – South Zone,

NAD 83, through Corpscon®. The data were not compared to the 1-foot topographic map for accuracy. Details about the methodology used to collect the data can be found in Dodd (2001).

The second set of data was collected for an experiment designed to examine the effect of DEM resolution on the accuracy of LOS prediction of a Geographic Information System (Appendix A.2). Details about this data set can be found in Rose (2001). The data set included X-Y State Plane coordinates (feet), nature of blockage, if existent, and received signal strengths (dBm). Data that was indicative of LOS pathways was excluded from this research due to accessibility. Signal strengths from reflected waves and pathways obstructed by vegetation were also excluded because the model is not currently designed to incorporate these parameters. The locations of the receiver points were not compared to the 1-foot topographic map for accuracy. The signal was transmitted at a frequency of 24.12 GHz.

The field data collected in this research consist of X-Y coordinates (decimal degrees), received signal strength (dBm), existence of one or more blockages, nature of blockage if existent and detailed field notes about location. The coordinates were transformed into Virginia State Plane – South Zone, NAD 83, through Corpscon® (Appendix A.3).

The design of the experiment included a signal generated at 2.40 GHz using a Hewlett Packard 6648C Signal Generator, a Hewlett Packard 491C Microwave Amplifier to increase the total output to 1-Watt, or 30 dBm (Figure 11), and a 0-dB gain monopole antenna erected on the southwest corner of Whittemore Hall's rooftop to transmit the signal (Figure 12). The receiver consisted of a 6-dB gain antenna attached to a Hewlett Packard 8594E Spectrum Analyzer powered by a 12-volt EverStart marine battery, and a Whistler PP300AC Power Inverter (Figure 13). Received signal strengths were collected for 63 locations throughout campus and the adjoining golf course (28 LOS and 35 obstructed). A Garmin GPS12® unit recorded the

geographic coordinates (decimal degrees) of the receiver locations. The satellite signal received by the Garmin GPS12® unit was time averaged for 30 seconds and the average error estimated by the unit was 16.4 feet (Appendix C). No single error estimate exceeded 30 feet (Figure 14). Once obtained, the data points were mapped onto the 1": 50' topographic map and evaluated for accuracy. If the detailed field note did not match the corresponding plotted location, the data point was moved to a more accurate location based on the field notes (Figure 15).

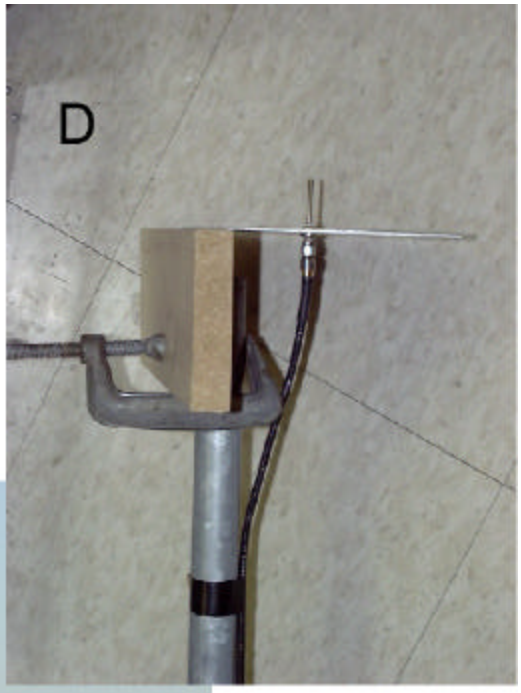

Figure 11: Transmitting system located on southwest corner of Whittemore Hall.

A) Hewlett Packard 6648C Signal Generator
B) Hewlett Packard 491C Microwave Amplifier
C) 2.1 dB Monopole Antenna
D) Antenna Closeup

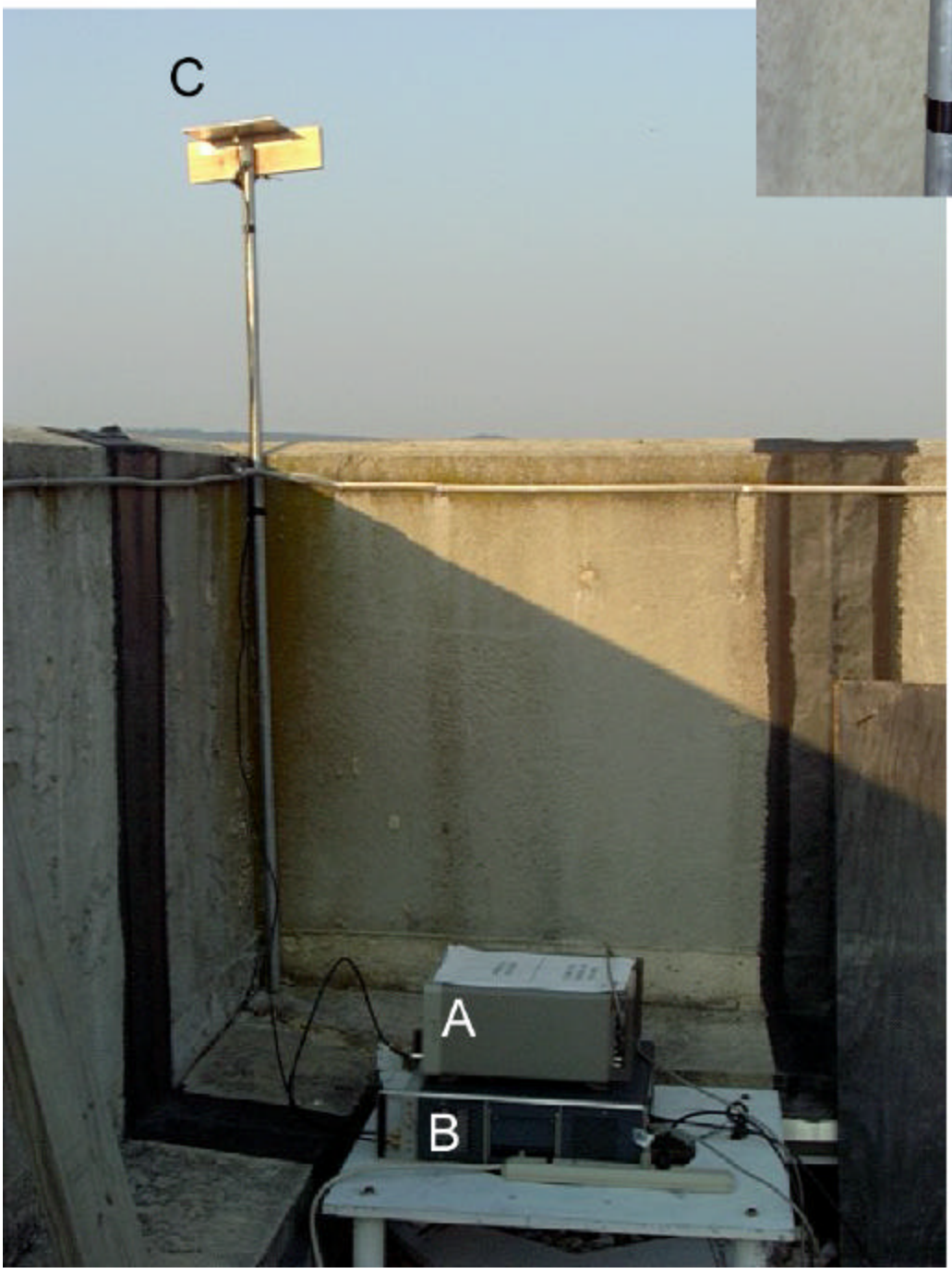

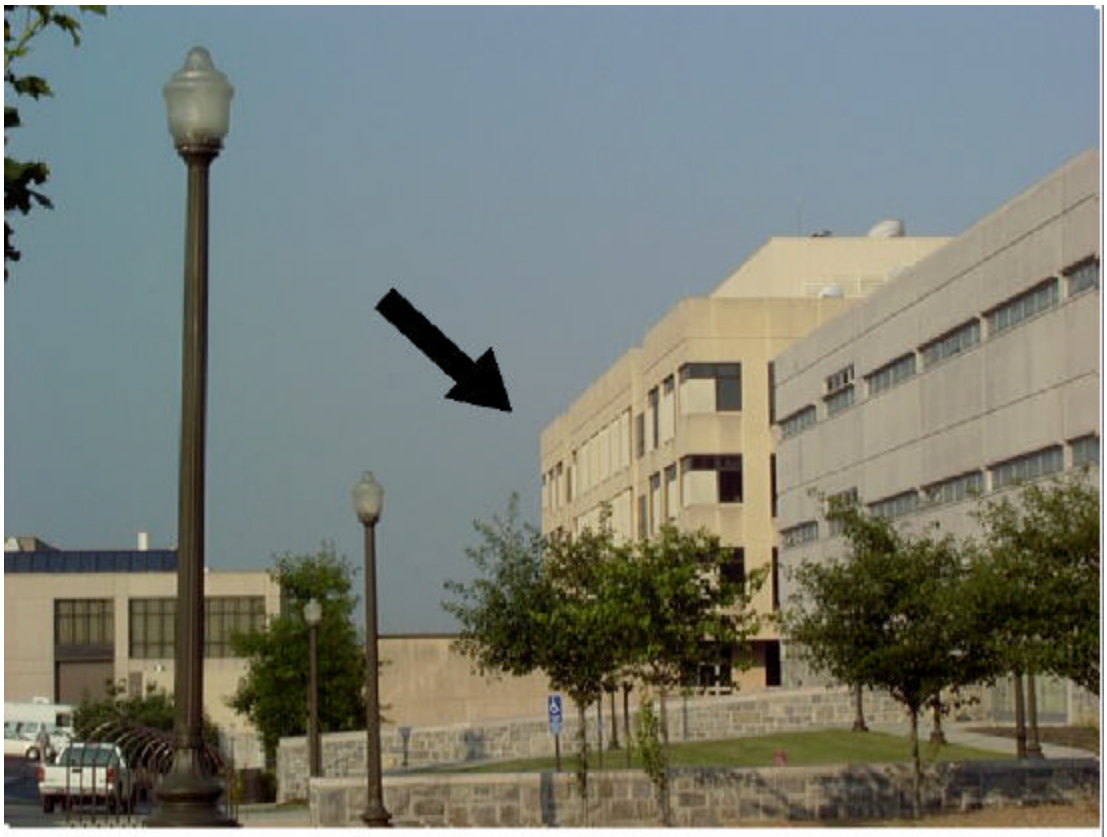

Figure 12: Arrow indicates location of transmitter on southwest corner of Whittemore Hall.

Figure 13: Receiving system used for experiments conducted in this study.
A) 12 volt EverStart Marine Battery
B) Whistler PP300AC Power Inverter
C) Hewlett Packard 8594E Spectrum Analyzer
D) 6-dB Gain Receiving Antenna

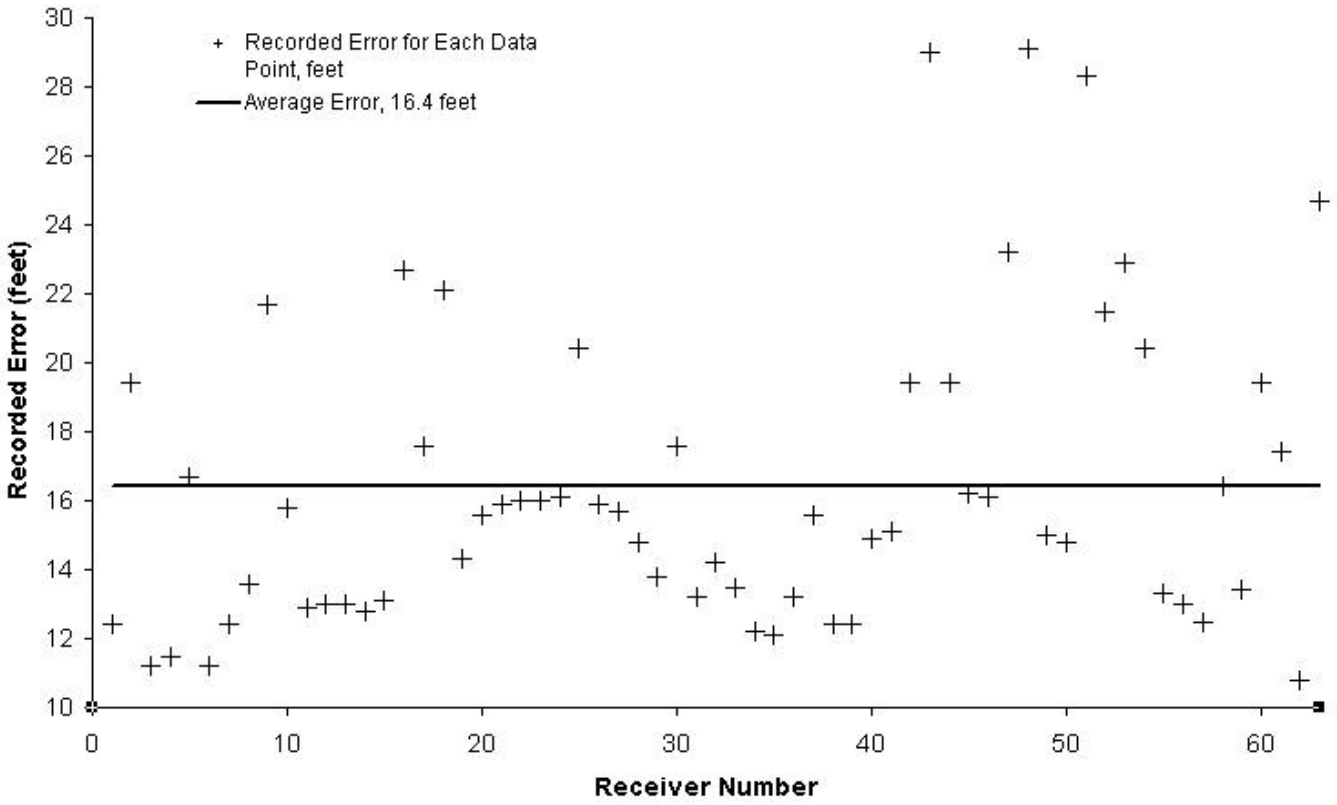

Figure 14: Graph depicting the recorded error for the location of each receiver and the average error for the data set (2.4 GHz).

The field notes are considered superior to the GPS measurements because they contain detailed information about the cultural and natural features surrounding the receiver location. The field notes are only superior when used in conjunction with the 1-foot contour maps, which contain the same type of information. If the topographic maps did not exist, or did not contain locations of such features as manhole covers, parking lot stripes or landscaping, then the field notes would not make the GPS locations any more accurate. For example, the field notes of receiver location #17 state that the location is at the "left top corner of parking lot in front of median." The location of the receiver recorded by the GPS unit is in the middle of the sidewalk, not in the parking lot, introducing significant error to the data point. Therefore, in an effort to reduce this error, the receiver was moved to a spot that more accurately reflected the field notes (Figure 16). Apparent State Plane coordinates, corrected State Plane coordinates (both in feet)

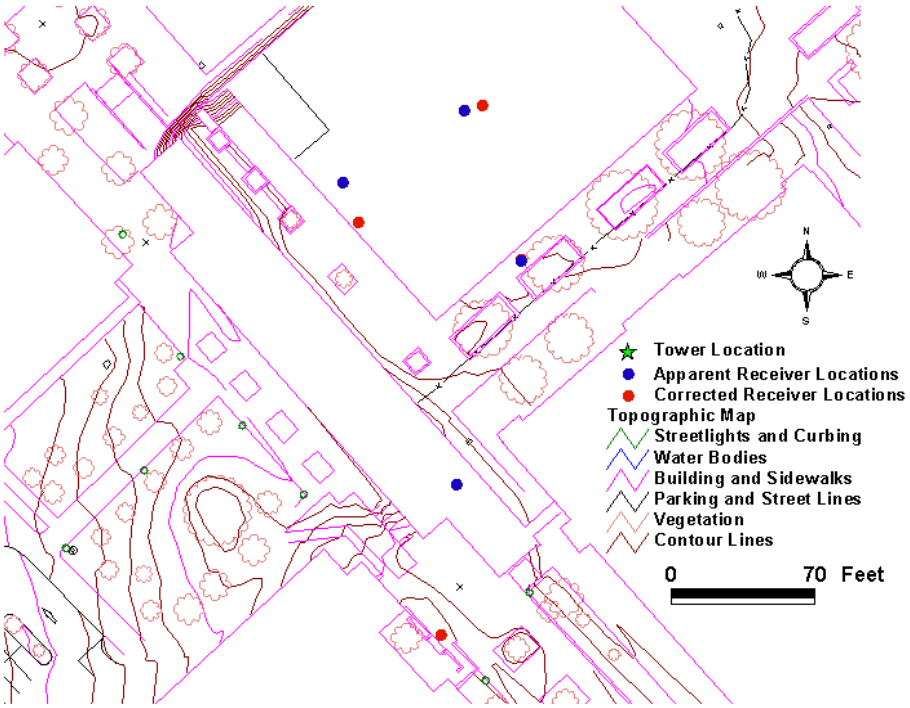

Figure 15: Sample comparison of apparent receiver locations based on the data recorded by the GPS unit to corrected receiver locations based on the detailed field notes collected in this study.

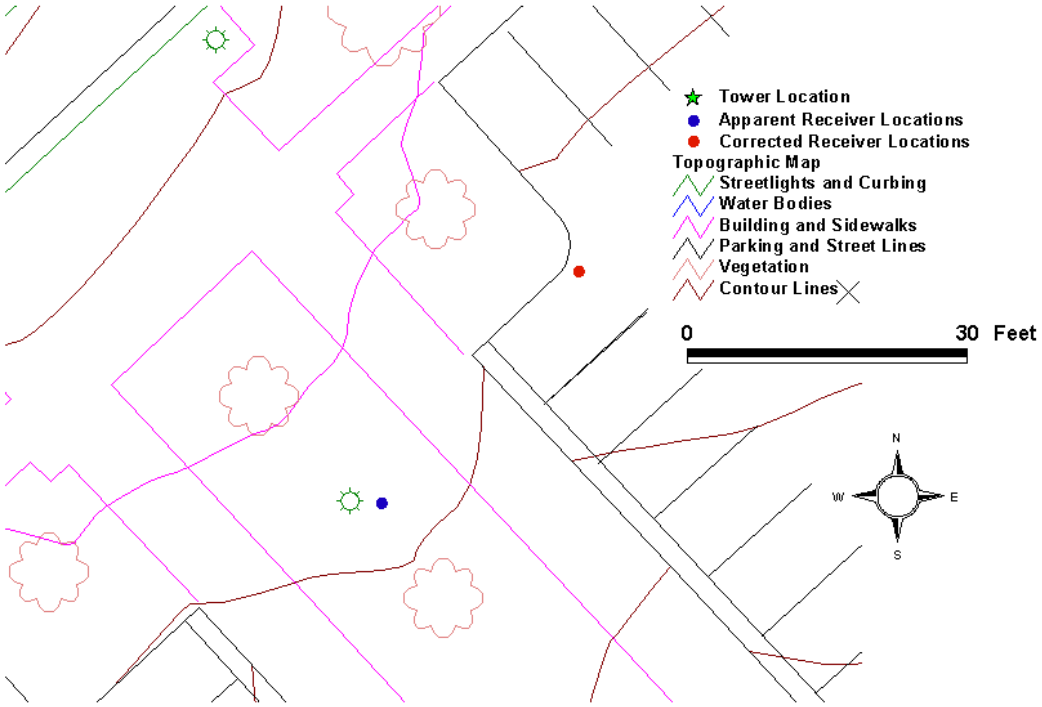

Figure 16: Example of field notes enabling the receiver to be located more accurately.

and distance moved (feet) are shown in Appendix D. The distance moved is also illustrated in Figure 17. The average distance a receiver location was moved is 16.7 feet, which is notably very close to the average error estimated by the GPS unit (16.4 feet).

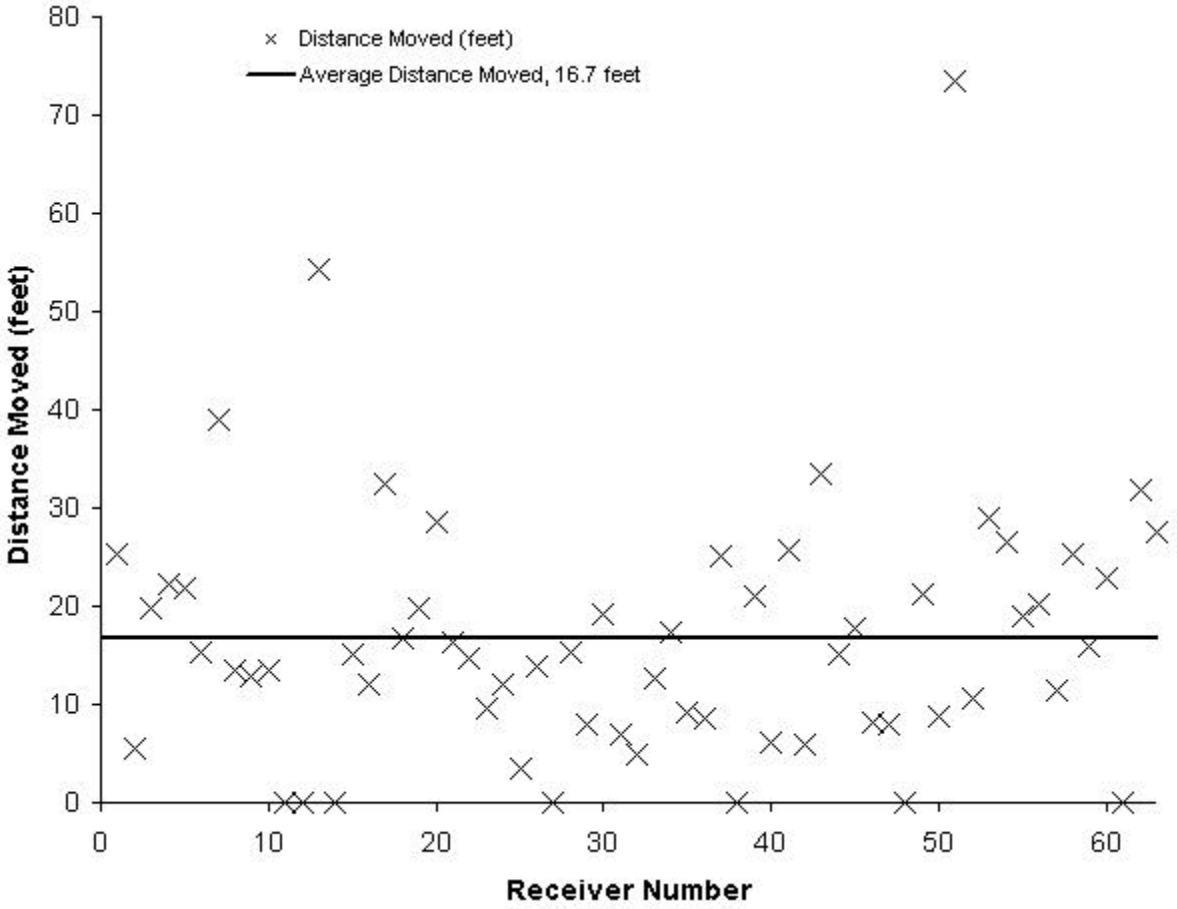

Figure 17: Graph of total distance each receiver location was moved based on detailed field notes and average distance moved for the entire data set (2.4 GHz).

The final data set used in the overall analysis was the output from the proposed model (Appendix B). There are 16 sets of results based on the technique used to calculate signal strength and frequency of data set. The model parameters for each frequency are listed in Table 1. The first four data sets are used to analyze the accuracy of prediction for path loss. The resultant data from the model includes: path length, blockage height(s), path loss, diffraction gain, predicted signal strength, distance to blockage(s) and distance to receiver from blockage(s)

and actual path loss (Appendix B.1a – B.1d). The remaining results were generated to better understand the effect of various modeling techniques on signal strength prediction and do not include path loss. The results are organized based on frequency, blockage type, interpolation of DEM elevations and inclusion of Fresnel zone clearance (Appendix B).

Table 1: Model parameters used for each frequency.

Frequency of Transmitted Signal	Transmitter Power (dBm)	Transmitter Gain (dB)	Receiver Gain (dB)	Tower Height (feet)	Receiver Height (feet)	Viewshed Radius (meters)
902 MHz	21.5	5.14	5.14	8.56	6.5	1,700
2.4 GHz	30.0	-2.0	10.0	7.33	3.0	1,700
24.12 GHz	13.0	12.0	20.0	3.28	3.0	1,700
27.525 GHz	22.3	37.0	11.5	8.56	6.5	1,700

Chapter 4. Algorithm Design

The algorithm developed in this research to predict the field strength was implemented in several stages (Figure 18). The first stage determined which cells in the base map constituted the LOS path from the transmitter to the receiver using the Bresenham Algorithm (Bresenham, 1965). Once the LOS path was determined, elevations were interpolated along the Bresenham line using the Inverse Distance Weighted Averaging Algorithm if the option was selected previously (Figure 19). Calculated elevations along the LOS path were then compared to the elevations along the Bresenham or interpolated line to find the maximum obstruction, if present. If the path was clear, Fresnel zone clearances were evaluated if this option was selected. If the **Double Blockage Type** option was selected, then a search for the second blockage was performed comparing elevations in the Bresenham or interpolated line to the calculated elevations from a new LOS path. The line connecting the primary blockage to the receiver defined the new LOS path. If two blockages were found, then the method described in Bullington (1947) was used to extract a single virtual blockage for the diffraction gain calculation. Diffraction gain, path loss and, finally, received power can be calculated, once the above stages are completed. Each stage of the algorithm is discussed in detail in the following sections.

The cells of the base map which represent the LOS path from the transmitter location to the receiver location were determined using a modified Bresenham Algorithm (Figure 20). Jack Bresenham published the original Bresenham Algorithm in 1965. The original algorithm drew the line by incrementing in both the horizontal and vertical direction and determining which of the two cells best satisfied the following equation.

$$f(x,y) = b * x - a * y = 0 \qquad (1)$$

x = X-coordinate of point on the line

y = Y-coordinate of point on the line

a = X-coordinate of test point

b = Y-coordinate of test point

The cell that best satisfied the equation was chosen to represent the line at that point. This algorithm was developed because the digital differential analyzers that were used to draw lines at that time were based on floating point arithmetic (Van Aken and Killebrew, 1988). In contrast,

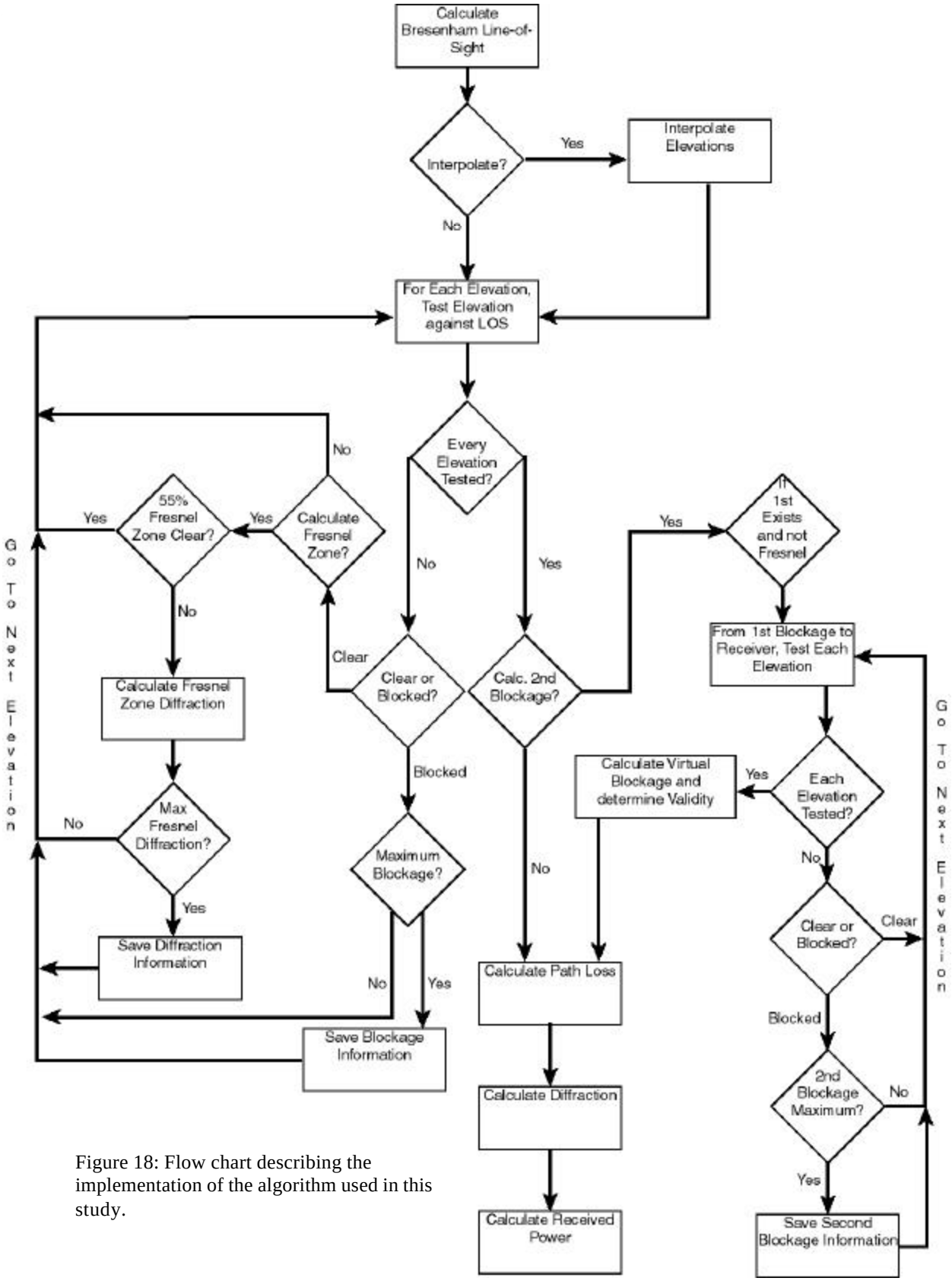

Figure 18: Flow chart describing the implementation of the algorithm used in this study.

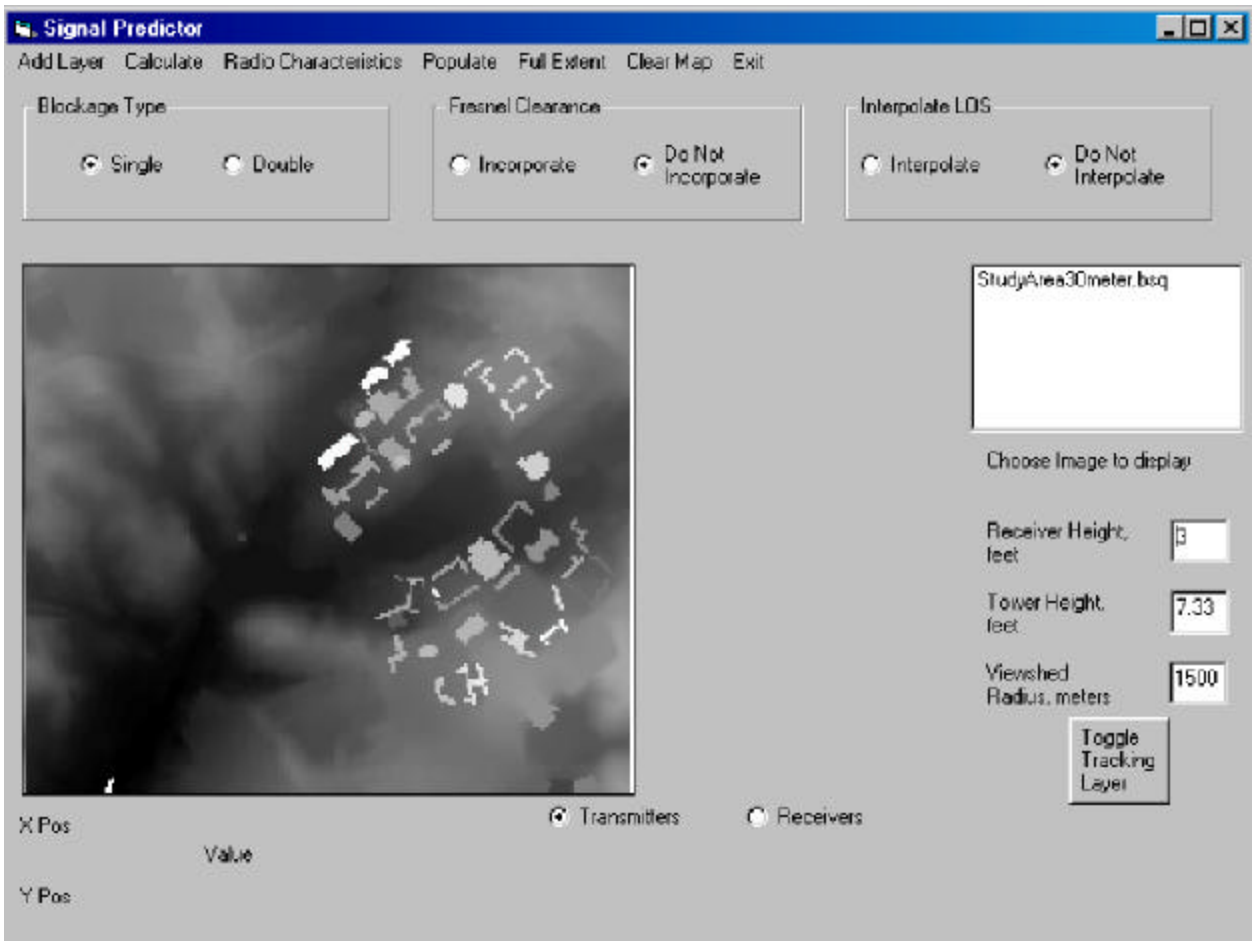

Figure 19: GUI interface for program showing optional techniques for predicting signal strength.

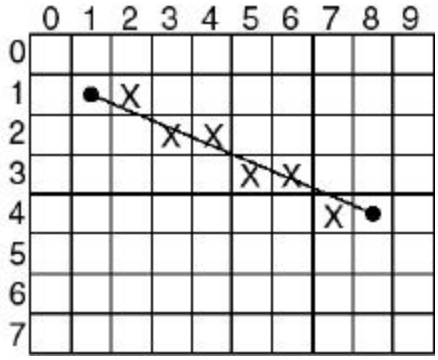

Figure 20: Schematic diagram illustrating the cells, marked with X's, that would represent the LOS path calculated by the modified Bresenham algorithm.

A part of the implementation of the Bresenham algorithm involves multiplication steps within the primary **For** loop, which is computationally more intense for a computer than simple addition or subtraction. Therefore, in order to reduce the computation time further, this research

uses a modified Bresenham Algorithm implemented by Patrick Caulfield and Alan Foster (former Geography students at Virginia Tech). This algorithm calculates the line by incrementally reducing an error factor. More specifically, the line is incremented in the longer direction (X or Y) until the error factor is reduced to zero, at which time the shorter direction (X or Y) is incremented. The error factor can be calculated a number of ways and is usually function of distance moved in the smaller direction per distance incremented in the larger direction, or slope. Because these increments involve integer addition and subtraction, rather than integer multiplication, the implementation of this line drawing algorithm is more efficient. Furthermore, the cells identified by the modified Bresenham algorithm also satisfy Equation 1.

As the line drawing algorithm progresses, the elevations from the DEM considered to be along the LOS path are saved (along with the corresponding row-column positions and X-Y coordinates) in a separate array. If the user has selected the **Interpolate** option (Figure 19), then this array is sent to a separate interpolation procedure. The method chosen to interpolate the elevations along the LOS path is the Inverse Distance Weighted Averaging Algorithm. Coordinates along the LOS path are incremented in the X and Y direction by a constant amount.

$$\text{X-Increment, feet} = dX / D \quad (2)$$

$$\text{Y-Increment, feet} = dY / D \quad (3)$$

dX = distance in the X-direction from the transmitter to receiver, feet

dY = distance in the Y-direction from transmitter to receiver, feet

D = Total Path Length, feet

As the point is incremented along the LOS path, distances from the point to each elevation of the Bresenham line are calculated. The two shortest distances (and their respective elevations) are selected to interpolate the new elevation (Figure 21). The equation used to interpolate the new elevation is

$$\text{Interpolated Elevation, meters} = ((E_1/D_1^2)+ (E_2/D_2^2))/ ((1/D_1^2)+ (1/D_2^2)) \quad (4)$$

E_1 and E_2 are the two closest elevations obtained from the Bresenham line and D_1 and D_2 are the corresponding distances from the point along the LOS path to these elevations.

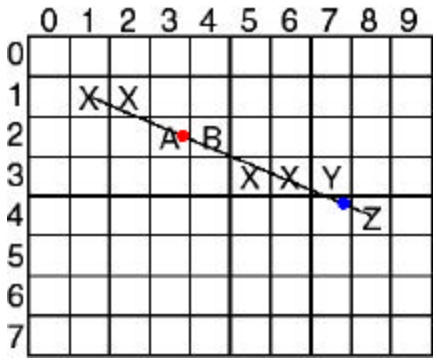

Figure 21: Schematic diagram illustrating the interpolation procedure. The Red dot would be interpolated using elevations and distances represented by A and B. The Blue dot would be interopolated using elevations and distances represented by Y and Z.

Once a final elevation line (either Bresenham or interpolated) is determined, a **For** loop is implemented so that each elevation can be compared to calculated elevations of the straight LOS path. If the Bresenham (or interpolated) elevation is less than the LOS elevation, then the path is considered clear. However, diffraction loss can still occur in a non-obstructed path. This occurs when an obstruction interferes with the Fresnel zones. Fresnel zones are zones of secondary waves which enclose the LOS path and have a path length $n\lambda/2$ greater than the total path length (Figure 22). These zones alternatively provide constructive and destructive interference to the total received signal strength (Rappaport, 1996). The general rule of thumb, as stated in Rappaport (1996), is that as long as 55% of the first Fresnel zone volume is clear, then no significant increase in diffraction loss will be observed with further clearance.

The user has to option to incorporate Fresnel zone clearance into the field strength calculations for points along the LOS path which are initially considered unobstructed. If this option is selected, then the radius of the first Fresnel zone, F_1, is calculated using the following equation.

$$F_1 = \sqrt{\frac{l d_1 d_2}{(d_1 + d_2)}} \qquad (5)$$

F_1 = radius of the first Fresnel zone, meters

λ = wavelength, meters

d_1 = distance from transmitter to blockage, meters

d_2 = distance from blockage to receiver, meters

Using the radius at this point, the area of the Fresnel circle is calculated. For the purposes of this study, a clearance of 55% of the Fresnel area is considered analogous to 55% of the Fresnel volume. The first Fresnel zone is the only zone that needs to be considered because it is the zone closest to the LOS path, with the smallest radius, and the largest potential for destructive or constructive interference. As a shortcut, a control statement is included such that the following calculations are performed only if the Fresnel radius, F_1, is greater than the distance, h, between the LOS elevation and the Bresenham (or interpolated) elevation (Figure 23).

The 55% clearance criterion is calculated by using the solution of the following integral

$$\text{Integral: } 2 * \int_0^h \sqrt{r^2 - h^2}\, dx \qquad (6)$$

$$\text{Solution: } 2 * \left(h/2 * \sqrt{r^2 - h^2} + r^2/2 * Arc\sin\left(h/|r| \right) \right) \qquad (7)$$

This integral calculates the area of the shaded region in Figure 23. If this area is greater than 5% of the total Fresnel area, then more than 55% of the entire Fresnel volume is unobstructed and the path is considered to be truly LOS at that point. If the area is less than or equal to 5%, then a diffraction loss is calculated. A detailed discussion of the calculation for diffraction loss will be presented in later sections. As the location of the test elevation proceeds along the LOS path, the most negative Fresnel diffraction loss is saved as long as no actual blockage has occurred. An actual blockage will cause significantly more diffraction loss than Fresnel zone interference. Therefore, once a real blockage is located, control statements prohibit further Fresnel zone calculations.

The path is considered obstructed when, if ever, the actual (or interpolated) elevation is greater than or equal to the calculated LOS elevation. As the location of the test point increments along the LOS path, only the information pertaining to the largest obstruction encountered is saved for the diffraction calculation. Unlike the Fresnel zone calculations, the actual diffraction calculation occurs later in the implementation of the algorithm. The program is implemented in this fashion to allow the user to calculate diffraction loss from two blockages.

If the user chooses the **Double Blockage Type** option, then once the maximum blockage is determined, the program attempts to locate a second blockage. A new LOS path is calculated

from the primary blockage to the receiver. The second blockage is defined as the maximum

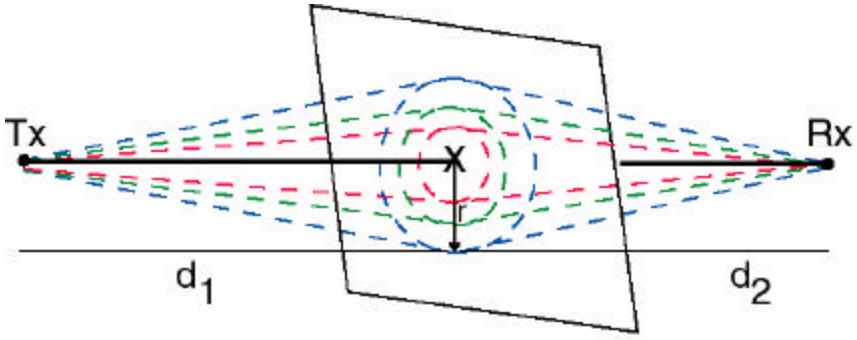

Figure 22: Schematic diagram illustrating Fresnel zones. The bold black line is the LOS path from the transmitter to the receiver. The dashed blue, green and red lines indicate successive Fresnel zones. Fresnel zones are an ellipsoidal volume, so a plane intersecting the Fresnel zones would generate Fresnel circles. The blue, green and red dashed circles are the planar intersections of the Fresnel zones at point X. The radius of the blue Fresnel zone (the third Fresnel zone in this illustration) is r. The first Fresnel zone is the red zone. The distance from the transmitter to point X is d_1, and the distance from point X to the receiver is d_2.

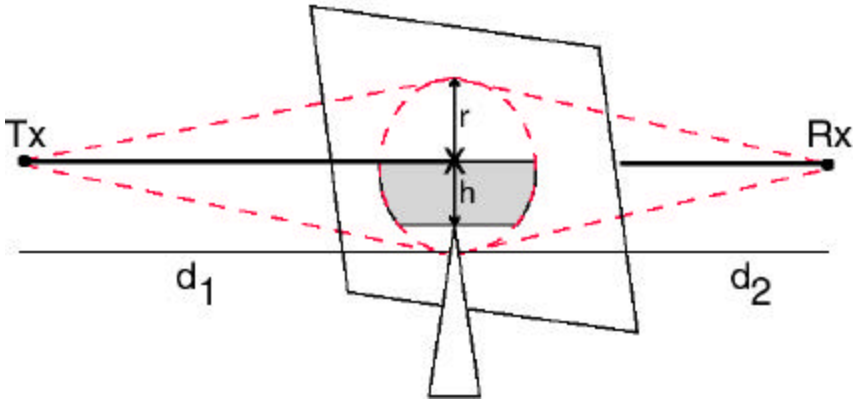

Figure 23: Schematic diagram illustrating calculation of the Fresnel zone clearance. The red dashed line represents the first Fresnel zone, and its radius is r. The red dashed circle is the planar intersection of the first Fresnel zone at point X. The white triangle is the knife-edge obstruction that is interfering with the first Fresnel zone. The distance from the LOS path to the obstruction is indicated by h. The shaded region represents 5% of the area of the circle that must be cleared in order to meet the 55% clearance criterion. (modified after Rappaport, 1996).

obstruction of this new LOS path. This part of the algorithm is only performed if a first blockage exists and it does not arise from interference with Fresnel zones. If a second blockage is found along this new path, then these two blockages are passed to an independent procedure to calculate a single virtual obstruction, and this virtual obstruction is used to calculate the diffraction loss.

The virtual obstruction is defined as the point of intersection of the line defined by the transmitter and primary blockage and a second line defined by the receiver and the secondary blockage (Figure 7a). The method provided by Bullington (1947) requires that the position of the virtual obstruction be between the two original obstructions. If the virtual obstruction is not positioned between the two original obstructions, then the diffraction loss calculation will produce erroneous results (Figure 24). A simple control statement determines if this requirement is met. If this requirement is met, then the virtual obstruction is used in the diffraction loss calculation. If not, then the primary obstruction alone is used.

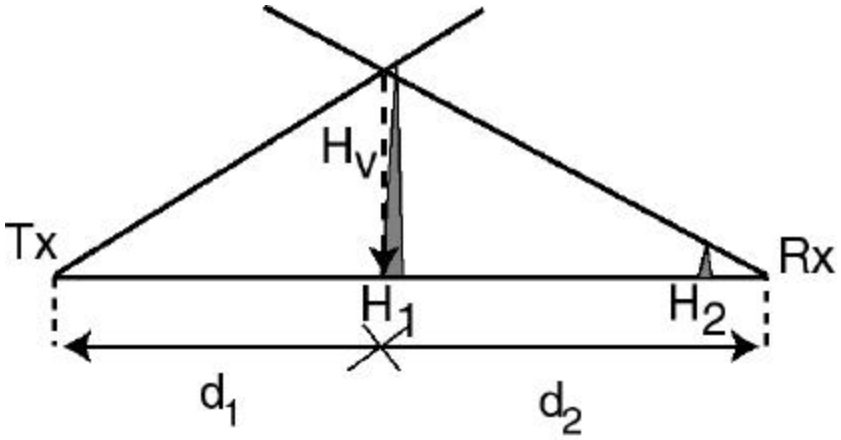

Figure 24: Model of an invalid virtual obstruction. The transmitter is Tx; the receiver is Rx. The height of the first and second blockage is H_1 and H_2, respectively. The height and distances of the virtual obstruction are H_v, d_1 and d_2, respectively.

At this point, all the necessary information has been collected from the model to calculate received power. Received power is a function of transmitter power, transmitter gain, receiver gain, path loss and diffraction loss. Transmitter power, transmitter gain and receiver gain are parameters entered by the user during runtime. Free-space path loss is calculated using the following equation

$$\text{Path Loss, dB} = 20 * \text{Log}_{10}(4 * \pi * D / \lambda) \qquad (8)$$

D = path length, meters

λ = wavelength, meters

Calculating diffraction loss is not a trivial matter. The exact solution for relative field strength (E/E_0) and corresponding diffraction loss is shown in Figure 25 (Lee, 1985).

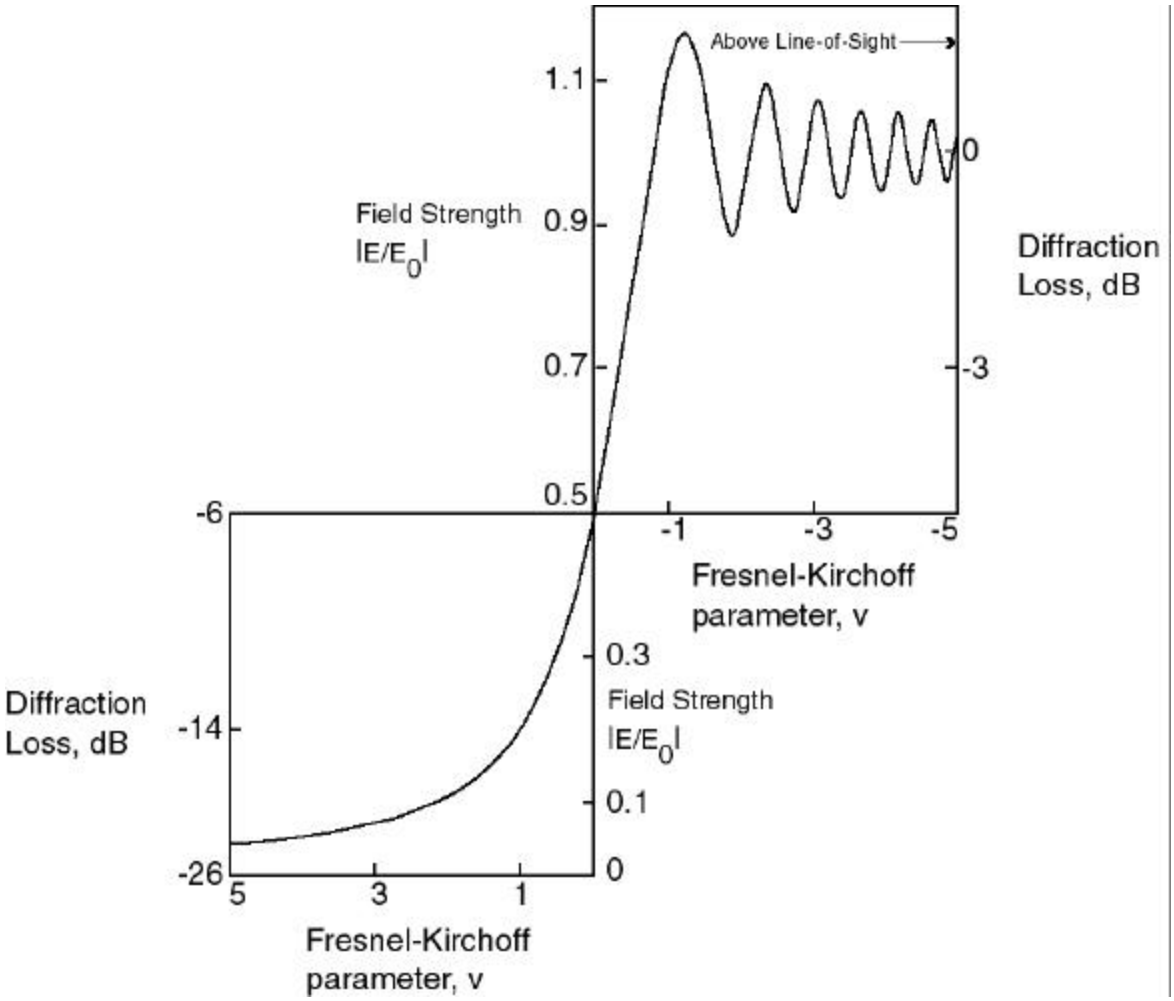

Figure 25: Graph of relative field strength (E/E_0) due to diffraction loss as a function of the Fresnel-Kirchoff parameter, v (Lee, 1985).

The approximation for diffraction loss used in this research can be found in Rappaport (1996) and was originally proposed by Lee (1985). The approximation is first determined by calculating the dimensionless Fresnel-Kirchoff diffraction parameter, v.

$$v = h * \sqrt{\frac{2*(d_1 + d_2)}{l d_1 d_2}} \qquad (9)$$

Using this parameter, diffraction loss is then calculated by the following set of approximation equations (Rappaport, 1996).

$G_d = 0$ $\quad v \leq -1$ (10)

$G_d = 20 * \text{Log}_{10}(0.5 - 0.62 * v)$ $\quad -1 < v < 0$ (11)

$G_d = 20 * \text{Log}_{10}(0.5 * \exp^{-0.95*v})$ $\quad 0 \leq v \leq 1$ (12)

$G_d = 20 * \text{Log}_{10}\left(0.4 - \sqrt{0.1184 - (0.38 - 0.1*v)^2}\right)$ $\quad 1 < v \leq 2.4$ (13)

$G_d = 20 * \text{Log}_{10}(0.225 / v)$ $\quad v > 2.4$ (14)

G_d = diffraction gain, dB

These equations have been developed to calculate diffraction for the various scenarios that can occur during propagation. The first scenario is indicated when the dimensionless Fresnel-Kirchoff parameter, v, is less than or equal to –1 (Equation 10). This would be an unobstructed path, or clear LOS. Other negative values for v ($-1 < v \geq 0$, Equation 11) indicate diffraction loss due to Fresnel zone interference. When v = 0 (Equation 12), then knife-edge diffraction is indicated and positive values of v (Equations 12-14) indicate diffraction loss due to obstructed pathways. Finally, the following equation is used to calculate received power.

Received Power, dBm = $P_{tx} + G_{tx} + G_{rx} + G_d - P_l$ (15)

P_{tx} = Transmitter Power, dBm

G_{tx} = Transmitter Gain, dB

G_{rx} = Receiver Gain, dB

G_d = Diffraction Gain, dB

P_l = Path Loss, dB

Chapter 5. Results

The ability of the various techniques to accurately predict field strength is illustrated in Figures 26 - 29 as a function of the difference between the measured and predicted values. The corresponding averages and standard deviations are summarized in Table 2, and graphically illustrated in Figure 30. All results were classified according to the calculation of Fresnel zones and interpolation of elevations. The various techniques were classified as follows: without Fresnel zones or interpolation (Figures 26a – 26d), with Fresnel zones but without interpolation (Figures 27a – 27d), without Fresnel zones but with interpolation (Figures 28a – 28d) and with Fresnel zones and interpolation (Figures 29a – 29d). All data is compiled from results using the single blockage technique unless otherwise noted. The double blockage technique was classified only into interpolated and non-interpolated techniques; Fresnel zone calculations were not included. The data set with the largest average difference is 902 MHz with an average difference between 11.4 and 12.1 dB. However, it has the lowest standard deviation (10.1 – 10.3 dB). The 2.4 GHz data set has an average difference between –0.35 to –1.1 dB, which is closest to ideal (0 db). The 24.12 GHz data set has the largest standard deviation (17.4 – 18.7 dB).

Table 2: Average and standard deviation of difference for each prediction technique.

Data Set (by Frequency)	No Fresnel No Interpolation	Yes Fresnel No Interpolation	No Fresnel Yes Interpolation	Yes Fresnel Yes Interpolation
902 MHz				
Average	-11.62 dB	-11.42 dB	-11.55 dB	-12.03 dB
Standard Deviation	10.25 dB	10.13 dB	10.26 dB	10.15 dB
2.4 GHz				
Average	-1.11 dB	-1.07 dB	-0.90 dB	-0.35 dB
Standard Deviation	15.68 dB	15.73 dB	16.50 dB	16.61 dB
24.12 GHz				
Average	2.07 dB	2.07 dB	0.02 dB	0.03 dB
Standard Deviation	18.64 dB	18.64 dB	17.43 dB	17.44 dB
27.525 GHz				
Average	3.57 dB	3.57 dB	3.64 dB	3.41 dB
Standard Deviation	15.18 dB	15.18 dB	15.20 dB	15.18 dB

In order to examine the contribution of different aspects of the program to field strength prediction, results have also been compiled for LOS prediction and Fresnel zone clearance. The accuracy of LOS prediction was determined by comparing the

number of predicted LOS pathways to the actual number indicated by the field notes. A prediction was considered accurate if the results match the field notes for both LOS and obstructed pathways. The results are summarized in Table 3. The percent accuracy is summarized in Table 4. All of the results are within the range of accuracy predicted by Dodd (2001) except for the 24.12 GHz data set.

Table 3: Predicted number of LOS pathways for each technique

Data Set (by Frequency)	Actual Number of LOS Pathways	No Fresnel No Interpolation	Yes Fresnel No Interpolation	No Fresnel Yes Interpolation	Yes Fresnel Yes Interpolation
902 MHz	21	32	31	32	32
2.4 GHz	28	30	30	30	29
24.12 GHz	0	10	10	11	11
27.525 GHz	21	32	32	32	32

Table 4: Percent accuracy of LOS prediction for each technique

Data Set (by Frequency)	Number of Receivers	No Fresnel No Interpolation	Yes Fresnel No Interpolation	No Fresnel Yes Interpolation	Yes Fresnel Yes Interpolation
902 MHz	81	84.0%	85.2%	84.0%	84.0%
2.4 GHz	63	90.5%	90.5%	87.3%	88.9%
24.12 GHz	33	69.7%	69.7%	66.7%	66.7%
27.525 GHz	80	83.8%	83.8%	83.8%	83.8%

The variation in the accuracy reported for a data set in Table 4 despite no apparent change in total number predicted is a function of the number of incorrectly predicted LOS paths relative to the number of incorrectly predicted obstructed paths. For example, the 2.4 GHz data set reports no change in total number of predicted LOS pathways between the non-interpolated and interpolated techniques, but the accuracy decreases by 3.2% when the elevations are interpolated (Table 4). For the non-interpolated data set, two were incorrectly omitted and four were incorrectly included. The total number of incorrect predictions is six, but the total number of predicted LOS pathways (incorrect or correct) is 30. When the elevations are interpolated, three were incorrectly omitted and five were incorrectly included, for a total of eight incorrectly predicted pathways. However, still only 30 actual LOS pathways are predicted (correct or incorrect).

Path loss is calculated by Equation 8 and the average difference between the predicted and measured values and standard deviation for each data set is illustrated in Figure 31 and summarized in Table 5. The results are compiled only for predicted LOS

pathways. It is not possible to accurately separate the effects of diffraction gain and path loss on received power for diffracted pathways. The data set with the highest average difference for path loss prediction is the 24.12 GHz data set. The data set with the lowest average difference is the 2.4 GHz data set. The 2.4 GHz data set is also the most variable set with a standard deviation of 10.28 dB.

Table 5: Average and standard deviation of difference in path loss for each data set.

Data Set (by Frequency)	Average Difference between Predicted and Measured Values of Path Loss	Standard Deviation of Difference for Path Loss
902 MHz	18.52	8.45
2.4 GHz	13.36	10.82
24.12 GHz	22.65	7.74
27.525 GHz	15.65	5.60

Diffraction gain's effect was evaluated by comparing new difference values between measured and predicted signal strength to the old difference values. The new difference values were based on predicted received signal strength calculated without diffraction gain (for the results that did not incorporate Fresnel zones, interpolate elevations or calculate a second blockage). The comparisons for each frequency are illustrated in Figures 32-35. Signal strength predictions based simply on LOS path loss do not adequately approximate the measured received signal strength for obstructed pathways.

The results from the double blockage computation are listed in Table 6. The obstructions in the single blockage technique are the same as the first obstructions calculated by the double blockage technique. In addition, the second obstructions found by the double blockage technique are located between the first obstruction and the receiver. However, the non-interpolated technique was unable to calculate any valid virtual obstructions from these two blockages. Interpolating elevations dramatically increased the number of second obstructions calculated, in addition to finding a very small number of valid virtual obstructions. However, calculating diffraction gain using the virtual obstruction did not improve the overall predictive power of the technique as indicated by the average change in predicted power listed in Table 6.

Table 6: Statistical summary of second blockage technique for non-interpolated and interpolated elevations.						
Data Set (by Frequency)	Number of First Blockages	Number of Second Blockages	Percentage of 2 Blockages	Number of Virtual Blockages	Percentage of Virtual Blockages	Average Change in Predicted Signal Strength, dBm
Non-interpolated Elevations						
902 MHz	49	34	69.39%	0	0%	0
2.4 GHz	33	26	78.79%	0	0%	0
24.12 GHz	23	16	69.57%	0	0%	0
27.525 GHz	48	33	67.35%	0	0%	0
Interpolated Elevations						
902 MHz	49	44	89.80%	4	9.09%	0.013
2.4 GHz	33	32	96.97%	3	9.38%	0.013
24.12 GHz	22	19	86.36%	0	0%	0
27.525 GHz	48	43	89.58%	3	6.98%	0.013

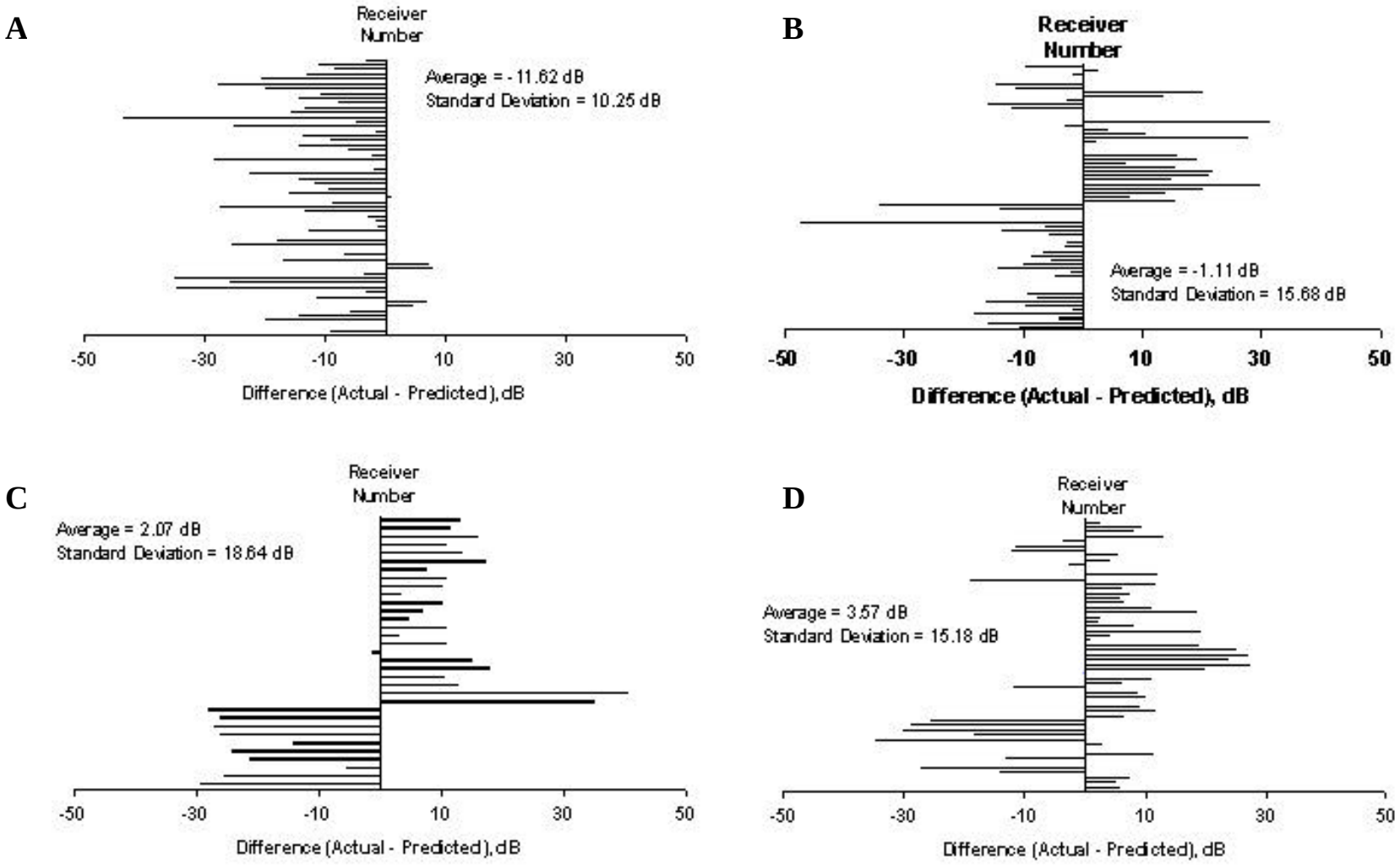

Figure 26: Difference, dB, in signal strength prediction for each receiver for the single blockage, without Fresnel zones and without interpolation technique: A) 902 MHz, B) 2.4 GHz, C) 24.12 GHz and D) 27.525 GHz.

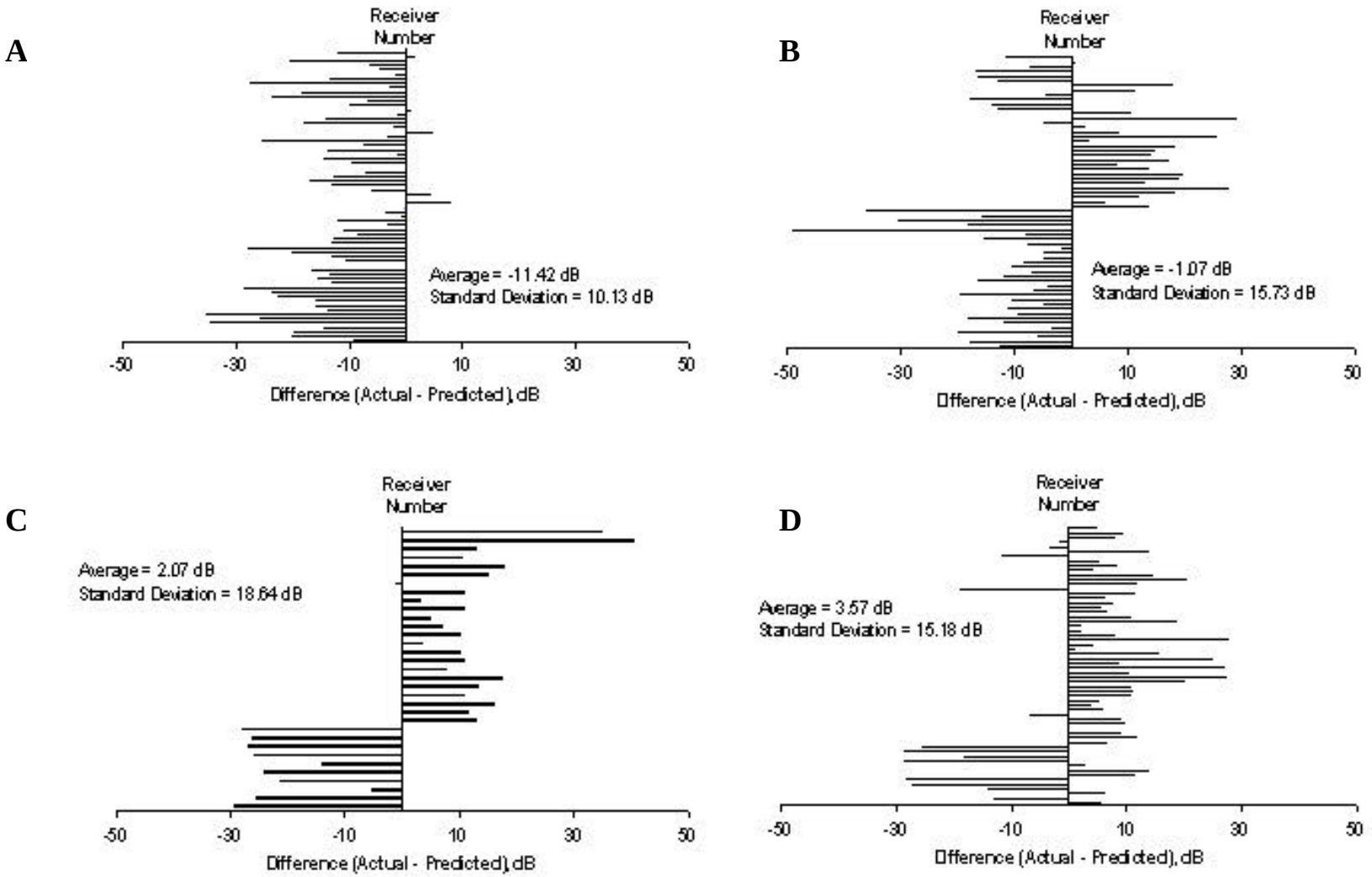

Figure 27: Difference, dB, in signal strength prediction for each receiver for the single blockage, with Fresnel zones and without interpolation technique: A) 902 MHz, B) 2.4 GHz, C) 24.12 GHz and D) 27.525 GHz.

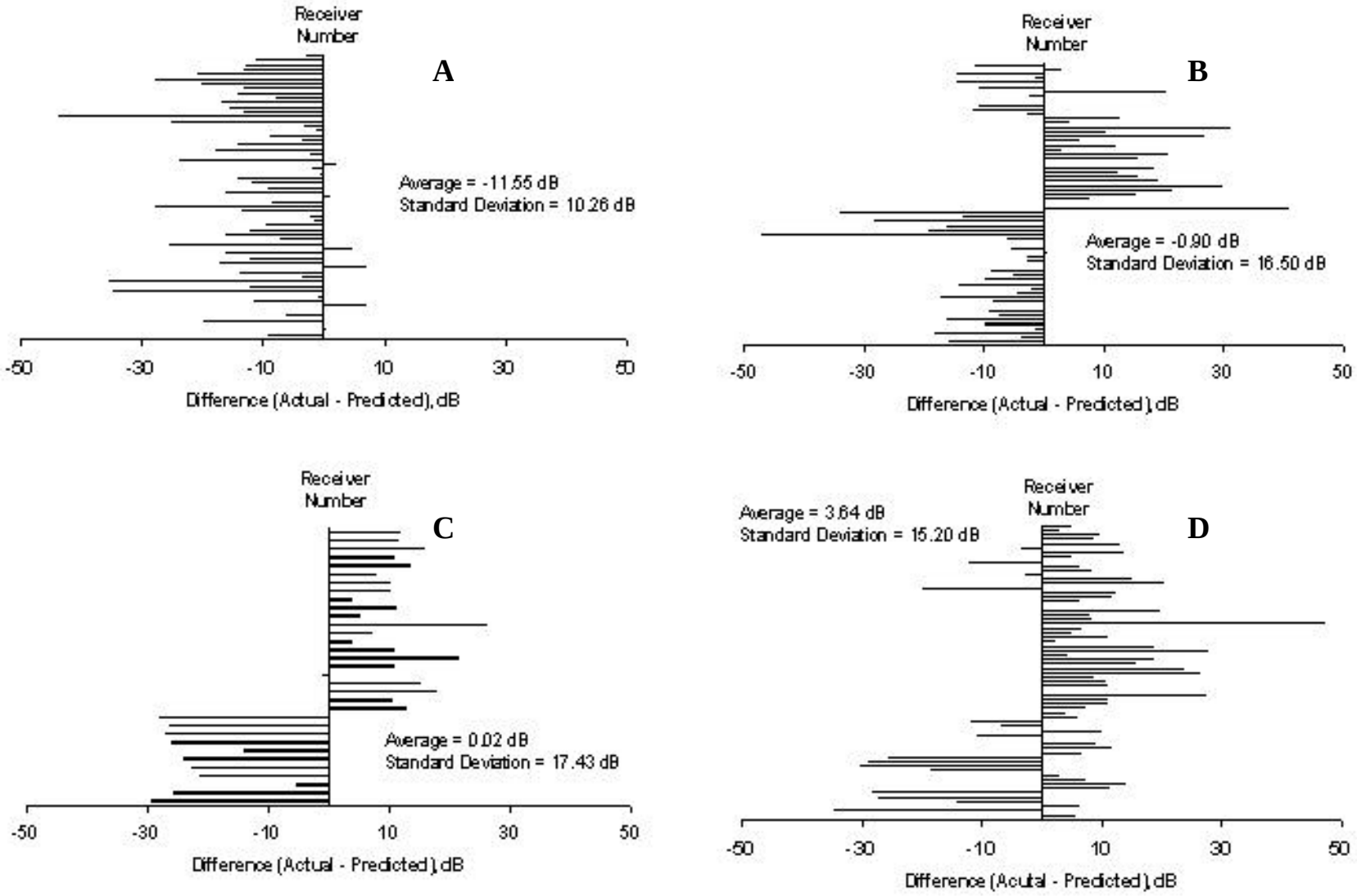

Figure 28: Difference, dB, in signal strength prediction for each receiver for the single blockage, without Fresnel zones and with interpolation technique: A) 902 MHz, B) 2.4 GHz, C) 24.12 GHz and D) 27.525 GHz.

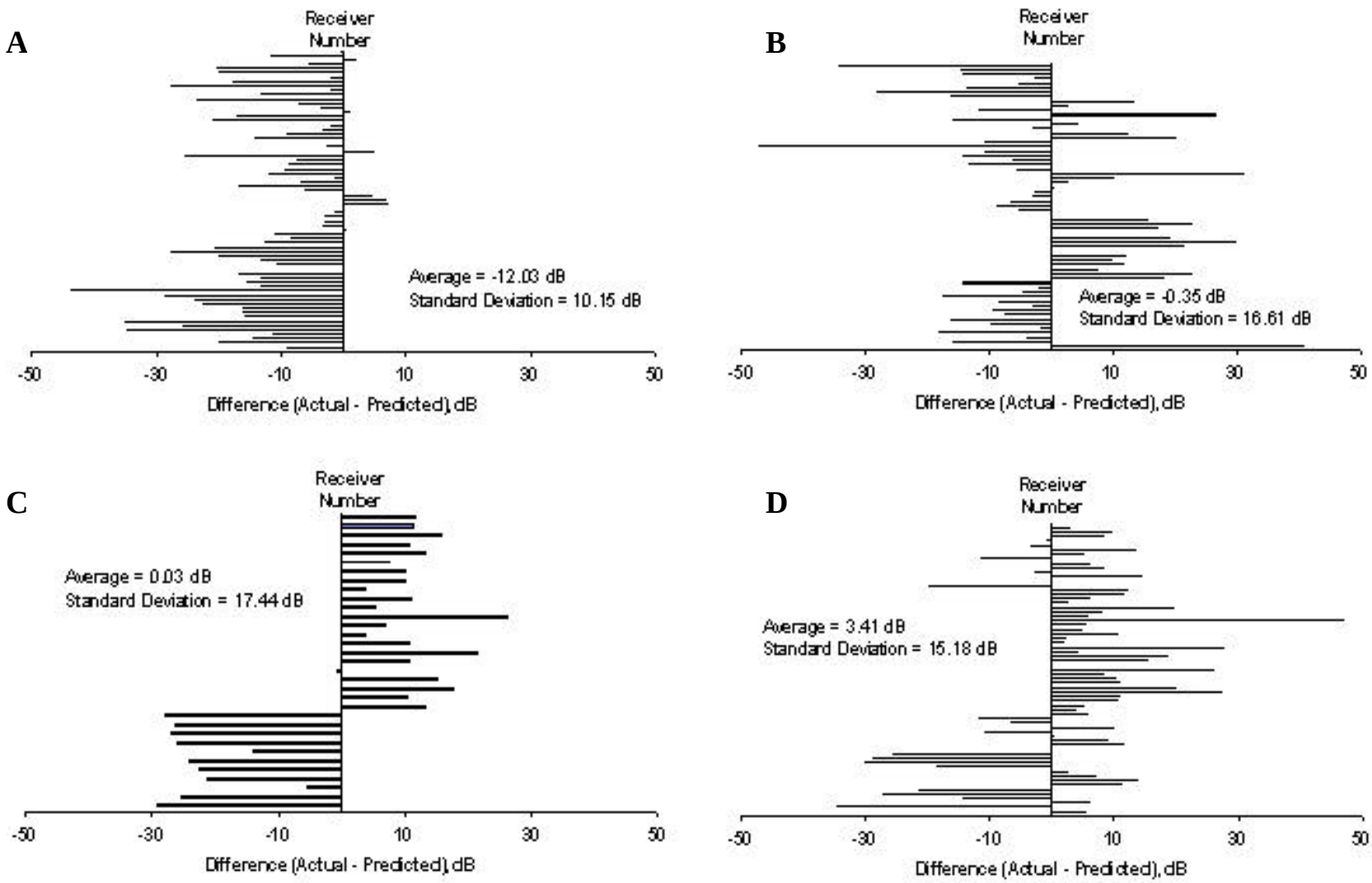

Figure 29: Difference, dB, in signal strength prediction for each receiver for the single blockage, with Fresnel zones and with interpolation technique: A) 902 MHz, B) 2.4 GHz, C) 24.12 GHz and D) 27.525 GHz.

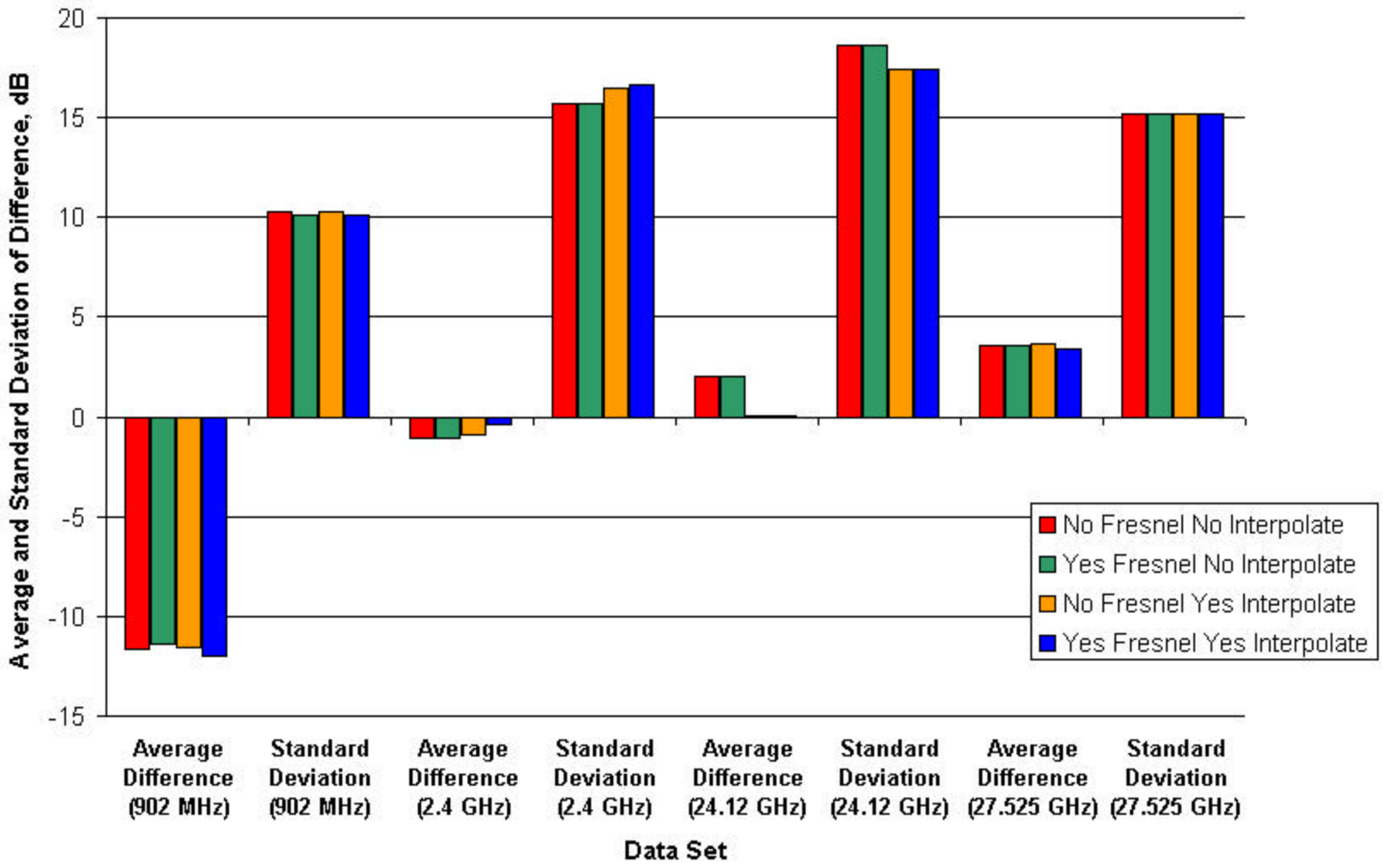

Figure 30: Average, dB, and standard deviation, dB, of difference in signal strength predictions for each technique only using single blockages to calculate diffraction.

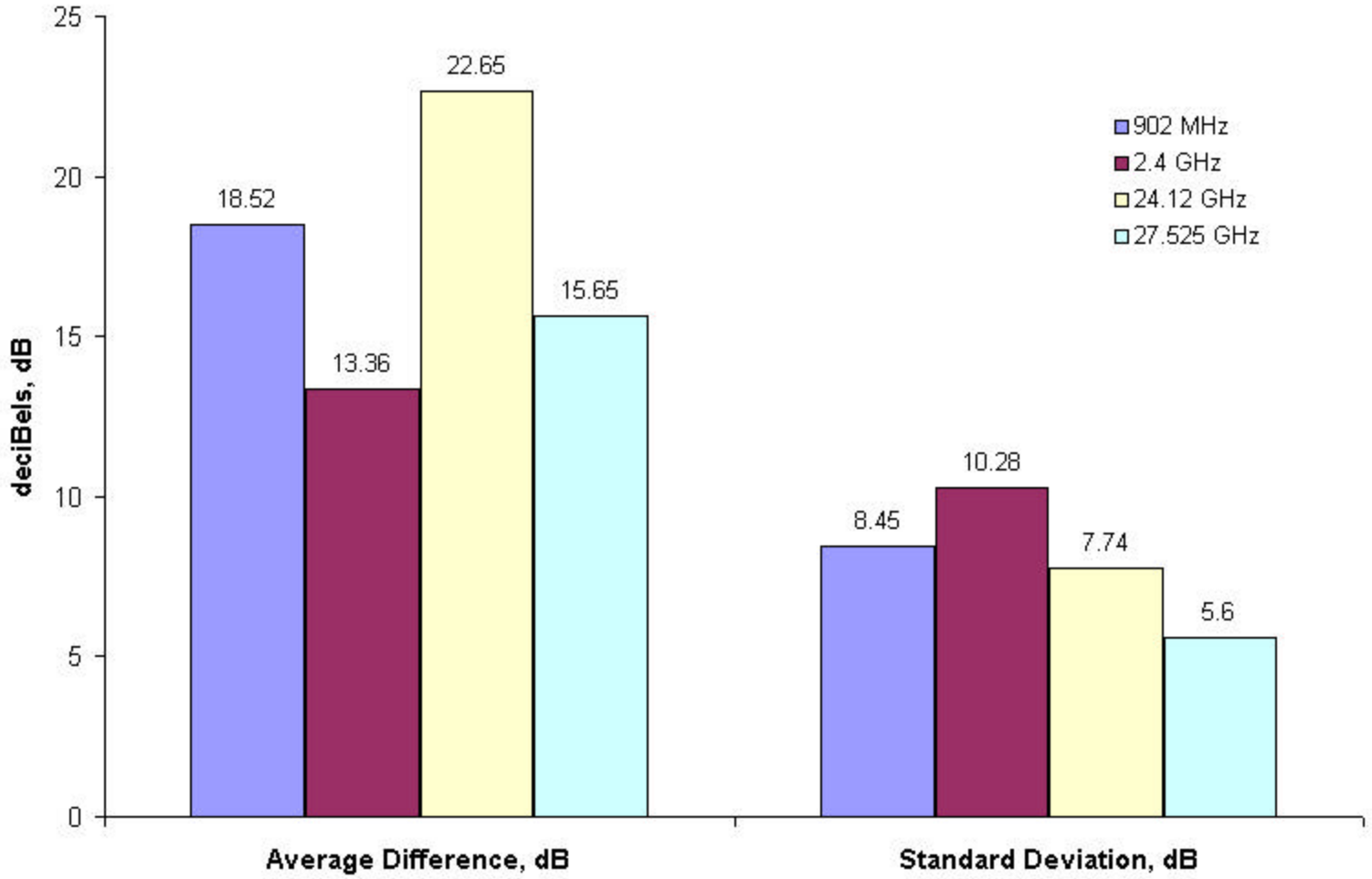

Figure 31: Average, dB, and standard deviation, dB, of difference in path loss for each frequency.

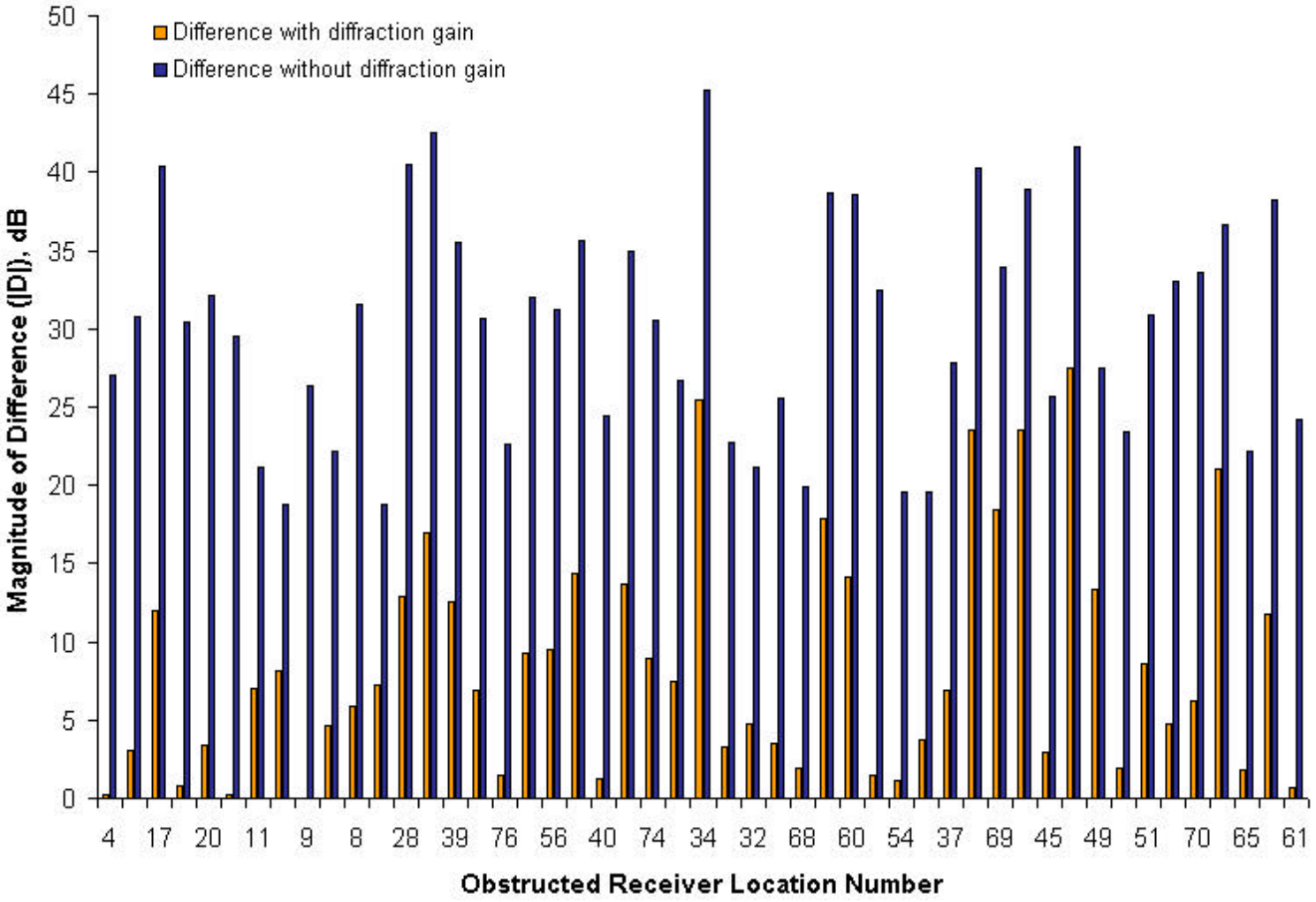

Figure 32: Graph comparing difference in signal strength prediction including diffraction gain to difference excluding diffraction gain (902 MHz).

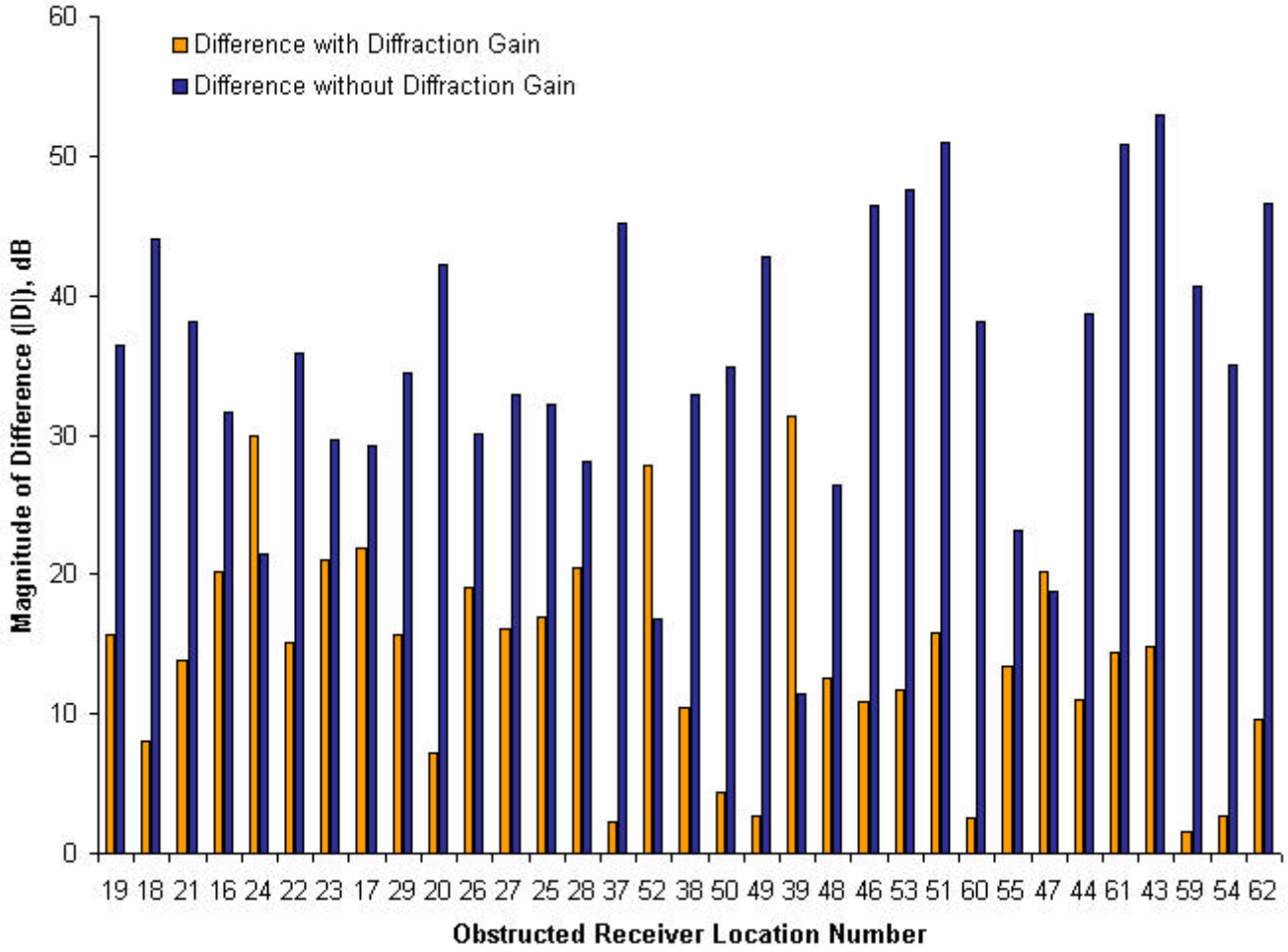

Figure 33: Graph comparing difference in signal strength prediction including diffraction gain to difference excluding diffraction gain (2.4 GHz).

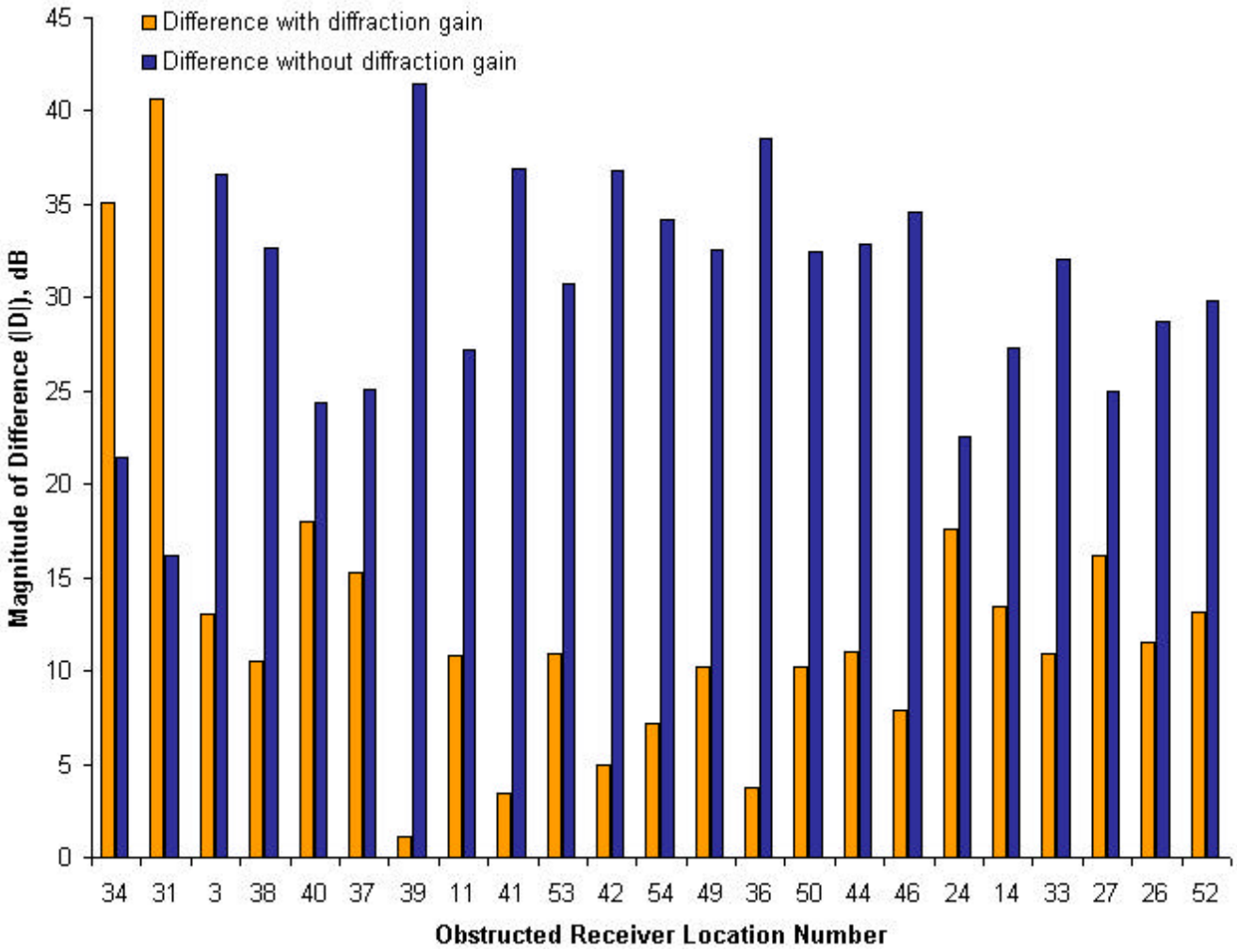

Figure 34: Graph comparing difference in signal strength prediction including diffraction gain to difference excluding diffraction gain (24.12 GHz).

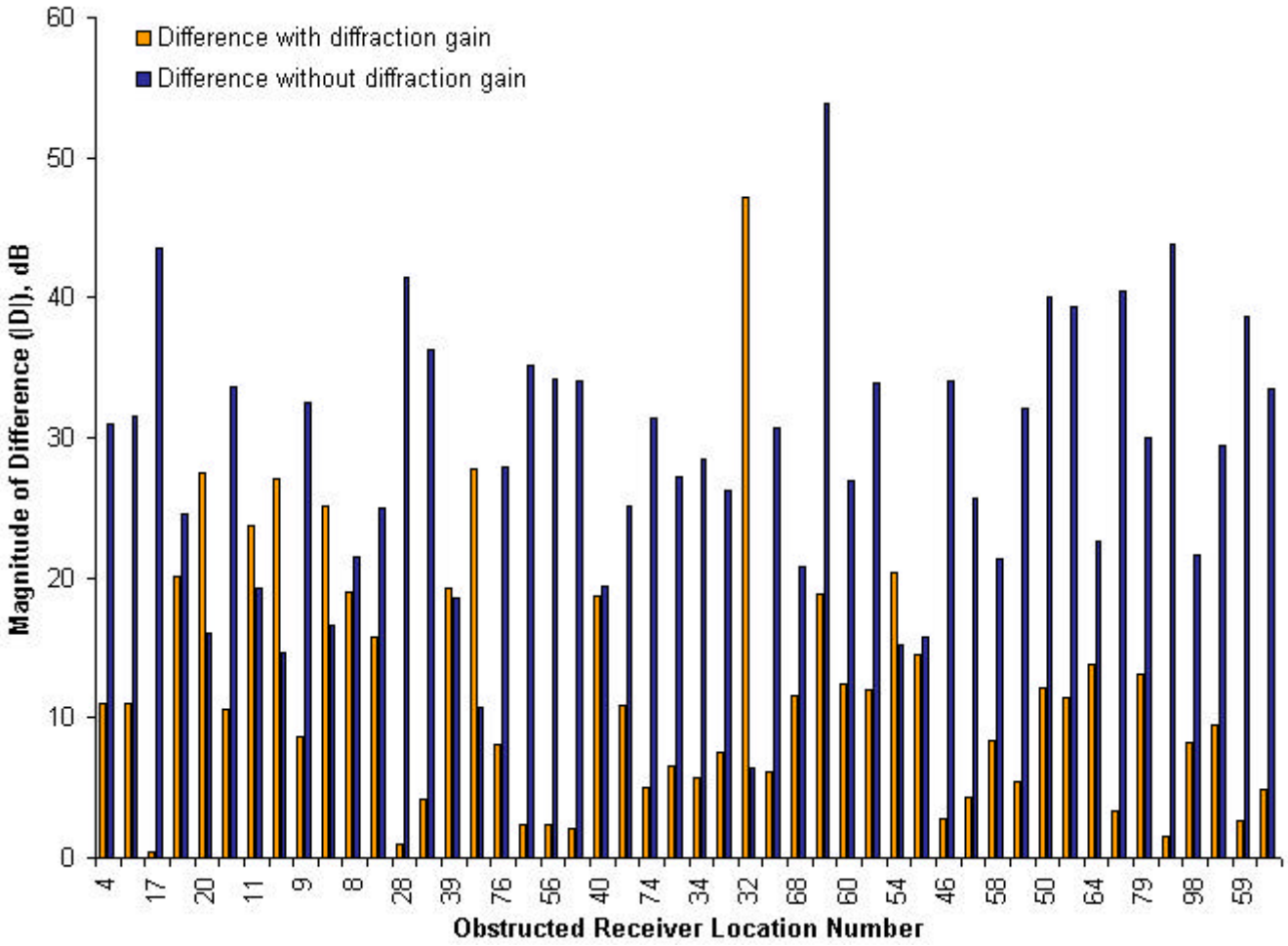

Figure 35: Graph comparing difference in signal strength prediction including diffraction gain to difference excluding diffraction gain (27.525 GHz).

Chapter 6. Discussion

The ability of the program to accurately predict signal strength for frequencies between 900 MHz and 28 GHz is illustrated in Figure 30. The average and standard deviation of the difference between measured and predicted signal strength for any given frequency varies by only 2 dB, indicating that the different techniques implemented in the program do not have an effect on the program's overall ability to predict signal strength. The standard deviation across the frequencies varies by 8-dB. This indicates that the program is independent of frequency. The average difference across the frequencies is positively correlated with frequency. Therefore, as frequency increases, so does average difference.

The higher frequencies (24.12 and 27.525 GHz) are underestimated, and the lower frequencies (902 MHz and 2.4 GHz) are overestimated. The higher frequencies are considered LOS due to their short wavelength; therefore the signal loss during propagation is primarily due to path loss. The lower frequencies have a longer wavelength and are more sensitive to losses due to diffraction and multipath reflection, effects that are not as easily modeled.

There are a variety of errors that are inherent in both the data sets and the program that could contribute to the departure of the results from the ideal average difference (0 dB). First, the DEM base map is a model of the earth's surface, and contains its own inaccuracies. 90% of the DEM base map has a vertical error up to seven meters, 10% has an error up to 15 meters, and the map has a horizontal error up to 15 meters (USGS, 2001). Additionally, building heights were included in the DEM, but only as a constant for each building footprint. Variations in the elevation of the roof of buildings occur due to the presence of physical plant facilities, air-conditioning units or external research buildings and are not represented in the DEM base map. Finally, the resolution of the base map (30 meters) introduces a certain amount of error. At this resolution, "an array of points will not encompass more than 49 contiguous elevations wherein the relative integrity is not in error by more than 21 meters" (USGS, 2001). Rose (2001) determined that resolution did not have much impact on LOS prediction; however, an elevation range of 21 meters could have a dramatic impact signal strength prediction.

The GPS device used to determine the location of the tower and receiver also introduces some inaccuracy to the results. The average error for the coordinates reported in Appendix C is 16.4 feet, or 5.0 meters. Comparing the plotted locations on the 1-foot contour map to the field

notes reduced this error. However, the remaining inaccuracy still has the potential to generate erroneous predictions in signal strength. The erroneous signal strength values can originate both from the prediction of LOS pathways and from diffraction gain calculations.

Predicting LOS pathways is the foundation upon which any field strength model is built. Therefore, it is crucial that an algorithm predict LOS pathways very accurately. Overall, the program predicts LOS pathways with an accuracy that is equivalent to or better than the accuracy reported for ArcView's viewshed function (84%; Dodd, 2001) with the exception of the 24.12 GHz frequency data set (Table 4). The entire 24.12 GHz data set is obstructed, yet a high number of receiver locations are predicted as LOS. It is possible that some of the above mentioned inherent inaccuracies of the GPS device and DEM base map are responsible for the low degree of accuracy for this data set.

One possible explanation for the relatively low accuracy in LOS prediction for the 24.12 GHz data set is that buildings obstructed all of the receiver locations. It was hypothesized that LOS prediction in urban environments will be less accurate than prediction in rural environments, therefore this could account for the low degree of accuracy for this data set. In order to test this theory, the data for all of the frequencies were separated into groups based on the nature of the pathway. If the wave must propagate over at least one building (obstructed or not), then that receiver location is considered urban. If no buildings are within the pathway, the receiver location is considered rural. An entirely urban area is considered less accurate due to the lack of accurate models of the earth's surface, which contain building elevation information. The accuracy of the grouped data points was calculated, and the results are reported in Table 7. Even though urban points are less accurate than rural ones, the overall accuracy of the other data sets still greatly exceeds the accuracy of the 24.12 GHz data set. Therefore, the presence of an urban environment does not accurately correlate to the lack of accuracy for this data set. This result is similar to one found by Rose (2001). He found that DEM resolution did not effect LOS prediction ability either when the data points were combined or grouped into urban and rural environments.

Table 7: Percent accuracy for LOS prediction in urban environments.

Data Set	Number of Urban Points	No Fresnel No Interpolation	Yes Fresnel No Interpolation	No Fresnel Yes Interpolation	Yes Fresnel Yes Interpolation
902 MHz	63	81.0%	82.5%	81.0%	81.0%
2.4 GHz	27	81.4%	81.4%	77.7%	81.4%
24.12 GHz	33	69.7%	69.7%	66.7%	66.7%
27.525 GHz	62	80.7%	80.7%	80.7%	80.7%

The Fresnel zones were incorporated to improve the prediction of obstructed pathways and diffraction gain. However, this technique does not significantly improve the accuracy of the program (Figure 30). Closer examination reveals that the cause is related to the wavelengths associated with each frequency and to the overall topography of the environment. The wavelengths that correspond to each frequency used in this study are listed in Table 8. For each receiver, the point of minimum clearance along the path was determined, and an average minimum clearance for each data set was calculated. The average Fresnel zone radius was also calculated at each point of minimum clearance (Table 8). The wavelengths for the higher frequencies are small enough that the Fresnel zones do not approach the obstructions along the path. There is a higher chance of interference at the lower frequencies indicated by the similar averages between minimum clearance and Fresnel zone radius. In addition, the average difference between the height of the transmitting tower and the height of the receiver is 37.5 meters, providing adequate natural clearance along each pathway. Therefore, the topography of the study area, small wavelengths and location of the transmitter and receivers, naturally provides adequate Fresnel zone clearance. In other environments, where there is not so much difference in topography, Fresnel zone clearance might have more impact.

Table 8: Wavelength of each frequency and corresponding average minimum clearance and Fresnel zone radius.

Frequency of Transmitted Signal	Wavelength of Transmitted Signal	Average Minimum Clearance	Average Fresnel Zone Radius
902 MHz	0.33 meters	3.69 meters	3.59 meters
2.4 GHz	0.12 meters	2.46 meters	1.65 meters
24.12 GHz	0.01 meters	4.56 meters	0.68 meters
27.525 GHz	0.01 meters	3.69 meters	0.65 meters

The impact of the interpolation technique is also a function of the topography of the study area as well as the fact that interpolation procedures average elevations. The method of interpolation chosen for this research averages the elevation data, and in urban environments, this could produce topographic profiles that reflect reality less than the original discrete cellular DEM model. In built-up environments the topography changes are often dramatic and discrete; therefore, the averaged model created by the interpolation procedure has the potential of introducing more errors than it eliminates.

The 24.12 GHz data set is used as a good example of interpolation error because that data set exhibited the largest decrease in accuracy due to interpolation. Receiver location 24 of this data set is originally an obstructed pathway; however, interpolation causes the pathway to become LOS. The reason this occurs is illustrated in Figure 36. In this figure, the transmitting tower (elevation 666.07 meters) is at 0 meters and the receiver is at 413.0 meters (elevation 629.7 meters). The black line is the clear line-of-sight path from the tower to the receiver. The red line is the topographic profile of the Bresenham, or original, cellular elevations. They clearly define the profile of the buildings over which the wave is propagating. The blue line is the interpolated path. Due to the nature of interpolating over discrete boundaries, the blue interpolated line is less smooth than the original Bresenham line. In this instance, more detail has been generated, but with less accuracy. Looking closer at the point of obstruction in Figure 37, it is apparent that, for this example, the LOS is actually obstructed, and calculations performed using the interpolated line would produce erroneous predictions of signal strength.

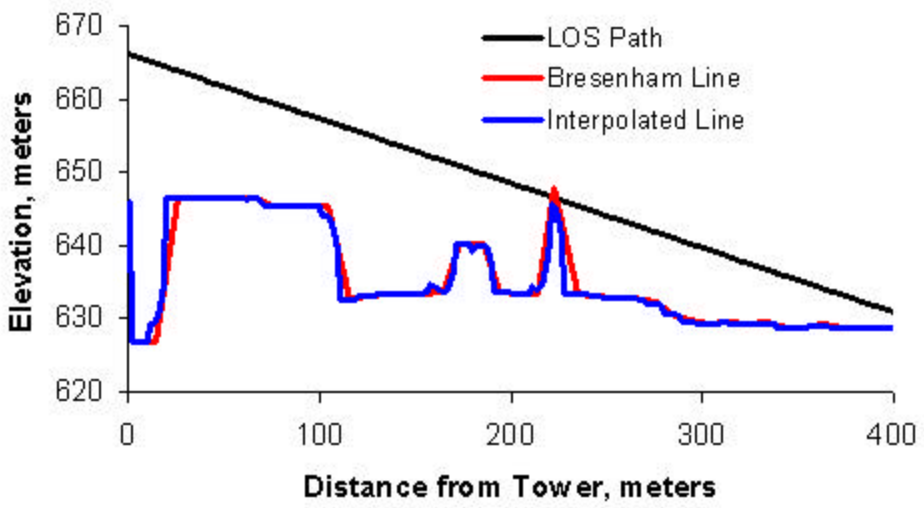

Figure 36: Graph illustrating the topographic profile of the LOS path, Bresenham line and interpolated line for receiver number 24 (2.4 GHz).

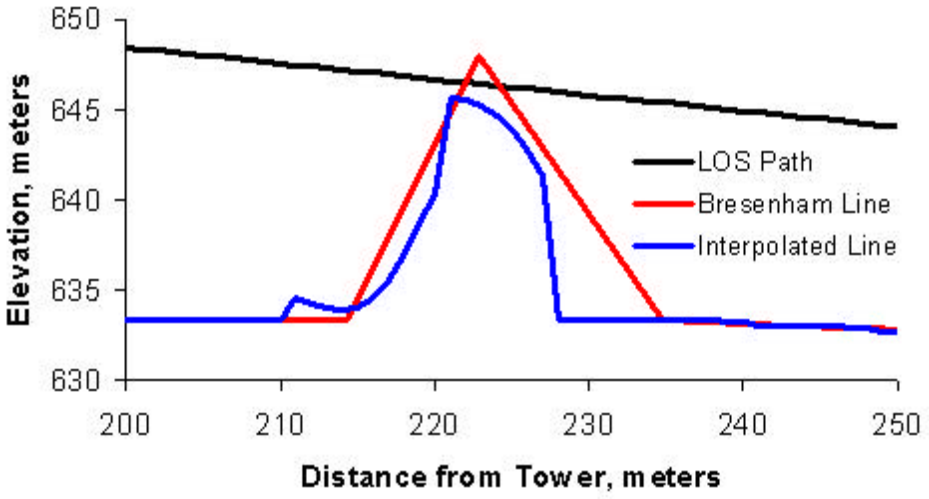

Figure 37: Graph highlighting the obstruction for receiver number 24 (2.4 GHz).

Path loss is another stage of the program that could be improved to produce more accurate signal strength predictions. Actual path loss was calculated for predicted LOS paths using the following equation.

$$\text{Actual Path Loss, dB} = P_{tx} + G_{tx} + G_{rx} - P_{rx} \quad (16)$$

P_{tx} = Transmitter Power, dBm

G_{tx} = Transmitter Gain, dB

G_{rx} = Receiver Gain, dB

P_{rx} = Measured Received Power, dBm

Actual path loss as a function of path length is illustrated in Figures 38 - 41. The figures illustrate that the equation to predict path loss (Equation 8) underestimates the actual path loss incurred by the signal as it propagates from transmitter to receiver. The excess path loss observed in the predicted signal strength is a function of propagation in a non-ideal environment. Equation 8 predicts path loss in an ideal environment (i.e. space). It is derived from the following equation for path loss.

$$\text{Path Loss, dB} = (4 * \pi * D / \lambda)^2 \quad (17)$$

In this equation, the exponent of two indicates that path loss is being predicted for ideal environments. However, when linear regression lines are calculated for the actual path loss values, the resulting slopes indicate that the actual value does not equal two (Table 9). Furthermore, the linear regression lines approach ideal path loss as frequency increases (except for the 24.12 GHz data set) indicating again that the higher frequencies are LOS frequencies and are not as sensitive to multipath reflection and diffraction as the lower frequencies. The 24.12 GHz data set is not unusual or incorrect. The field notes of this data set indicated that all of the receiver locations were obstructed. However, the program predicted that over 65% of them were LOS. These incorrectly predicted LOS pathways were used to calculate the exponent that predicts the excess path loss. A value greater than four provides further evidence that the pathways were truly obstructed and incorrectly predicted as LOS. Obstructed pathways incur greater path loss and exhibit steeper slopes than LOS pathways.

Table 9: Linear regression equations for actual path loss.

Data Set (by Frequency)	Equation of Regression Line for LOS Path Loss
902 MHz	Y = 1.88X + 90.90
2.4 GHz	Y = 2.72X + 89.84
24.12 GHz	Y = 4.06X + 110.77
27.525 GHz	Y = 2.17X + 105.68

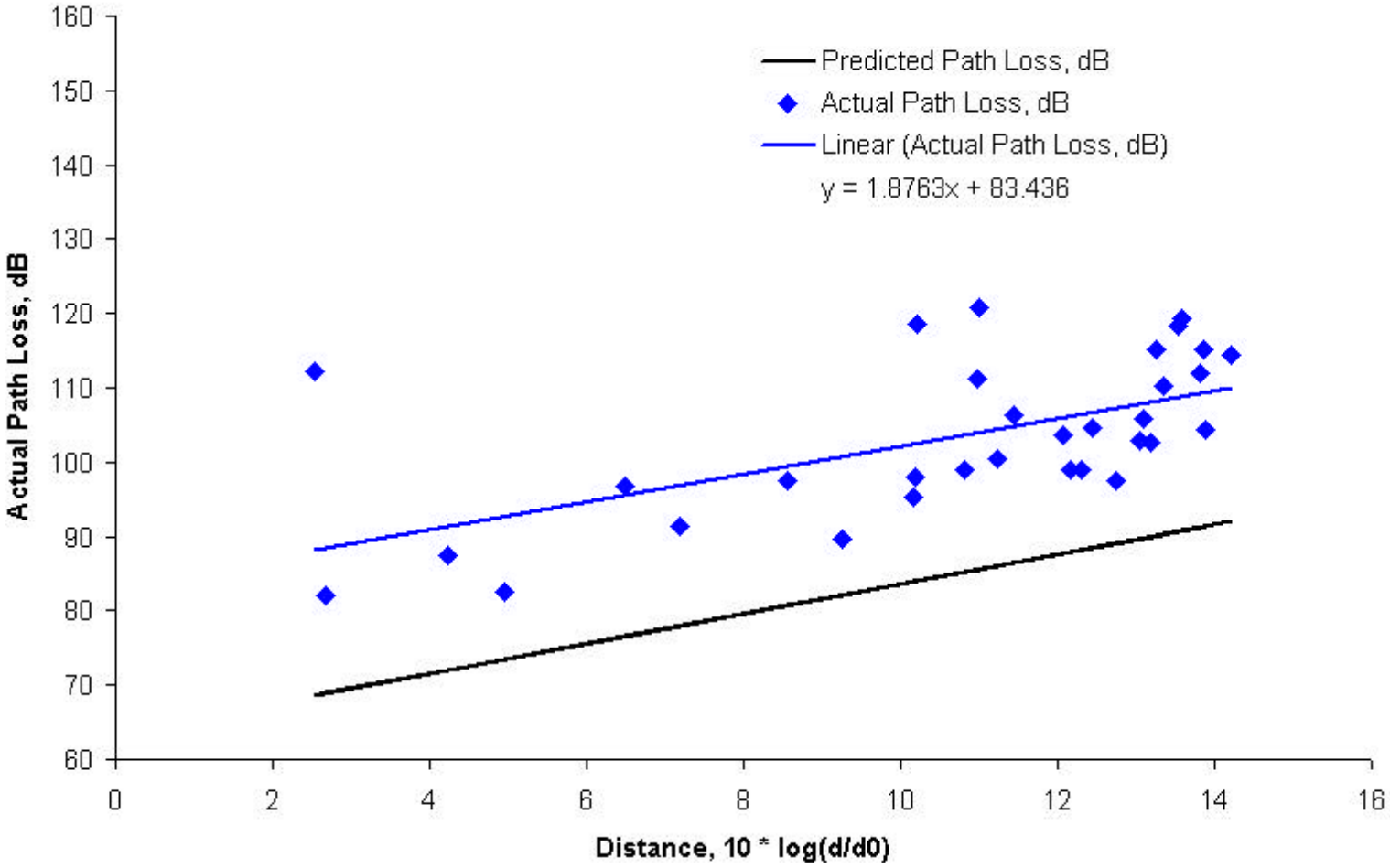

Figure 38: Actual path loss as a function of distance for 902 MHz.

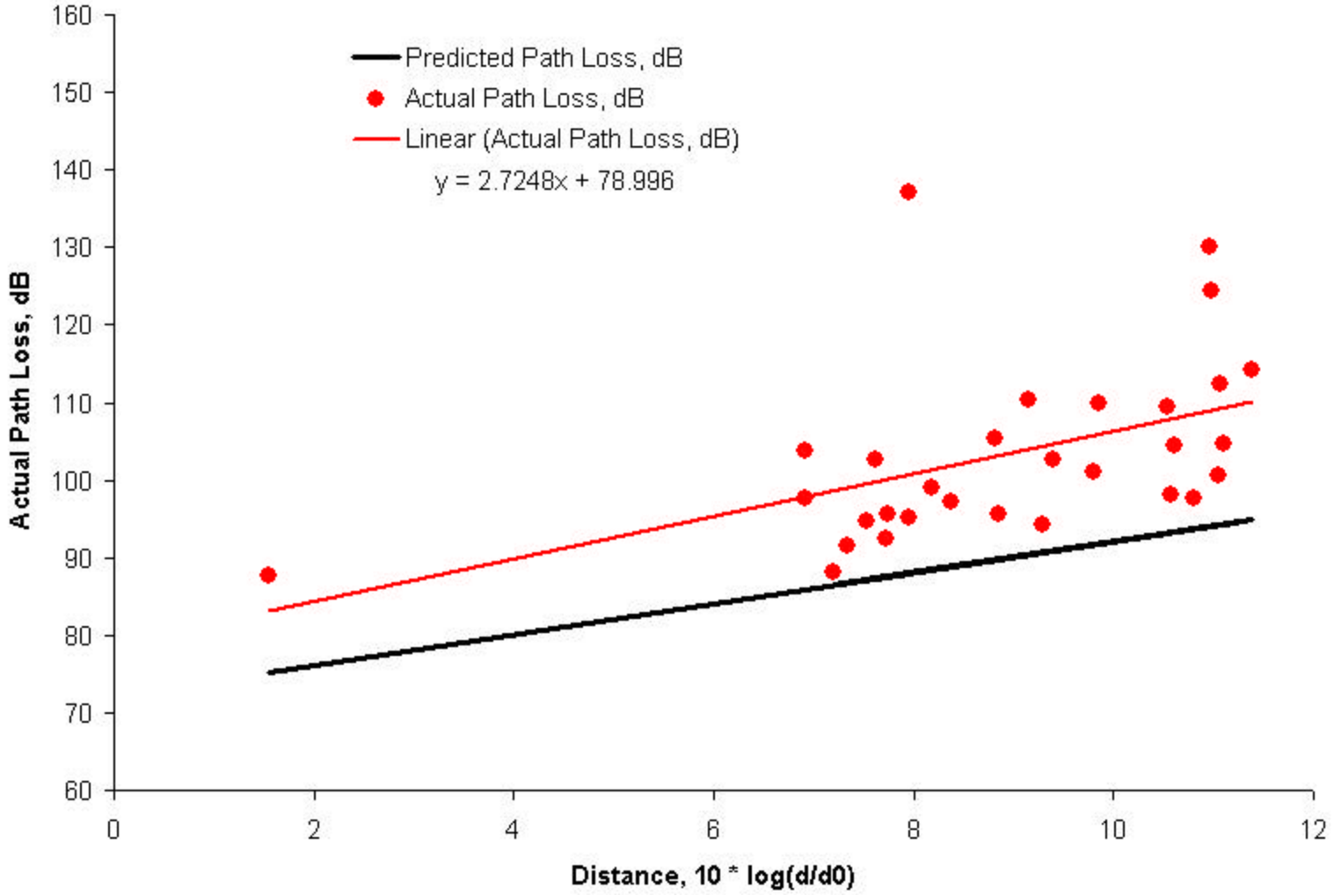

Figure 39: Actual path loss as a function of distance for 2.4 GHz.

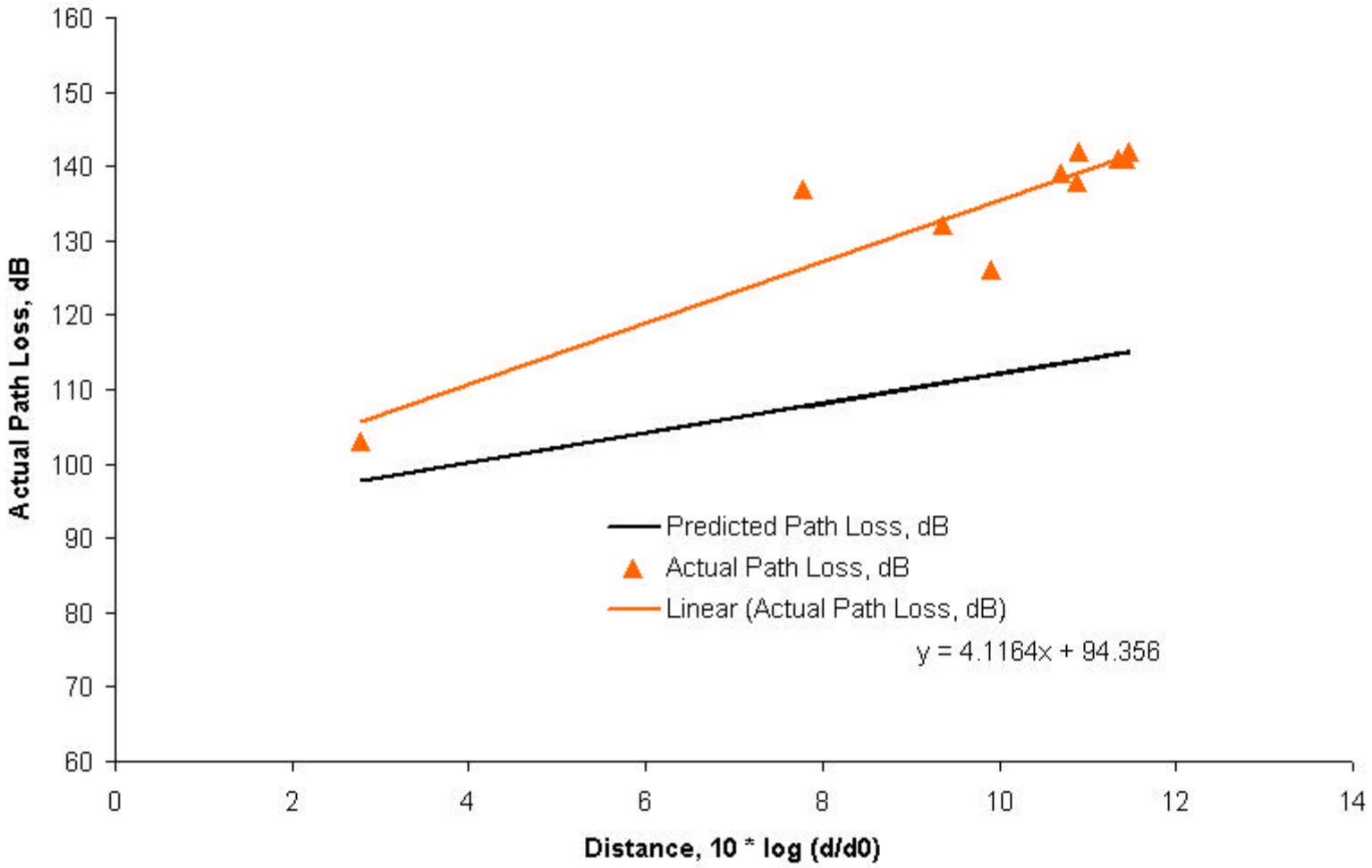

Figure 40: Actual path loss as a function of distance for 24.12 GHz.

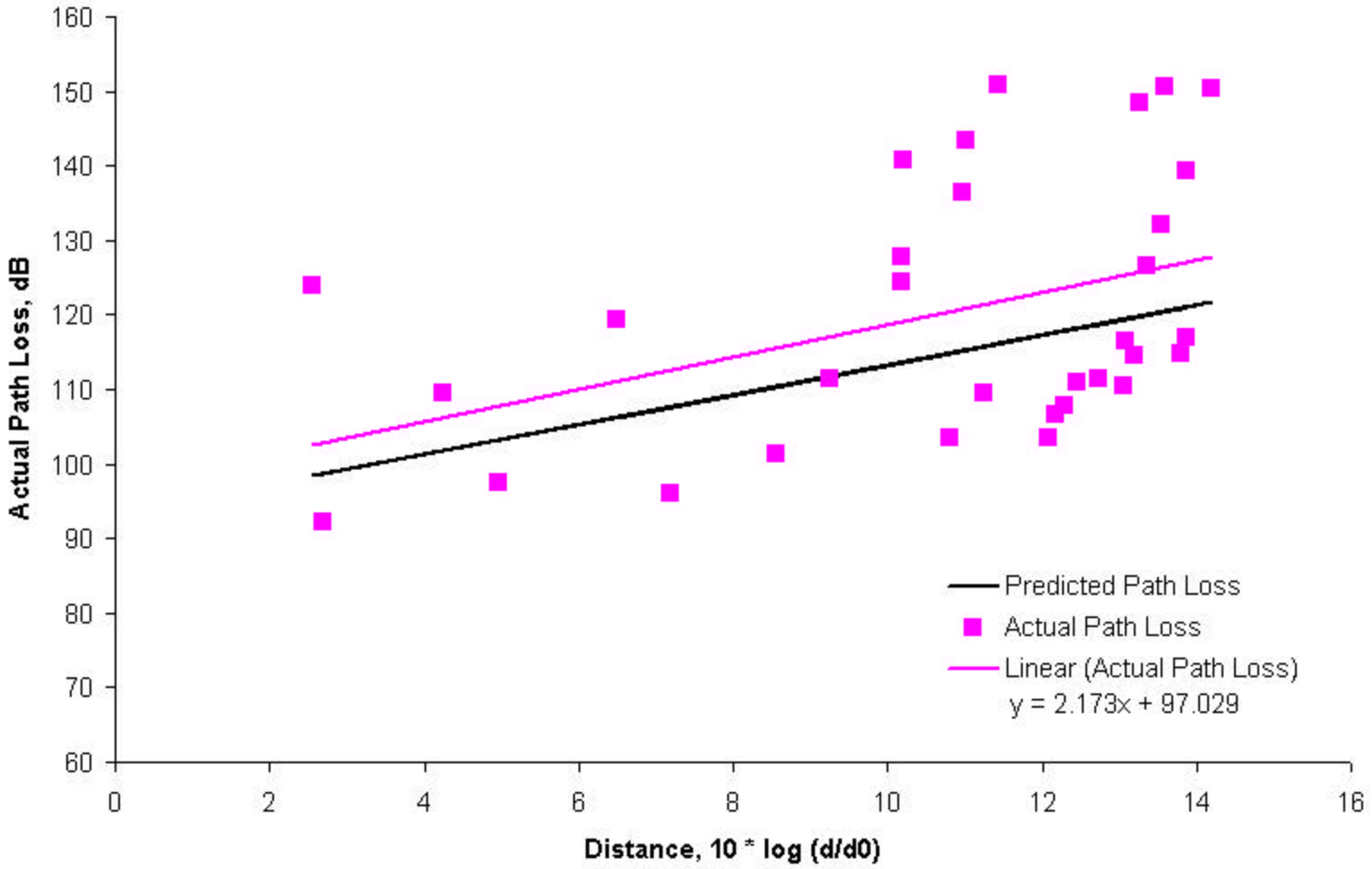

Figure 41: Actual path loss as a function of distance for 27.525 GHz.

Chapter 7. Conclusion

Various techniques have been examined to predict received signal strength for frequencies between 900 MHz and 28 GHz. The different techniques implemented in the program do not have an effect on the program's overall ability to predict signal strength. However, it is not adequate to simply use LOS path loss as an estimate of signal strength for obstructed pathways. In addition, examination of the standard deviation for the data sets indicates that the program is independent of frequency. The average difference across the frequencies is positively correlated with frequency, indicating that the program predicts signal strength better for higher frequencies, whose smaller wavelengths are less sensitive to diffraction loss and multipath interference. This program can be used to obtain estimates of received signal strength for the frequency range used in this study.

Adding techniques such as Fresnel zones and interpolation will not necessarily improve predictions of received signal strength. Oftentimes, these techniques introduce more detail, and are more computationally intensive, but they do not increase accuracy. However, it is necessary to include methods that accurately calculate diffraction gain and path loss. The exclusion of accurate estimates of diffraction gain and path dramatically increase the magnitude of error associated with signal strength prediction.

There are two additional techniques that could be implemented in the program to increase the accuracy of diffraction gain prediction. First, vegetation could be included. This model does not incorporate vegetation into the program; however, experiments have shown that vegetation can play a key role in signal attenuation, especially at high frequencies. Additional research should also consider ray-tracing techniques as an

enhancement to the existing program. Ray tracing techniques incorporate a more detailed model of the earth's surface and would accommodate for multipath reflection. The effect of multipath reflection on received power is illustrated in Figure 42. Certain reflected waves can arrive at the receiver out of phase with the primary wave. This phase shift can cause both constructive and destructive interference. Ray tracing models have been designed to predict the existence of such waves and calculate their effect on received power. In summary, whereas this model effectively predicts received signal strength, further refinements to include more detailed descriptions of the terrain and more accurate modeling of wave propagation should produce more accurate predictions of received signal strength.

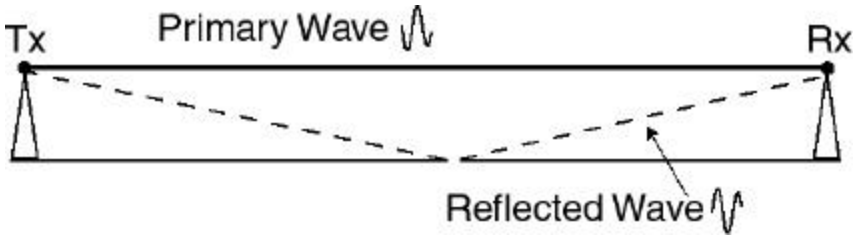

Figure 42: Schematic diagram of 2-ray model illustrating how certain reflected waves can have an arrival time that places the wave out of phase with the reflected wave. This causes destructive interference with the received signal. In this example, the wave arrives 180 degrees out of phase, completely destroying the transmitted signal. A similar situation can occur for any degree of phase shifting causing either constructive or destructive interference.

Bibliography

Bachynski, M. (1963) Scale-model investigations of electromagnetic wave propagation over natural obstacles. RCA Review, March, pp 135-144.

Bi, Q., Zysman, G. and Menkes, H. (2001) Wireless mobile communications at the start of the 21st century. IEEE Communications Magazine, January 2001, pp 110-116.

Bölcskei, H., Paulraj, A., Hari, K. and Nabar, R. (2001) Fixed broadband wireless access: State of the art, challenges and future directions. IEEE Communications Magazine, January 2001, pp 100-107.

Bresenham, J. (1965) Algorithm for computer control of a digital plotter. IBM Systems Journal, v. 4, n. 1 pp 25-30.

Bullington, K. (1947) Radio propagation at frequencies above 30 megacycles. Proceedings of the Institute of Radio Engineers, v. 35, pp 1122-1136.

Deygout, J. (1966) Multiple knife-edge diffraction of microwaves. IEEE Transactions on Antennas and Propagation, v. AP14, n. 4, pp480-489.

Dodd, M. (2001) The Validity of Using a Geographic Information System'[s Viewshed Function as a Predictor for the Reception of Line-of-Sight Radio Waves. Thesis, Virginia Polytechnic Institute and State University.

Epstein, J. and Peterson, D. (1953) An experimental study of wave propagation at 840 MC. Proceedings of the Institute of Radio Engineers, v. 41, n. 5, pp 595-611.

Erricolo, D. and Uslenghi, P. (2001) Two-dimensional simulator for propagation in urban environments. *In publication.*

Furutsu, K. (1963) On the theory of radio wave propagation over inhomogeneous earth. Journal of Research of the National Bureau of Standards –D. Radio Propagation, v. 67d, pp 39-62.

Furutsu, K. (1957a) Wave propagation over an irregular terrain, Part I. Journal of Radio Research (Japan), v. 4, pp 135-153.

Furutsu, K. (1957b) Wave propagation over an irregular terrain, Part II. Journal of Radio Research (Japan), v. 4, pp 349-393.

Furutsu, K. (1959) Wave propagation over an irregular terrain, Part III. Journal of Radio Research (Japan), v. 5, pp 71-102.

Ikegami, F., Takeuchi, T. and Yoshida, S. (1991) Theoretical prediction of mean field strength for urban mobile radio. IEEE Transactions on Antennas and Propagation, v. 39, n. 3, pp 299-302.

Krzanowski, R. and Raper, J. (1999) Hybrid genetic algorithm for transmitter location in wireless networks. Computers, Environment and Urban Systems, v. 23, pp 359-382.

Lee, W. (1985) Mobile Communications Engineering. McGraw-Hill, Inc., New York.

MacDonald, V. (1979) The cellular concept. The Bell Systems Technical Journal, v. 58, n. 1, pp 15-43.

Millington, G., Hewitt, R. and Immirzi, F. (1962) Double knife-edge diffraction in field-strength predictions. The Proceedings of the Institution of Electrical Engineers, v. 109c, pp 419-429.

Papazian, P., Jones, D. and Espeland, R. (1992) Wideband Propagation Measurements at 30.3 GHz through a Pecan Orchard in Texas. NTIA Report 92-287, September, 1992.

Rappaport, T. (1996) Wireless Communications, Principles and Practices. Prentice Hall PTR, Upper Saddle River, New Jersey.

Rose, S. (2001) The Effect of Digital Elevation Model Resolution on Wave Propagation Predictions at 24 GHz. Thesis, Virginia Polytechnic Institute and State University.

Sandrasegaran, K. and Prag, K. (1999) Planning point-to-multipoint radio access networks using expert systems. Expert Systems with Applications, v. 17, pp 145-166.

Schelleng, J., Burrows, C. and Ferrell, E. (1933) Ultra-short-wave propagation. Proceedings of the IRE, v. 21, March, pp 427-463.

Schiff, A., Tang, A., Wong, L. and Cusa, L. (1998) The Loma Prieta, California, earthquake of October 17, 1989: Performance of the built environment. U.S. Geological Survey Professional Paper, 1552-A.

Schwering, Violette and Espeland, R. (1988) Millimeter-wave propagation in vegetation: experiments and theory. IEEE Transactions in Geoscience and Remote Sensing, v. 26, n. 3, pp 355-367.

Van Aken, J. and Killebrew, C., Jr. (1988) Better bit-mapped lines. Byte, March, 1988, pp 249-252.

Vogler, L. (1982) An attenuation function for multiple knife-edge diffraction. Radio Science, v. 17, n. 6, pp 1541-1546.

Zhang, W. and Lähteenmäki, J. (1999) A practical aspect of over-rooftop mutiple-building forward diffraction from a low source. IEEE Transactions on Electromagnetic Compatibility, v. 41, n. 2, pp 115-118.

Appendix A: Field Data

A.1 Data from Dodd (2001) compiled for this research.

Receiver Location Number	X Coordinate (ft)	Y Coordinate (ft)	LOS Path	Obstruction	Received Signal Strength for 902 MHz Transmitting Frequency (dBm)	Received Signal Strength for 27.525 GHz Transmitting Frequency (dBm)
1	10922765	3612895	Yes		-50.80	-26.66
2	10922955	3612804	No	Building	-65.00	-48.50
4	10923162	3612395	No	Building	-76.80	-71.50
5	10923311	3611952	No	Building	-82.50	-77.20
6	10923583	3611728	No	Both	-74.50	-80.00
7	10923736	3611943	Yes		-68.70	-38.60
8	10924002	3612295	No	Building	-85.60	-66.20
9	10923816	3612451	No	Building	-79.10	-75.90
10	10923804	3612466	No	Building	-74.80	-59.90
11	10923575	3612347	No	Building	-73.15	-61.88
12	10923396	3612158	No	Building	-63.58	-56.98
14	10923206	3612125	No	Building	-82.18	-66.91
15	10923091	3612029	No	Both	-82.72	-74.17
16	10922908	3611931	No	Both	-86.75	-70.00
17	10922775	3611828	No	Both	-93.08	-86.94
18	10922964	3611671	No	Both	-79.44	-65.68
19	10923201	3611732	No	Both	-88.90	-72.62
20	10923381	3611841	No	Both	-85.83	-60.45
22	10923654	3612087	Yes		-67.10	-32.74
23	10923808	3612186	No	Both	-72.41	-59.00
24	10923925	3612256	No	Both	-72.69	-69.58
26	10924174	3612018	No	Building	-98.00	-82.39
28	10924031	3612025	No	Both	-95.50	-87.14
30	10924072	3611736	No	Building	-86.60	-57.40
31	10924016	3611693	Yes		-71.90	-32.62
32	10923973	3611600	Yes		-77.31	-40.43
34	10924586	3611806	No	Building	-102.51	-76.36
36	10924709	3611989	No	Building	-95.99	-101.86
37	10924812	3611757	No	Building	-85.78	
38	10924132	3611542	No	Both	-72.78	-40.17
39	10924065	3611390	No	Building	-92.51	-66.25
40	10924047	3611376	No	Building	-81.42	-67.00
41	10923990	3611293	No	Building	-89.11	-83.00
44	10923322	3611099	No	Building	-89.13	-81.18
45	10923564	3610825	No	Building	-83.55	-80.62
46	10923792	3610726	No	Building	-98.70	-83.11
49	10923949	3610409	No	Both	-86.92	-89.54
50	10924049	3610480	No	Both	-100.98	-90.13
51	10924195	3610626	No	Building	-90.13	-90.39
53	10924216	3610936	No	Building	-85.26	-76.36
54	10924392	3611154	No	Building	-77.89	-64.15
55	10924401	3611296	Yes		-73.96	-45.81
56	10924140	3611221	No	Building	-88.85	-82.51

58	10923932	3610264	No	Building	-98.73	-71.77
59	10923816	3610168	No	Building	-98.18	-89.23
60	10923677	3610058	No	Building	-98.67	-77.61
61	10923543	3609944	No	Both	-84.42	-84.41
63	10923213	3609878	No	Building	-82.69	-79.56
64	10923251	3610034	No	Building	-83.22	-73.05
65	10923373	3610162	No	Both	-81.80	-79.65
66	10923549	3610228	No	Both	-83.26	-68.57
67	10923454	3610398	No	Building	-87.51	-79.77
68	10923424	3610660	No	Building	-78.12	-69.72
69	10923905	3610698	No	Building	-92.60	-74.94
70	10923946	3610814	No	Both	-92.05	-92.93
71	10924076	3611077	No	Building	-93.53	-82.66
73	10923987	3611119	No	Building	-83.16	-79.05
74	10924083	3611113	No	Building	-88.31	-79.91
75	10924152	3611104	No	Building	-92.87	-73.79
76	10924230	3611176	No	Building	-80.57	-76.52
77	10924482	3611407	No	Building	-77.42	-64.30
78	10924555	3611289	No	Building	-83.43	-77.70
79	10924613	3611124	No	Both	-91.84	-79.47
83	10922379	3613245	Yes		-80.45	-53.13
84	10922429	3613117	Yes		-50.26	-21.34
85	10922446	3612971	Yes		-55.79	-38.73
87	10922159	3612762	Yes		-59.50	-25.16
88	10921972	3612584	Yes		-65.65	-30.56
89	10921854	3612473	Yes		-57.91	-40.70
90	10921706	3612250	Yes		-66.30	-53.55
94	10920920	3611826	Yes		-67.09	-37.14
95	10920723	3611426	Yes		-71.02	-39.66
96	10920603	3611275	Yes		-78.51	-55.79
97	10920520	3611182	No	Hill	-86.56	-61.26
98	10920240	3611326	No	Hill/ Veg.	-95.84	-71.54
99	10920067	3611421	Yes		-80.10	-44.00
101	10919680	3611993	Yes		-72.58	-46.26
104	10919987	3612493	Yes		-70.85	-43.72
106	10920392	3612212	Yes		-65.63	-40.63
107	10920832	3612053	Yes		-67.07	-35.93
109	10921320	3611737	No	Building	-78.25	-72.41

A.2 Data from Rose (2001) compiled for this research.

Receiver Location Number	X Coordinate (ft)	Y Coordinate (ft)	Obstruction	Received Signal Strength for 24.12 GHz Transmitting Frequency (dBm)
3	10923108.20	3613744.38	Durham Hall	-98.0
10	10923369.42	3613498.22	Price Hall	-92.0
11	10923317.82	3613254.89	Randolph Hall	-89.0
14	10923864.62	3613235.39	Major Williams, Performing Arts Building	-94.0
16	10924077.52	3613752.91	Roof Tops	-94.0
22	10922860.83	3613262.15	Hancock Hall Roof	-58.0
23	10923616.03	3612754.02	Building, Trees	-87.0
24	10923856.12	3612738.96	Building, Trees	-90.0
25	10924032.02	3612520.35	Building, Trees	-93.0
26	10923873.61	3612486.28	Patton Hall, Trees	-97.0
27	10923859.80	3612235.98	Patton Hall	-94.0
31	10923611.15	3612257.95	Building	-84.0
32	10923380.41	3612245.43	Top of Hancock	-81.0
33	10923617.65	3612477.39	Patton Hall	-99.0
34	10923368.22	3612488.72	Building	-87.0
36	10923408.41	3612957.49	Holden Hall	-102.0
37	10923070.07	3613047.30	Randolph Hall, Tree	-84.0
38	10922857.17	3612988.37	Hancock Hall, Randolph Hall	-89.0
39	10923158.22	3613217.51	Randolph Hall	-101.0
40	10922912.04	3612809.26	Randolph Hall, Tree	-84.0
41	10922861.59	3612488.68	Burruss Hall	-100.0
42	10923110.31	3612490.78	Burruss Hall	-101.0
44	10923281.72	3611968.72	Burruss Hall	-101.0
45	10923580.28	3611735.99	Burruss Hall	-96.0
46	10923356.47	3611748.96	Burruss Hall	-104.0
47	10923105.38	3611502.75	Burruss Hall	-97.0
48	10922862.07	3611504.80	Burruss Hall, Williams Hall	-96.0
49	10922606.95	3611755.45	Williams Hall, Tree	-101.0
50	10922848.23	3611755.48	Burruss Hall, Tree	-101.0
51	10923086.29	3611733.95	Burruss Hall	-97.0
52	10922863.70	3611990.26	Burruss Hall	-97.0
53	10922858.01	3612249.44	Burruss Hall	-96.0
54	10922564.65	3612149.94	Pamplin Hall	-100.0

A.3 Data collected for this research.

Receiver Location Number	Longitude	Latitude	Signal Strength (dBm)	Error (ft)	LOS Path	Blockage
1	80.4254	37.2308	-47.66	12.4	Yes	
2	80.4267	37.2300	-63.80	19.4	Yes	
3	80.4275	37.2291	-55.63	11.2	Yes	
4	80.4280	37.2295	-70.42	11.5	Yes	
5	80.4283	37.2298	-54.19	16.7	Yes	
6	80.4285	37.2301	-62.55	11.2	Yes	
7	80.4291	37.2309	-69.95	12.4	Yes	
8	80.4289	37.2314	-61.05	13.6	Yes	
9	80.4299	37.2312	-64.53	21.7	Yes	
10	80.4298	37.2308	-58.17	15.8	Yes	
11	80.4305	37.2308	-64.73	12.9	Yes	
12	80.4309	37.2308	-74.22	13.0	No	Golf Course Hill
13	80.4305	37.2303	-60.70	13.0	Yes	
14	80.4300	37.2298	-57.72	12.8	Yes	
15	80.4295	37.2293	-69.44	13.1	Yes	
16	80.4253	37.2317	-71.18	22.7	No	Whittemore Hall
17	80.4257	37.2315	-69.11	17.6	No	Whittemore Hall
18	80.4251	37.2318	-84.32	22.1	No	Whittemore Hall
19	80.4248	37.2320	-77.79	14.3	No	Whittemore Hall
20	80.4244	37.2324	-85.31	15.6	No	Whittemore Hall
21	80.4254	37.2322	-80.72	15.9	No	Whittemore Hall
22	80.4259	37.2318	-77.74	16.0	No	Whittemore Hall
23	80.4261	37.2319	-72.74	16.0	No	Whittemore Hall
24	80.4258	37.2322	-65.12	16.1	No	Whittemore Hall
25	80.4255	37.2324	-76.23	20.4	No	Whittemore Hall
26	80.4250	37.2328	-75.34	15.9	No	Whittemore Hall
27	80.4253	37.2330	-79.12	15.7	No	Whittemore Hall
28	80.4260	37.2324	-72.95	14.8	No	Whittemore Hall
29	80.4263	37.2320	-78.53	13.8	No	Whittemore Hall
30	80.4265	37.2318	-57.47	17.6	Yes	
31	80.4268	37.2322	-55.06	13.2	Yes	
32	80.4273	37.2319	-59.07	14.2	Yes	
33	80.4276	37.2317	-57.29	13.5	Yes	
34	80.4273	37.2314	-52.32	12.2	Yes	
35	80.4269	37.2316	-51.47	12.1	Yes	
36	80.4267	37.2317	-48.02	13.2	Yes	
37	80.4234	37.2322	-89.56	15.6	No	Whittemore Hall, Durham Hall
38	80.4230	37.2321	-77.60	12.4	No	Whittemore Hall, Durham Hall
39	80.4227	37.2320	-56.37	12.4	Yes	
40	80.4225	37.2318	-54.63	14.9	Yes	
41	80.4223	37.2317	-62.69	15.1	Yes	
42	80.4222	37.2315	-55.67	19.4	Yes	
43	80.4212	37.2304	-101.01	29.0	No	McBryde Hall, Randolph Hall

44	80.4218	37.2302	-84.96	19.4	No	Randolph Hall, Norris Hall
45	80.4222	37.2298	-97.13	16.2	No	Randolph Hall, Norris Hall
46	80.4225	37.2296	-91.86	16.1	No	Randolph Hall, Norris Hall
47	80.4232	37.2291	-63.81	23.2	No	Cowgill Hall
48	80.4243	37.2294	-68.13	29.1	No	Cowgill Hall
49	80.4246	37.2295	-83.90	15.0	No	Cowgill Hall
50	80.4244	37.2296	-75.01	14.8	No	Cowgill Hall
51	80.4244	37.2291	-95.17	28.3	No	GBJ Student Center and Cowgill Hall
52	80.4248	37.2304	-47.05	21.5	Yes	
53	80.4216	37.2292	-95.87	22.9	No	Drillfield, Multiple blockages
54	80.4216	37.2287	-84.27	20.4	No	Drillfield, Multiple blockages
55	80.4215	37.2279	-73.86	13.3	No	Drillfield, Multiple blockages
56	80.4209	37.2273	-72.33	13.0	No	Drillfield, Multiple blockages
57	80.4215	37.2270	-84.38	12.5	No	Drillfield, Multiple blockages
58	80.4225	37.2287	-65.36	16.4	Yes	
59	80.4230	37.2284	-88.31	13.4	No	Drillfield, Multiple blockages
60	80.4234	37.2280	-86.40	19.4	No	Drillfield, Multiple blockages
61	80.4240	37.2276	-99.79	17.4	No	Drillfield, Multiple blockages
62	80.4237	37.2273	-96.65	10.8	No	Drillfield, Multiple blockages
63	80.4231	37.2265	-90.13	24.7	No	Drillfield, Multiple blockages

Appendix B: Model Data

B.1a 902 MHz: single blockage, without Fresnel zones, without interpolation.

Receiver Location Number	Tower Height (m)	Path Length (m)	Receiver Height (m)	D1 (m)	Blockage Height (m)	D2 (m)	Diffraction Gain (dB)	Path Loss (dBm)	Predicted Received Power (dBm)	Measured Received Power (dBm)	Difference (dB)	Actual Path Loss (dBm)
1	667.68	125.38	632.31	--	--	--	0.00	73.52	-41.74	-50.80	-9.06	82.58
2	667.68	178.00	632.31	--	--	--	0.00	76.56	-44.78	-65.00	-20.22	96.78
4	667.68	316.75	625.91	190.05	644.35	126.70	-27.26	81.57	-77.04	-76.80	0.24	--
5	667.68	456.55	621.94	213.06	650.44	243.49	-29.29	84.74	-82.25	-82.50	-0.25	--
6	667.68	557.16	625.60	--	--	--	0.00	86.47	-54.69	-74.50	-19.81	106.28
7	667.68	531.60	624.38	--	--	--	0.00	86.06	-54.28	-68.70	-14.42	100.48
8	667.68	518.61	626.82	270.11	646.79	248.50	-25.64	85.85	-79.70	-85.60	-5.90	--
9	667.68	444.91	627.13	264.83	646.79	180.08	-26.32	84.52	-79.06	-79.10	-0.04	--
10	667.68	439.31	626.21	267.87	646.79	171.44	-26.82	84.41	-79.45	-74.80	4.65	--
11	667.68	407.95	624.08	259.60	646.79	148.34	-28.12	83.76	-80.11	-73.15	6.96	--
12	667.68	416.37	623.16	--	--	--	0.00	83.94	-52.16	-63.58	-11.42	95.36
14	667.68	395.00	622.55	212.69	650.44	182.31	-29.74	83.48	-81.44	-82.18	-0.74	--
15	667.68	407.40	621.94	208.44	644.35	198.96	-27.68	83.75	-79.65	-82.72	-3.07	--
16	667.68	420.04	621.03	--	--	--	0.00	84.02	-52.24	-86.75	-34.51	118.53
17	667.68	444.44	620.12	208.61	645.26	235.82	-28.32	84.51	-81.05	-93.08	-12.03	--
18	667.68	501.11	621.03	--	--	--	0.00	85.55	-53.77	-79.44	-25.67	111.22
19	667.68	503.93	622.55	--	--	--	0.00	85.60	-53.82	-88.90	-35.08	120.68
20	667.68	496.44	622.86	212.76	650.44	283.68	-28.72	85.47	-82.40	-85.83	-3.43	--
22	667.68	482.01	623.77	--	--	--	0.00	85.21	-53.43	-67.10	-13.67	98.88
23	667.68	493.32	624.38	264.71	646.79	228.61	-26.87	85.41	-80.50	-72.41	8.09	--
24	667.68	506.84	626.21	270.31	646.79	236.53	-26.01	85.65	-79.88	-72.69	7.19	--
26	667.68	611.38	624.38	530.63	638.86	80.75	-25.51	87.28	-81.01	-98.00	-16.99	--
28	667.68	576.68	624.38	529.61	638.86	47.08	-27.61	86.77	-82.60	-95.50	-12.90	--
30	667.68	646.93	625.30	534.96	638.86	111.97	-23.73	87.77	-79.72	-86.60	-6.88	--
31	667.68	645.06	625.91	--	--	--	0.00	87.74	-55.96	-71.90	-15.94	103.68
32	667.68	658.21	632.31	554.28	649.22	103.93	-25.90	87.92	-82.03	-77.31	4.72	--
34	667.68	750.24	628.65	548.68	638.86	201.56	-19.75	89.06	-77.02	-102.51	-25.49	--
36	667.68	749.97	628.35	602.09	638.56	147.88	-20.88	89.05	-78.15	-95.99	-17.84	--
37	667.68	814.92	631.39	706.26	641.30	108.66	-20.93	89.77	-78.92	-85.78	-6.86	--
38	667.68	702.97	633.53	--	--	--	0.00	88.49	-56.71	-72.78	-16.07	104.56
39	667.68	725.82	633.83	533.03	649.22	192.80	-22.99	88.77	-79.97	-92.51	-12.54	--
40	667.68	725.89	633.83	544.42	649.22	181.47	-23.16	88.77	-80.15	-81.42	-1.27	--

41	667.68	736.20	634.14	538.41	649.22	197.78	-22.72	88.89	-79.83	-89.11	-9.28	--
44	667.68	698.20	633.22	603.85	662.64	94.35	-31.00	88.43	-87.66	-89.13	-1.47	--
45	667.68	801.68	638.71	734.07	648.61	67.61	-22.75	89.63	-80.60	-83.55	-2.95	--
46	667.68	856.64	642.06	717.19	648.61	139.45	-16.76	90.21	-75.19	-98.70	-23.51	--
49	667.68	964.43	643.28	755.64	648.61	208.79	-14.12	91.24	-73.58	-86.92	-13.34	--
50	667.68	958.40	643.28	744.29	648.61	214.11	-14.07	91.18	-73.47	-100.98	-27.51	--
51	667.68	941.05	642.98	793.02	656.23	148.03	-22.24	91.02	-81.48	-90.13	-8.65	--
53	667.68	864.88	637.79	547.39	649.22	317.49	-19.32	90.29	-77.83	-85.26	-7.43	--
54	667.68	844.35	636.27	609.81	649.22	234.54	-20.71	90.08	-79.01	-77.89	1.12	--
55	667.68	813.49	660.65	--	--	--	0.00	89.76	-57.98	-73.96	-15.98	105.74
56	667.68	780.70	634.75	543.09	649.22	237.60	-21.78	89.40	-79.40	-88.85	-9.45	--
58	667.68	1002.58	641.45	724.63	648.61	277.94	-15.39	91.57	-75.18	-98.73	-23.55	--
59	667.68	1016.16	640.23	890.35	660.50	125.81	-26.46	91.69	-86.38	-98.18	-11.80	--
60	667.68	1033.42	638.40	602.83	662.64	430.59	-24.44	91.84	-84.50	-98.67	-14.17	--
61	667.68	1054.76	636.57	922.91	651.36	131.84	-23.52	92.01	-83.76	-84.42	-0.66	--
63	667.68	1052.07	636.27	--	--	--	0.00	91.99	-60.21	-82.69	-22.48	114.47
64	667.68	1007.46	635.36	776.39	649.83	231.07	-21.46	91.62	-81.30	-83.22	-1.92	--
65	667.68	977.35	636.27	856.34	651.36	121.01	-24.07	91.35	-83.64	-81.80	1.84	--
66	667.68	972.20	637.79	--	--	--	0.00	91.31	-59.53	-83.26	-23.73	115.04
67	667.68	914.25	637.18	--	--	--	0.00	90.77	-58.99	-87.51	-28.52	119.29
68	667.68	835.14	637.49	578.91	646.79	256.24	-17.95	89.99	-76.16	-78.12	-1.96	--
69	667.68	879.28	642.67	717.57	648.61	161.71	-15.55	90.43	-74.21	-92.60	-18.39	--
70	667.68	853.70	642.67	812.56	656.23	41.14	-27.47	90.18	-85.87	-92.05	-6.18	--
71	667.68	805.38	635.05	544.18	649.22	261.21	-21.31	89.67	-79.20	-93.53	-14.33	--
73	667.68	779.85	634.75	566.20	649.22	213.66	-22.06	89.39	-79.67	-83.16	-3.49	--
74	667.68	797.47	634.75	546.21	649.22	251.26	-21.61	89.59	-79.41	-88.31	-8.90	--
75	667.68	811.71	635.05	544.85	649.22	266.86	-21.25	89.74	-79.21	-92.87	-13.66	--
76	667.68	808.19	635.05	535.00	649.22	273.19	-21.21	89.70	-79.13	-80.57	-1.44	--
77	667.68	805.96	635.36	654.84	641.30	151.12	-15.81	89.68	-73.71	-77.42	-3.71	--
78	667.68	847.19	635.66	--	--	--	0.00	90.11	-58.33	-83.43	-25.10	115.21
79	667.68	895.79	637.79	809.90	658.67	85.90	-28.24	90.60	-87.06	-91.84	-4.78	--
83	667.68	71.85	624.38	--	--	--	0.00	68.68	-36.90	-80.45	-43.55	112.23
84	667.68	74.22	627.43	--	--	--	0.00	68.96	-37.18	-50.26	-13.08	82.04
85	667.68	106.20	627.74	--	--	--	0.00	72.07	-40.29	-55.79	-15.50	87.57
87	667.68	209.18	623.47	--	--	--	0.00	77.96	-46.18	-59.50	-13.32	91.28
88	667.68	287.64	622.86	--	--	--	0.00	80.73	-48.95	-65.65	-16.70	97.43
89	667.68	336.92	620.73	--	--	--	0.00	82.10	-50.32	-57.91	-7.59	89.69
90	667.68	417.55	619.51	--	--	--	0.00	83.97	-52.19	-66.30	-14.11	98.08
94	667.68	679.52	628.65	--	--	--	0.00	88.20	-56.42	-67.09	-10.67	98.87
95	667.68	806.24	625.60	--	--	--	0.00	89.68	-57.90	-71.02	-13.12	102.80

96	667.68	864.60	622.55	--	--	--	0.00	90.29	-58.51	-78.51	-20.00	110.29
97	667.68	902.53	619.81	--	--	--	0.00	90.66	-58.88	-86.56	-27.68	118.34
98	667.68	936.26	620.12	830.93	625.14	105.33	-15.59	90.98	-74.79	-95.84	-21.05	--
99	667.68	960.22	621.94	--	--	--	0.00	91.20	-59.42	-80.10	-20.68	111.88
101	667.68	975.77	633.53	--	--	--	0.00	91.34	-59.56	-72.58	-13.02	104.36
104	667.68	835.18	632.31	--	--	--	0.00	89.99	-58.21	-70.85	-12.64	102.63
106	667.68	750.64	628.65	--	--	--	0.00	89.06	-57.28	-65.63	-8.35	97.41
107	667.68	658.58	626.82	--	--	--	0.00	87.92	-56.14	-67.07	-10.93	98.85
109	667.68	612.82	618.59	553.90	624.54	58.93	-19.42	87.30	-74.94	-78.25	-3.31	--

B.1b 2.4 GHz: single blockage, without Fresnel zones and without interpolation.

Receiver Location Number	Tower Height (m)	Path Length (m)	Receiver Height (m)	D1 (m)	Blockage Height (m)	D2 (m)	Diffraction Gain (dB)	Path Loss (dBm)	Predicted Received Power (dBm)	Measured Received Power (dBm)	Difference (dB)	Actual Path Loss (dBm)
1	667.31	57.15	623.32	--	--	--	0.00	75.19	-37.19	-47.66	-10.47	87.66
2	667.31	196.74	623.62	--	--	--	0.00	85.93	-47.93	-63.80	-15.87	103.80
3	667.31	307.10	622.71	--	--	--	0.00	89.80	-51.80	-55.63	-3.83	95.63
4	667.31	329.40	626.06	--	--	--	0.00	90.41	-52.41	-70.42	-18.01	110.42
5	667.31	339.46	628.80	--	--	--	0.00	90.67	-52.67	-54.19	-1.52	94.19
6	667.31	348.59	631.24	--	--	--	0.00	90.90	-52.90	-62.55	-9.65	102.55
7	667.31	386.19	636.42	--	--	--	0.00	91.79	-53.79	-69.95	-16.16	109.95
8	667.31	381.52	637.34	--	--	--	0.00	91.68	-53.68	-61.05	-7.37	101.05
9	667.31	460.90	638.56	--	--	--	0.00	93.32	-55.32	-64.53	-9.21	104.53
10	667.31	456.55	636.42	--	--	--	0.00	93.24	-55.24	-58.17	-2.93	98.17
11	667.31	514.73	635.20	--	--	--	0.00	94.28	-56.28	-64.73	-8.45	104.73
12	667.31	550.23	633.07	--	--	--	0.00	94.86	-56.86	-74.22	-17.36	114.22
13	667.31	510.00	632.76	--	--	--	0.00	94.20	-56.20	-60.70	-4.50	100.70
14	667.31	481.50	627.28	--	--	--	0.00	93.70	-55.70	-57.72	-2.02	97.72
15	667.31	453.34	627.28	--	--	--	0.00	93.18	-55.18	-69.44	-14.26	109.44
16	667.31	118.42	624.54	9.11	665.07	109.31	-47.91	81.52	-91.43	-71.18	20.25	--
17	667.31	124.37	624.54	11.31	665.07	113.06	-47.04	81.95	-90.98	-69.11	21.87	--
18	667.31	128.78	624.84	8.59	665.07	120.19	-48.05	82.25	-92.30	-84.32	7.98	--
19	667.31	145.90	624.54	8.58	665.07	137.32	-48.09	83.33	-93.42	-77.79	15.63	--
20	667.31	179.62	623.93	17.11	665.07	162.52	-45.39	85.14	-92.53	-85.31	7.22	--
21	667.31	169.65	624.23	8.93	665.07	160.72	-47.95	84.64	-94.59	-80.72	13.87	--
22	667.31	155.54	625.14	11.11	665.07	144.43	-46.89	83.89	-92.78	-77.74	15.04	--
23	667.31	179.20	625.75	11.20	665.07	168.00	-46.68	85.12	-93.80	-72.74	21.06	--
24	667.31	189.35	624.54	9.97	665.07	179.38	-47.41	85.60	-95.00	-65.12	29.88	--
25	667.31	199.34	623.93	18.12	665.07	181.22	-45.12	86.04	-93.16	-76.23	16.93	--

26	667.31	229.97	623.93	17.69	665.07	212.28	-45.16	87.29	-94.44	-75.34	19.10	--
27	667.31	257.48	624.84	17.76	665.07	239.72	-44.91	88.27	-95.18	-79.12	16.06	--
28	667.31	217.58	624.54	19.78	665.07	197.80	-44.61	86.80	-93.41	-72.95	20.46	--
29	667.31	200.02	627.28	11.77	665.07	188.25	-46.11	86.07	-94.18	-78.53	15.65	--
30	667.31	196.25	627.28	--	--	--	0.00	85.91	-47.91	-57.74	-9.83	97.74
31	667.31	249.64	630.63	--	--	--	0.00	88.00	-50.00	-55.06	-5.06	95.06
32	667.31	263.24	631.85	--	--	--	0.00	88.46	-50.46	-59.07	-8.61	99.07
33	667.31	275.16	631.85	--	--	--	0.00	88.84	-50.84	-57.29	-6.45	97.29
34	667.31	237.22	629.11	--	--	--	0.00	87.56	-49.56	-52.32	-2.76	92.32
35	667.31	216.60	628.80	--	--	--	0.00	86.77	-48.77	-51.47	-2.70	91.47
36	667.31	209.74	628.50	--	--	--	0.00	86.49	-48.49	-48.02	0.47	88.02
37	667.31	207.07	627.89	21.80	665.07	185.27	-43.51	86.37	-91.88	-89.56	2.32	--
38	667.31	214.18	630.63	59.49	665.07	154.68	-39.41	86.67	-88.08	-77.60	10.48	--
39	667.31	221.94	632.16	63.41	665.07	158.53	-38.79	86.98	-87.77	-56.37	31.40	--
40	667.31	226.62	633.37	--	--	--	0.00	87.16	-49.16	-54.63	-5.47	94.63
41	667.31	231.19	634.29	--	--	--	0.00	87.33	-49.33	-62.69	-13.36	102.69
42	667.31	237.73	634.59	--	--	--	0.00	87.57	-49.57	-55.67	-6.10	95.67
43	667.31	317.68	635.51	220.61	658.98	97.07	-34.12	90.09	-86.22	-101.01	-14.79	--
44	667.31	259.36	634.90	214.64	640.08	44.72	-23.61	88.33	-73.94	-84.96	-11.02	--
45	667.31	250.07	633.07	--	--	--	0.00	88.01	-50.01	-97.13	-47.12	137.13
46	667.31	232.23	631.85	158.34	647.09	73.89	-31.64	87.37	-81.01	-91.86	-10.85	--
47	667.31	223.83	630.63	202.51	644.35	21.32	-34.89	87.05	-83.94	-63.81	20.13	--
48	667.31	151.81	630.02	71.44	649.53	80.37	-35.03	83.68	-80.70	-68.13	12.57	--
49	667.31	142.89	628.50	62.52	649.53	80.38	-36.00	83.15	-81.15	-83.90	-2.75	--
50	667.31	128.13	631.24	59.79	649.53	68.34	-35.21	82.21	-79.41	-75.01	4.40	--
51	667.31	204.66	628.80	169.06	639.78	35.59	-31.12	86.27	-79.40	-95.17	-15.77	--
52	667.31	40.45	627.58	24.27	646.48	16.18	-40.66	72.19	-74.85	-47.05	27.80	--
53	667.31	323.89	627.28	161.95	647.09	161.95	-31.86	90.26	-84.12	-95.87	-11.75	--
54	667.31	363.61	623.62	261.34	646.79	102.26	-33.63	91.26	-86.90	-84.27	2.63	--
55	667.31	428.04	622.40	190.24	647.09	237.80	-32.61	92.68	-87.29	-73.86	13.43	--
56	667.31	510.48	623.01	--	--	--	0.00	94.21	-56.21	-72.33	-16.12	112.33
57	667.31	501.79	622.71	--	--	--	0.00	94.06	-56.06	-84.38	-28.32	124.38
58	667.31	304.96	625.45	--	--	--	0.00	89.74	-51.74	-65.36	-13.62	105.36
59	667.31	303.98	626.06	222.92	650.44	81.06	-35.00	89.71	-86.71	-88.31	-1.60	--
60	667.31	323.97	625.14	171.51	644.35	152.46	-31.60	90.26	-83.86	-86.40	-2.54	--
61	667.31	352.86	623.93	217.15	645.26	135.72	-32.37	91.00	-85.37	-99.79	-14.42	--
62	667.31	400.19	620.57	291.05	642.82	109.14	-32.95	92.10	-87.05	-96.65	-9.60	--
63	667.31	498.44	620.27	--	--	--	0.00	94.00	-56.00	-90.13	-34.13	130.13

B.1c 24.12 GHz: single blockage, without Fresnel zones and without interpolation.

Receiver Location Number	Tower Height (m)	Path Length (m)	Receiver Height (m)	D1 (m)	Blockage Height (m)	D2 (m)	Diffraction Gain (dB)	Path Loss (dBm)	Predicted Received Power (dBm)	Measured Received Power (dBm)	Difference (dB)	Actual Path Loss (dBm)
3	666.07	207.64	630.63	58	665	150	-49.57	106.44	-111.01	-98	13.01	--
10	666.07	240.35	635.20	--	--	--	0.00	107.71	-62.71	-92	-29.29	137.00
11	666.07	215.08	635.51	146	645	69	-38.10	106.75	-99.85	-89	10.85	--
14	666.07	381.85	640.38	222	659	160	-40.73	111.73	-107.46	-94	13.46	--
16	666.07	469.49	639.47	--	--	--	0.00	113.53	-68.53	-94	-25.47	139.00
22	666.07	75.82	646.18	--	--	--	0.00	97.69	-52.69	-58	-5.31	103.00
23	666.07	344.92	628.50	--	--	--	0.00	110.85	-65.85	-87	-21.15	132.00
24	666.07	413.01	629.72	220.91	648.00	192.10	-40.15	112.41	-107.56	-90	17.56	--
25	666.07	490.30	629.41	--	--	--	0.00	113.90	-68.90	-93	-24.10	138.00
26	666.07	453.69	627.58	274.33	646.79	179.37	-40.34	113.23	-108.57	-97	11.57	--
27	666.07	495.19	624.23	264.87	646.79	230.32	-41.18	113.99	-110.17	-94	16.17	--
31	666.07	434.89	622.71	12	665	422	-56.75	112.86	-124.61	-84	40.61	--
32	666.07	391.98	622.40	--	--	--	0.00	111.96	-66.96	-81	-14.04	126.00
33	666.07	391.49	623.32	257.26	646.79	134.22	-42.98	111.95	-109.93	-99	10.93	--
34	666.07	332.85	623.93	12.33	665.07	320.52	-56.56	110.54	-122.10	-87	35.10	--
36	666.07	261.41	633.68	214.73	648.00	46.68	-42.31	108.44	-105.75	-102	3.75	--
37	666.07	156.05	634.29	101	645	55	-40.31	103.96	-99.27	-84	15.27	--
38	666.07	115.33	632.76	62.91	646.48	52.42	-43.20	101.33	-99.54	-89	10.54	--
39	666.07	167.31	634.29	117.12	645.26	50.19	-40.37	104.57	-99.94	-101	-1.06	--
40	666.07	169.30	631.55	95.23	646.48	74.07	-42.31	104.67	-101.98	-84	17.98	--
41	666.07	252.00	630.33	158.67	644.35	93.33	-40.27	108.12	-103.39	-100	3.39	--
42	666.07	283.64	626.97	189.10	644.35	94.55	-41.82	109.15	-105.98	-101	4.98	--
44	666.07	447.91	620.88	218.98	650.44	228.93	-43.95	113.12	-112.07	-101	11.07	--
45	666.07	554.65	650.14	--	--	--	0.00	114.98	-69.98	-96	-26.02	141.00
46	666.07	518.02	623.93	219.16	650.44	298.86	-42.47	114.38	-111.86	-104	7.86	--
47	666.07	561.28	625.14	--	--	--	0.00	115.08	-70.08	-97	-26.92	142.00
48	666.07	545.51	636.73	--	--	--	0.00	114.83	-69.83	-96	-26.17	141.00
49	666.07	463.79	619.05	205	645	259	-42.81	113.42	-111.23	-101	10.23	--
50	666.07	469.31	619.05	217	645	253	-42.72	113.52	-111.25	-101	10.25	--
51	666.07	492.00	620.27	--	--	--	0.00	113.93	-68.93	-97	-28.07	142.00
52	666.07	399.61	620.57	290.63	642.82	108.99	-42.98	112.13	-110.11	-97	13.11	--
53	666.07	322.03	625.14	175	644	147	-41.66	110.25	-106.92	-96	10.92	--
54	666.07	343.85	626.06	190.02	645.26	153.83	-41.39	110.82	-107.22	-100	7.22	--

B.1d 27.525 GHz: single blockage, without Fresnel zones and without interpolation.

Receiver Location Number	Tower Height (m)	Path Length (m)	Receiver Height (m)	D1 (m)	Blockage Height (m)	D2 (m)	Diffraction Gain (dB)	Path Loss (dBm)	Predicted Received Power (dBm)	Measured Received Power (dBm)	Difference (dB)	Actual Path Loss (dB)
1	667.68	125.38	632.31	--	--	--	0.00	103.21	-32.41	-26.66	5.75	97.46
2	667.68	178.00	632.31	--	--	--	0.00	106.25	-35.45	-48.50	-13.05	119.30
4	667.68	316.75	625.91	190.05	644.35	126.70	-42.10	111.26	-82.56	-71.50	11.06	--
5	667.68	456.55	621.94	213.06	650.44	243.49	-44.14	114.43	-87.77	-77.20	10.57	--
6	667.68	557.16	625.60	--	--	--	0.00	116.16	-45.36	-80.00	-34.64	150.80
7	667.68	531.60	624.38	--	--	--	0.00	115.75	-44.95	-38.60	6.35	109.40
8	667.68	518.61	626.82	270.11	646.79	248.50	-40.48	115.54	-85.22	-66.20	19.02	--
9	667.68	444.91	627.13	265	647	180	-41.17	114.21	-84.57	-75.90	8.67	--
10	667.68	439.31	626.21	267.87	646.79	171.44	-41.67	114.10	-84.97	-59.90	25.07	--
11	667.68	407.95	624.08	260	647	148	-42.97	113.45	-85.62	-61.88	23.74	--
12	667.68	416.37	623.16	--	--	--	0.00	113.63	-42.83	-56.98	-14.15	127.78
14	667.68	395.00	622.55	213	650	182	-44.58	113.17	-86.96	-66.91	20.05	--
15	667.68	407.40	621.94	208	644	199	-42.52	113.44	-85.17	-74.17	11.00	--
16	667.68	420.04	621.03	--	--	--	0.00	113.71	-42.91	-70.00	-27.09	140.80
17	667.68	444.44	620.12	209	645	236	-43.16	114.20	-86.56	-86.94	-0.38	--
18	667.68	501.11	621.03	--	--	--	0.00	115.24	-44.44	-65.68	-21.24	136.48
19	667.68	503.93	622.55	--	--	--	0.00	115.29	-44.49	-72.62	-28.13	143.42
20	667.68	496.44	622.86	212.76	650.44	283.68	-43.56	115.16	-87.92	-60.45	27.47	--
22	667.68	482.01	623.77	--	--	--	0.00	114.90	-44.10	-32.74	11.36	103.54
23	667.68	493.32	624.38	265	647	229	-41.71	115.10	-86.02	-59.00	27.02	--
24	667.68	506.84	626.21	270	647	237	-40.85	115.34	-85.39	-69.58	15.81	--
26	667.68	611.38	624.38	531	639	81	-40.35	116.97	-86.52	-82.39	4.13	--
28	667.68	576.68	624.38	529.61	638.86	47.08	-42.45	116.46	-88.11	-87.14	0.97	--
30	667.68	646.93	625.30	534.96	638.86	111.97	-38.58	117.46	-85.24	-57.40	27.84	--
31	667.68	645.06	625.91	--	--	--	0.00	117.43	-46.63	-32.62	14.01	103.42
32	667.68	658.21	632.31	554	649	104	-40.74	117.61	-87.55	-40.43	47.12	--
34	667.68	750.24	628.65	548.68	638.86	201.56	-34.09	118.75	-82.04	-76.36	5.68	--
36	667.68	749.97	628.35	602.09	638.56	147.88	-35.03	118.74	-82.97	-101.86	-18.89	--
38	667.68	702.97	633.53	--	--	--	0.00	118.18	-47.38	-40.17	7.21	110.97
39	667.68	725.82	633.83	533.03	649.22	192.80	-37.83	118.46	-85.49	-66.25	19.24	--
40	667.68	725.89	633.83	544	649	181	-38.00	118.46	-85.66	-67.00	18.66	--

41	667.68	736.20	634.14	538	649	198	-37.57	118.58	-85.35	-83.00	2.35	--
44	667.68	698.20	633.22	604	663	94	-45.85	118.12	-93.17	-81.18	11.99	--
45	667.68	801.68	638.71	734	649	68	-37.60	119.32	-86.12	-80.62	5.50	--
46	667.68	856.64	642.06	717.19	648.61	139.45	-31.25	119.90	-80.35	-83.11	-2.76	--
49	667.68	964.43	643.28	756	649	209	-28.00	120.93	-78.13	-89.54	-11.41	--
50	667.68	958.40	643.28	744	649	214	-27.93	120.87	-78.00	-90.13	-12.13	--
51	667.68	941.05	642.98	793.02	656.23	148.03	-37.09	120.71	-87.00	-90.39	-3.39	--
53	667.68	864.88	637.79	547.39	649.22	317.49	-33.73	119.98	-82.91	-76.36	6.55	--
54	667.68	844.35	636.27	610	649	235	-35.55	119.77	-84.53	-64.15	20.38	--
55	667.68	813.49	660.65	--	--	--	0.00	119.45	-48.65	-45.81	2.84	116.61
56	667.68	780.70	634.75	543.09	649.22	237.60	-36.63	119.09	-84.92	-82.51	2.41	--
58	667.68	1002.58	641.45	724.63	648.61	277.94	-29.67	121.26	-80.13	-71.77	8.36	--
59	667.68	1016.16	640.23	890.35	660.50	125.81	-41.31	121.38	-91.89	-89.23	2.66	--
60	667.68	1033.42	638.40	602.83	662.64	430.59	-39.28	121.53	-90.01	-77.61	12.40	--
61	667.68	1054.76	636.57	922.91	651.36	131.84	-38.37	121.71	-89.28	-84.41	4.87	--
63	667.68	1052.07	636.27	--	--	--	0.00	121.68	-50.88	-79.56	-28.68	150.36
64	667.68	1007.46	635.36	776.39	649.83	231.07	-36.30	121.31	-86.81	-73.05	13.76	--
65	667.68	977.35	636.27	856.34	651.36	121.01	-38.91	121.04	-89.16	-79.65	9.51	--
66	667.68	972.20	637.79	--	--	--	0.00	121.00	-50.20	-68.57	-18.37	139.37
67	667.68	914.25	637.18	--	--	--	0.00	120.46	-49.66	-79.77	-30.11	150.57
68	667.68	835.14	637.49	579	647	256	-32.47	119.68	-81.34	-69.72	11.62	--
69	667.68	879.28	642.67	718	649	162	-29.87	120.12	-79.20	-74.94	4.26	--
70	667.68	853.70	642.67	813	656	41	-42.31	119.87	-91.38	-92.93	-1.55	--
71	667.68	805.38	635.05	544.18	649.22	261.21	-36.16	119.36	-84.72	-82.66	2.06	--
73	667.68	779.85	634.75	566.20	649.22	213.66	-36.90	119.08	-85.19	-79.05	6.14	--
74	667.68	797.47	634.75	546.21	649.22	251.26	-36.45	119.28	-84.93	-79.91	5.02	--
75	667.68	811.71	635.05	544.85	649.22	266.86	-36.09	119.43	-84.72	-73.79	10.93	--
76	667.68	808.19	635.05	535	649	273	-36.05	119.39	-84.64	-76.52	8.12	--
77	667.68	805.96	635.36	654.84	641.30	151.12	-30.19	119.37	-78.75	-64.30	14.45	--
78	667.68	847.19	635.66	--	--	--	0.00	119.80	-49.00	-77.70	-28.70	148.50
79	667.68	895.79	637.79	809.90	658.67	85.90	-43.09	120.29	-92.57	-79.47	13.10	--
83	667.68	71.85	624.38	--	--	--	0.00	98.37	-27.57	-53.13	-25.56	123.93
84	667.68	74.22	627.43	--	--	--	0.00	98.65	-27.85	-21.34	6.51	92.14
85	667.68	106.20	627.74	--	--	--	0.00	101.76	-30.96	-38.73	-7.77	109.53
87	667.68	209.18	623.47	--	--	--	0.00	107.65	-36.85	-25.16	11.69	95.96
88	667.68	287.64	622.86	--	--	--	0.00	110.42	-39.62	-30.56	9.06	101.36
89	667.68	336.92	620.73	--	--	--	0.00	111.79	-40.99	-40.70	0.29	111.50
90	667.68	417.55	619.51	--	--	--	0.00	113.66	-42.86	-53.55	-10.69	124.35
94	667.68	679.52	628.65	--	--	--	0.00	117.89	-47.09	-37.14	9.95	107.94
95	667.68	806.24	625.60	--	--	--	0.00	119.37	-48.57	-39.66	8.91	110.46

96	667.68	864.60	622.55	--	--	--	0.00	119.98	-49.18	-55.79	-6.61	126.59
97	667.68	902.53	619.81	--	--	--	0.00	120.35	-49.55	-61.26	-11.71	132.06
98	667.68	936.26	620.12	830.93	625.14	105.33	-29.92	120.67	-79.79	-71.54	8.25	--
99	667.68	960.22	621.94	--	--	--	0.00	120.89	-50.09	-44.00	6.09	114.80
101	667.68	975.77	633.53	--	--	--	0.00	121.03	-50.23	-46.26	3.97	117.06
104	667.68	835.18	632.31	--	--	--	0.00	119.68	-48.88	-43.72	5.16	114.52
106	667.68	750.64	628.65	--	--	--	0.00	118.75	-47.95	-40.63	7.32	111.43
107	667.68	658.58	626.82	--	--	--	0.00	117.61	-46.81	-35.93	10.88	106.73
109	667.68	612.82	618.59	554	625	59	-33.81	116.99	-80.00	-72.41	7.59	--

B.2a 902 MHz: single blockage, with Fresnel zones and without interpolation.

Receiver Location Number	Tower Height (m)	Path Length (m)	Receiver Height (m)	D1 (m)	Blockage Height (m)	D2 (m)	Diffraction Gain (dB)	Path Loss (dBm)	Predicted Received Power (dBm)	Measured Received Power (dBm)	Difference (dB)
1	667.68	125.38	632.31	--	--	--	0.00	73.52	-41.74	-50.80	-9.06
2	667.68	178.00	632.31	--	--	--	0.00	76.56	-44.78	-65.00	-20.22
4	667.68	316.75	625.91	190.05	644.35	126.70	-27.26	81.57	-77.04	-76.80	0.24
5	667.68	456.55	621.94	213.06	650.44	243.49	-29.29	84.74	-82.25	-82.50	-0.25
6	667.68	557.16	625.60	--	--	--	0.00	86.47	-54.69	-74.50	-19.81
7	667.68	531.60	624.38	--	--	--	0.00	86.06	-54.28	-68.70	-14.42
8	667.68	518.61	626.82	270.11	646.79	248.50	-25.64	85.85	-79.70	-85.60	-5.90
9	667.68	444.91	627.13	264.83	646.79	180.08	-26.32	84.52	-79.06	-79.10	-0.04
10	667.68	439.31	626.21	267.87	646.79	171.44	-26.82	84.41	-79.45	-74.80	4.65
11	667.68	407.95	624.08	259.60	646.79	148.34	-28.12	83.76	-80.11	-73.15	6.96
12	667.68	416.37	623.16	--	--	--	0.00	83.94	-52.16	-63.58	-11.42
14	667.68	395.00	622.55	212.69	650.44	182.31	-29.74	83.48	-81.44	-82.18	-0.74
15	667.68	407.40	621.94	208.44	644.35	198.96	-27.68	83.75	-79.65	-82.72	-3.07
16	667.68	420.04	621.03	--	--	--	0.00	84.02	-52.24	-86.75	-34.51
17	667.68	444.44	620.12	208.61	645.26	235.82	-28.32	84.51	-81.05	-93.08	-12.03
18	667.68	501.11	621.03	--	--	--	0.00	85.55	-53.77	-79.44	-25.67
19	667.68	503.93	622.55	--	--	--	0.00	85.60	-53.82	-88.90	-35.08
20	667.68	496.44	622.86	212.76	650.44	283.68	-28.72	85.47	-82.40	-85.83	-3.43
22	667.68	482.01	623.77	--	--	--	0.00	85.21	-53.43	-67.10	-13.67
23	667.68	493.32	624.38	264.71	646.79	228.61	-26.87	85.41	-80.50	-72.41	8.09
24	667.68	506.84	626.21	270.31	646.79	236.53	-26.01	85.65	-79.88	-72.69	7.19

26	667.68	611.38	624.38	530.63	638.86	80.75	-25.51	87.28	-81.01	-98.00	-16.99
28	667.68	576.68	624.38	529.61	638.86	47.08	-27.61	86.77	-82.60	-95.50	-12.90
30	667.68	646.93	625.30	534.96	638.86	111.97	-23.73	87.77	-79.72	-86.60	-6.88
31	667.68	645.06	625.91	--	--	--	0.00	87.74	-55.96	-71.90	-15.94
32	667.68	658.21	632.31	554.28	649.22	103.93	-25.90	87.92	-82.03	-77.31	4.72
34	667.68	750.24	628.65	548.68	638.86	201.56	-19.75	89.06	-77.02	-102.51	-25.49
36	667.68	749.97	628.35	602.09	638.56	147.88	-20.88	89.05	-78.15	-95.99	-17.84
37	667.68	814.92	631.39	706.26	641.30	108.66	-20.93	89.77	-78.92	-85.78	-6.86
38	667.68	702.97	633.53	--	--	--	0.00	88.49	-56.71	-72.78	-16.07
39	667.68	725.82	633.83	533.03	649.22	192.80	-22.99	88.77	-79.97	-92.51	-12.54
40	667.68	725.89	633.83	544.42	649.22	181.47	-23.16	88.77	-80.15	-81.42	-1.27
41	667.68	736.20	634.14	538.41	649.22	197.78	-22.72	88.89	-79.83	-89.11	-9.28
44	667.68	698.20	633.22	603.85	662.64	94.35	-31.00	88.43	-87.66	-89.13	-1.47
45	667.68	801.68	638.71	734.07	648.61	67.61	-22.75	89.63	-80.60	-83.55	-2.95
46	667.68	856.64	642.06	717.19	648.61	139.45	-16.76	90.21	-75.19	-98.70	-23.51
49	667.68	964.43	643.28	755.64	648.61	208.79	-14.19	91.24	-73.65	-86.92	-13.27
50	667.68	958.40	643.28	744.29	648.61	214.11	-14.07	91.18	-73.47	-100.98	-27.51
51	667.68	941.05	642.98	793.02	656.23	148.03	-22.24	91.02	-81.48	-90.13	-8.65
53	667.68	864.88	637.79	547.39	649.22	317.49	-19.32	90.29	-77.83	-85.26	-7.43
54	667.68	844.35	636.27	609.81	649.22	234.54	-20.71	90.08	-79.01	-77.89	1.12
55	667.68	813.49	660.65	--	--	--	0.00	89.76	-57.98	-73.96	-15.98
56	667.68	780.70	634.75	543.09	649.22	237.60	-21.78	89.40	-79.40	-88.85	-9.45
58	667.68	1002.58	641.45	724.63	648.61	277.94	-15.39	91.57	-75.18	-98.73	-23.55
59	667.68	1016.16	640.23	890.35	660.50	125.81	-26.46	91.69	-86.38	-98.18	-11.80
60	667.68	1033.42	638.40	602.83	662.64	430.59	-24.44	91.84	-84.50	-98.67	-14.17
61	667.68	1054.76	636.57	922.91	651.36	131.84	-23.52	92.01	-83.76	-84.42	-0.66
63	667.68	1052.07	636.27	--	--	--	0.00	91.99	-60.21	-82.69	-22.48
64	667.68	1007.46	635.36	776.39	649.83	231.07	-21.46	91.62	-81.30	-83.22	-1.92
65	667.68	977.35	636.27	856.34	651.36	121.01	-24.07	91.35	-83.64	-81.80	1.84
66	667.68	972.20	637.79	--	--	--	0.00	91.31	-59.53	-83.26	-23.73
67	667.68	914.25	637.18	--	--	--	0.00	90.77	-58.99	-87.51	-28.52
68	667.68	835.14	637.49	578.91	646.79	256.24	-17.86	89.99	-76.07	-78.12	-2.05
69	667.68	879.28	642.67	717.57	648.61	161.71	-15.55	90.43	-74.21	-92.60	-18.39
70	667.68	853.70	642.67	812.56	656.23	41.14	-27.47	90.18	-85.87	-92.05	-6.18
71	667.68	805.38	635.05	544.18	649.22	261.21	-21.31	89.67	-79.20	-93.53	-14.33
73	667.68	779.85	634.75	566.20	649.22	213.66	-22.06	89.39	-79.67	-83.16	-3.49
74	667.68	797.47	634.75	546.21	649.22	251.26	-21.61	89.59	-79.41	-88.31	-8.90
75	667.68	811.71	635.05	544.85	649.22	266.86	-21.25	89.74	-79.21	-92.87	-13.66
76	667.68	808.19	635.05	535.00	649.22	273.19	-21.21	89.70	-79.13	-80.57	-1.44
77	667.68	805.96	635.36	654.84	641.30	151.12	-15.59	89.68	-73.49	-77.42	-3.93

78	667.68	847.19	635.66	682.81	641.30	164.38	-15.17	90.11	-73.50	-83.43	-9.93
79	667.68	895.79	637.79	809.90	658.67	85.90	-28.24	90.60	-87.06	-91.84	-4.78
83	667.68	71.85	624.38	--	--	--	0.00	68.68	-36.90	-80.45	-43.55
84	667.68	74.22	627.43	--	--	--	0.00	68.96	-37.18	-50.26	-13.08
85	667.68	106.20	627.74	--	--	--	0.00	72.07	-40.29	-55.79	-15.50
87	667.68	209.18	623.47	--	--	--	0.00	77.96	-46.18	-59.50	-13.32
88	667.68	287.64	622.86	--	--	--	0.00	80.73	-48.95	-65.65	-16.70
89	667.68	336.92	620.73	--	--	--	0.00	82.10	-50.32	-57.91	-7.59
90	667.68	417.55	619.51	--	--	--	0.00	83.97	-52.19	-66.30	-14.11
94	667.68	679.52	628.65	--	--	--	0.00	88.20	-56.42	-67.09	-10.67
95	667.68	806.24	625.60	--	--	--	0.00	89.68	-57.90	-71.02	-13.12
96	667.68	864.60	622.55	--	--	--	0.00	90.29	-58.51	-78.51	-20.00
97	667.68	902.53	619.81	--	--	--	0.00	90.66	-58.88	-86.56	-27.68
98	667.68	936.26	620.12	830.93	625.14	105.33	-16.30	90.98	-75.50	-95.84	-20.34
99	667.68	960.22	621.94	--	--	--	0.00	91.20	-59.42	-80.10	-20.68
101	667.68	975.77	633.53	--	--	--	0.00	91.34	-59.56	-72.58	-13.02
104	667.68	835.18	632.31	--	--	--	0.00	89.99	-58.21	-70.85	-12.64
106	667.68	750.64	628.65	--	--	--	0.00	89.06	-57.28	-65.63	-8.35
107	667.68	658.58	626.82	--	--	--	0.00	87.92	-56.14	-67.07	-10.93
109	667.68	612.82	618.59	553.90	624.54	58.93	-19.42	87.30	-74.94	-78.25	-3.31

B.2b 2.4 GHz: single blockage, with Fresnel zones and without interpolation.

Receiver Location Number	Tower Height (m)	Path Length (m)	Receiver Height (m)	D1 (m)	Blockage Height (m)	D2 (m)	Diffraction Gain (dB)	Path Loss (dBm)	Predicted Received Power (dBm)	Measured Received Power (dBm)	Difference (dB)
1	667.31	57.15	623.32	--	--	--	0.00	75.19	-37.19	-47.66	-10.47
2	667.31	196.74	623.62	--	--	--	0.00	85.93	-47.93	-63.80	-15.87
3	667.31	307.10	622.71	--	--	--	0.00	89.80	-51.80	-55.63	-3.83
4	667.31	329.40	626.06	--	--	--	0.00	90.41	-52.41	-70.42	-18.01
5	667.31	339.46	628.80	--	--	--	0.00	90.67	-52.67	-54.19	-1.52
6	667.31	348.59	631.24	--	--	--	0.00	90.90	-52.90	-62.55	-9.65
7	667.31	386.19	636.42	--	--	--	0.00	91.79	-53.79	-69.95	-16.16
8	667.31	381.52	637.34	--	--	--	0.00	91.68	-53.68	-61.05	-7.37
9	667.31	460.90	638.56	--	--	--	0.00	93.32	-55.32	-64.53	-9.21
10	667.31	456.55	636.42	--	--	--	0.00	93.24	-55.24	-58.17	-2.93

11	667.31	514.73	635.20	--	--	--	0.00	94.28	-56.28	-64.73	-8.45
12	667.31	550.23	633.07	--	--	--	0.00	94.86	-56.86	-74.22	-17.36
13	667.31	510.00	632.76	--	--	--	0.00	94.20	-56.20	-60.70	-4.50
14	667.31	481.50	627.28	--	--	--	0.00	93.70	-55.70	-57.72	-2.02
15	667.31	453.34	627.28	--	--	--	0.00	93.18	-55.18	-69.44	-14.26
16	667.31	118.42	624.54	9.11	665.07	109.31	-47.91	81.52	-91.43	-71.18	20.25
17	667.31	124.37	624.54	11.31	665.07	113.06	-47.04	81.95	-90.98	-69.11	21.87
18	667.31	128.78	624.84	8.59	665.07	120.19	-48.05	82.25	-92.30	-84.32	7.98
19	667.31	145.90	624.54	8.58	665.07	137.32	-48.09	83.33	-93.42	-77.79	15.63
20	667.31	179.62	623.93	17.11	665.07	162.52	-48.18	85.14	-95.32	-85.31	10.01
21	667.31	169.65	624.23	8.93	665.07	160.72	-47.95	84.64	-94.59	-80.72	13.87
22	667.31	155.54	625.14	11.11	665.07	144.43	-46.89	83.89	-92.78	-77.74	15.04
23	667.31	179.20	625.75	11.20	665.07	168.00	-46.68	85.12	-93.80	-72.74	21.06
24	667.31	189.35	624.54	9.97	665.07	179.38	-47.41	85.60	-95.00	-65.12	29.88
25	667.31	199.34	623.93	18.12	665.07	181.22	-45.12	86.04	-93.16	-76.23	16.93
26	667.31	229.97	623.93	17.69	665.07	212.28	-45.16	87.29	-94.44	-75.34	19.10
27	667.31	257.48	624.84	17.76	665.07	239.72	-44.91	88.27	-95.18	-79.12	16.06
28	667.31	217.58	624.54	19.78	665.07	197.80	-44.61	86.80	-93.41	-72.95	20.46
29	667.31	200.02	627.28	11.77	665.07	188.25	-46.11	86.07	-94.18	-78.53	15.65
30	667.31	196.25	627.28	--	--	--	0.00	85.91	-47.91	-57.74	-9.83
31	667.31	249.64	630.63	--	--	--	0.00	88.00	-50.00	-55.06	-5.06
32	667.31	263.24	631.85	--	--	--	0.00	88.46	-50.46	-59.07	-8.61
33	667.31	275.16	631.85	--	--	--	0.00	88.84	-50.84	-57.29	-6.45
34	667.31	237.22	629.11	--	--	--	0.00	87.56	-49.56	-52.32	-2.76
35	667.31	216.60	628.80	--	--	--	0.00	86.77	-48.77	-51.47	-2.70
36	667.31	209.74	628.50	--	--	--	0.00	86.49	-48.49	-48.02	0.47
37	667.31	207.07	627.89	21.80	665.07	185.27	-46.27	86.37	-94.64	-89.56	5.08
38	667.31	214.18	630.63	59.49	665.07	154.68	-39.41	86.67	-88.08	-77.60	10.48
39	667.31	221.94	632.16	63.41	665.07	158.53	-38.79	86.98	-87.77	-56.37	31.40
40	667.31	226.62	633.37	--	--	--	0.00	87.16	-49.16	-54.63	-5.47
41	667.31	231.19	634.29	--	--	--	0.00	87.33	-49.33	-62.69	-13.36
42	667.31	237.73	634.59	--	--	--	0.00	87.57	-49.57	-55.67	-6.10
43	667.31	317.68	635.51	220.61	658.98	97.07	-34.12	90.09	-86.22	-101.01	-14.79
44	667.31	259.36	634.90	214.64	640.08	44.72	-23.61	88.33	-73.94	-84.96	-11.02
45	667.31	250.07	633.07	--	--	--	0.00	88.01	-50.01	-97.13	-47.12
46	667.31	232.23	631.85	158.34	647.09	73.89	-31.64	87.37	-81.01	-91.86	-10.85
47	667.31	223.83	630.63	202.51	644.35	21.32	-34.89	87.05	-83.94	-63.81	20.13
48	667.31	151.81	630.02	71.44	649.53	80.37	-35.03	83.68	-80.70	-68.13	12.57
49	667.31	142.89	628.50	62.52	649.53	80.38	-36.00	83.15	-81.15	-83.90	-2.75
50	667.31	128.13	631.24	59.79	649.53	68.34	-35.21	82.21	-79.41	-75.01	4.40

51	667.31	204.66	628.80	169.06	639.78	35.59	-31.12	86.27	-79.40	-95.17	-15.77
52	667.31	40.45	627.58	24.27	646.48	16.18	-40.66	72.19	-74.85	-47.05	27.80
53	667.31	323.89	627.28	161.95	647.09	161.95	-31.86	90.26	-84.12	-95.87	-11.75
54	667.31	363.61	623.62	261.34	646.79	102.26	-33.63	91.26	-86.90	-84.27	2.63
55	667.31	428.04	622.40	190.24	647.09	237.80	-32.61	92.68	-87.29	-73.86	13.43
56	667.31	510.48	623.01	--	--	--	0.00	94.21	-56.21	-72.33	-16.12
57	667.31	501.79	622.71	--	--	--	0.00	94.06	-56.06	-84.38	-28.32
58	667.31	304.96	625.45	--	--	--	0.00	89.74	-51.74	-65.36	-13.62
59	667.31	303.98	626.06	222.92	650.44	81.06	-31.46	89.71	-83.16	-88.31	-5.15
60	667.31	323.97	625.14	171.51	644.35	152.46	-31.60	90.26	-83.86	-86.40	-2.54
61	667.31	352.86	623.93	217.15	645.26	135.72	-32.37	91.00	-85.37	-99.79	-14.42
62	667.31	400.19	620.57	291.05	642.82	109.14	-32.95	92.10	-87.05	-96.65	-9.60
63	667.31	498.44	620.27	--	--	--	0.00	94.00	-56.00	-90.13	-34.13

B.2c 24.12 GHz: single blockage, with Fresnel zones and without interpolation.

Receiver Location Number	Tower Height (m)	Path Length (m)	Receiver Height (m)	D1 (m)	Blockage Height (m)	D2 (m)	Diffraction Gain (dB)	Path Loss (dBm)	Predicted Received Power (dBm)	Measured Received Power (dBm)	Difference (dB)
3	666.07	207.64	630.63	57.68	665.07	149.96	-49.57	106.44	-111.01	-98	13.01
10	666.07	240.35	635.20	--	--	--	0.00	107.71	-62.71	-92	-29.29
11	666.07	215.08	635.51	146.25	645.26	68.82	-38.10	106.75	-99.85	-89	10.85
14	666.07	381.85	640.38	222.00	658.98	159.84	-40.73	111.73	-107.46	-94	13.46
16	666.07	469.49	639.47	--	--	--	0.00	113.53	-68.53	-94	-25.47
22	666.07	75.82	646.18	--	--	--	0.00	97.69	-52.69	-58	-5.31
23	666.07	344.92	628.50	--	--	--	0.00	110.85	-65.85	-87	-21.15
24	666.07	413.01	629.72	220.91	648.00	192.10	-40.15	112.41	-107.56	-90	17.56
25	666.07	490.30	629.41	--	--	--	0.00	113.90	-68.90	-93	-24.10
26	666.07	453.69	627.58	274.33	646.79	179.37	-40.34	113.23	-108.57	-97	11.57
27	666.07	495.19	624.23	264.87	646.79	230.32	-41.18	113.99	-110.17	-94	16.17
31	666.07	434.89	622.71	12.43	665.07	422.47	-56.75	112.86	-124.61	-84	40.61
32	666.07	391.98	622.40	--	--	--	0.00	111.96	-66.96	-81	-14.04
33	666.07	391.49	623.32	257.26	646.79	134.22	-42.98	111.95	-109.93	-99	10.93
34	666.07	332.85	623.93	12.33	665.07	320.52	-56.56	110.54	-122.10	-87	35.10
36	666.07	261.41	633.68	214.73	648.00	46.68	-42.31	108.44	-105.75	-102	3.75
37	666.07	156.05	634.29	100.97	645.26	55.08	-40.31	103.96	-99.27	-84	15.27
38	666.07	115.33	632.76	62.91	646.48	52.42	-43.20	101.33	-99.54	-89	10.54
39	666.07	167.31	634.29	117.12	645.26	50.19	-40.37	104.57	-99.94	-101	-1.06

40	666.07	169.30	631.55	95.23	646.48	74.07	-42.31	104.67	-101.98	-84	17.98
41	666.07	252.00	630.33	158.67	644.35	93.33	-40.27	108.12	-103.39	-100	3.39
42	666.07	283.64	626.97	189.10	644.35	94.55	-41.82	109.15	-105.98	-101	4.98
44	666.07	447.91	620.88	218.98	650.44	228.93	-43.95	113.12	-112.07	-101	11.07
45	666.07	554.65	650.14	--	--	--	0.00	114.98	-69.98	-96	-26.02
46	666.07	518.02	623.93	219.16	650.44	298.86	-42.47	114.38	-111.86	-104	7.86
47	666.07	561.28	625.14	--	--	--	0.00	115.08	-70.08	-97	-26.92
48	666.07	545.51	636.73	--	--	--	0.00	114.83	-69.83	-96	-26.17
49	666.07	463.79	619.05	205.14	645.26	258.65	-42.81	113.42	-111.23	-101	10.23
50	666.07	469.31	619.05	216.60	645.26	252.70	-42.72	113.52	-111.25	-101	10.25
51	666.07	492.00	620.27	--	--	--	0.00	113.93	-68.93	-97	-28.07
52	666.07	399.61	620.57	290.63	642.82	108.99	-42.98	112.13	-110.11	-97	13.11
53	666.07	322.03	625.14	174.81	644.35	147.21	-41.63	110.25	-106.89	-96	10.89
54	666.07	343.85	626.06	190.02	645.26	153.83	-41.39	110.82	-107.22	-100	7.22

B.2d 27.525 GHz: single blockage, with Fresnel zones and without interpolation.

Receiver Location Number	Tower Height (m)	Path Length (m)	Receiver Height (m)	D1 (m)	Blockage Height (m)	D2 (m)	Diffraction Gain (dB)	Path Loss (dBm)	Predicted Received Power (dBm)	Measured Received Power (dBm)	Difference (dB)
1	667.68	125.38	632.31	--	--	--	0.00	103.21	-32.41	-26.66	5.75
2	667.68	178.00	632.31	--	--	--	0.00	106.25	-35.45	-48.50	-13.05
4	667.68	316.75	625.91	190.05	644.35	126.70	-42.10	111.26	-82.56	-71.50	11.06
5	667.68	456.55	621.94	213.06	650.44	243.49	-44.14	114.43	-87.77	-77.20	10.57
6	667.68	557.16	625.60	--	--	--	0.00	116.16	-45.36	-80.00	-34.64
7	667.68	531.60	624.38	--	--	--	0.00	115.75	-44.95	-38.60	6.35
8	667.68	518.61	626.82	270.11	646.79	248.50	-40.48	115.54	-85.22	-66.20	19.02
9	667.68	444.91	627.13	264.83	646.79	180.08	-41.17	114.21	-84.57	-75.90	8.67
10	667.68	439.31	626.21	267.87	646.79	171.44	-41.67	114.10	-84.97	-59.90	25.07
11	667.68	407.95	624.08	259.60	646.79	148.34	-42.97	113.45	-85.62	-61.88	23.74
12	667.68	416.37	623.16	--	--	--	0.00	113.63	-42.83	-56.98	-14.15
14	667.68	395.00	622.55	212.69	650.44	182.31	-44.58	113.17	-86.96	-66.91	20.05
15	667.68	407.40	621.94	208.44	644.35	198.96	-42.52	113.44	-85.17	-74.17	11.00
16	667.68	420.04	621.03	--	--	--	0.00	113.71	-42.91	-70.00	-27.09
17	667.68	444.44	620.12	208.61	645.26	235.82	-43.16	114.20	-86.56	-86.94	-0.38
18	667.68	501.11	621.03	--	--	--	0.00	115.24	-44.44	-65.68	-21.24
19	667.68	503.93	622.55	--	--	--	0.00	115.29	-44.49	-72.62	-28.13
20	667.68	496.44	622.86	212.76	650.44	283.68	-43.56	115.16	-87.92	-60.45	27.47

22	667.68	482.01	623.77	--	--	--	0.00	114.90	-44.10	-32.74	11.36
23	667.68	493.32	624.38	264.71	646.79	228.61	-41.71	115.10	-86.02	-59.00	27.02
24	667.68	506.84	626.21	270.31	646.79	236.53	-40.85	115.34	-85.39	-69.58	15.81
26	667.68	611.38	624.38	530.63	638.86	80.75	-40.35	116.97	-86.52	-82.39	4.13
28	667.68	576.68	624.38	529.61	638.86	47.08	-42.45	116.46	-88.11	-87.14	0.97
30	667.68	646.93	625.30	534.96	638.86	111.97	-38.58	117.46	-85.24	-57.40	27.84
31	667.68	645.06	625.91	--	--	--	0.00	117.43	-46.63	-32.62	14.01
32	667.68	658.21	632.31	554.28	649.22	103.93	-40.74	117.61	-87.55	-40.43	47.12
34	667.68	750.24	628.65	548.68	638.86	201.56	-34.09	118.75	-82.04	-76.36	5.68
36	667.68	749.97	628.35	602.09	638.56	147.88	-35.03	118.74	-82.97	-101.86	-18.89
38	667.68	702.97	633.53	--	--	--	0.00	118.18	-47.38	-40.17	7.21
39	667.68	725.82	633.83	533.03	649.22	192.80	-37.83	118.46	-85.49	-66.25	19.24
40	667.68	725.89	633.83	544.42	649.22	181.47	-38.00	118.46	-85.66	-67.00	18.66
41	667.68	736.20	634.14	538.41	649.22	197.78	-37.57	118.58	-85.35	-83.00	2.35
44	667.68	698.20	633.22	603.85	662.64	94.35	-45.85	118.12	-93.17	-81.18	11.99
45	667.68	801.68	638.71	734.07	648.61	67.61	-37.60	119.32	-86.12	-80.62	5.50
46	667.68	856.64	642.06	717.19	648.61	139.45	-31.25	119.90	-80.35	-83.11	-2.76
49	667.68	964.43	643.28	755.64	648.61	208.79	-27.85	120.93	-77.98	-89.54	-11.56
50	667.68	958.40	643.28	744.29	648.61	214.11	-27.93	120.87	-78.00	-90.13	-12.13
51	667.68	941.05	642.98	793.02	656.23	148.03	-37.09	120.71	-87.00	-90.39	-3.39
53	667.68	864.88	637.79	547.39	649.22	317.49	-33.73	119.98	-82.91	-76.36	6.55
54	667.68	844.35	636.27	609.81	649.22	234.54	-35.55	119.77	-84.53	-64.15	20.38
55	667.68	813.49	660.65	--	--	--	0.00	119.45	-48.65	-45.81	2.84
56	667.68	780.70	634.75	543.09	649.22	237.60	-36.63	119.09	-84.92	-82.51	2.41
58	667.68	1002.58	641.45	724.63	648.61	277.94	-29.67	121.26	-80.13	-71.77	8.36
59	667.68	1016.16	640.23	890.35	660.50	125.81	-41.31	121.38	-91.89	-89.23	2.66
60	667.68	1033.42	638.40	602.83	662.64	430.59	-39.28	121.53	-90.01	-77.61	12.40
61	667.68	1054.76	636.57	922.91	651.36	131.84	-38.37	121.71	-89.28	-84.41	4.87
63	667.68	1052.07	636.27	--	--	--	0.00	121.68	-50.88	-79.56	-28.68
64	667.68	1007.46	635.36	776.39	649.83	231.07	-36.30	121.31	-86.81	-73.05	13.76
65	667.68	977.35	636.27	856.34	651.36	121.01	-38.91	121.04	-89.16	-79.65	9.51
66	667.68	972.20	637.79	--	--	--	0.00	121.00	-50.20	-68.57	-18.37
67	667.68	914.25	637.18	--	--	--	0.00	120.46	-49.66	-79.77	-30.11
68	667.68	835.14	637.49	578.91	646.79	256.24	-32.38	119.68	-81.26	-69.72	11.54
69	667.68	879.28	642.67	717.57	648.61	161.71	-29.87	120.12	-79.20	-74.94	4.26
70	667.68	853.70	642.67	812.56	656.23	41.14	-42.31	119.87	-91.38	-92.93	-1.55
71	667.68	805.38	635.05	544.18	649.22	261.21	-36.16	119.36	-84.72	-82.66	2.06
73	667.68	779.85	634.75	566.20	649.22	213.66	-36.90	119.08	-85.19	-79.05	6.14
74	667.68	797.47	634.75	546.21	649.22	251.26	-36.45	119.28	-84.93	-79.91	5.02
75	667.68	811.71	635.05	544.85	649.22	266.86	-36.09	119.43	-84.72	-73.79	10.93

76	667.68	808.19	635.05	535.00	649.22	273.19	-36.05	119.39	-84.64	-76.52	8.12
77	667.68	805.96	635.36	654.84	641.30	151.12	-30.19	119.37	-78.75	-64.30	14.45
78	667.68	847.19	635.66	--	--	--	0.00	119.80	-49.00	-77.70	-28.70
79	667.68	895.79	637.79	809.90	658.67	85.90	-43.09	120.29	-92.57	-79.47	13.10
83	667.68	71.85	624.38	--	--	--	0.00	98.37	-27.57	-53.13	-25.56
84	667.68	74.22	627.43	--	--	--	0.00	98.65	-27.85	-21.34	6.51
85	667.68	106.20	627.74	--	--	--	0.00	101.76	-30.96	-38.73	-7.77
87	667.68	209.18	623.47	--	--	--	0.00	107.65	-36.85	-25.16	11.69
88	667.68	287.64	622.86	--	--	--	0.00	110.42	-39.62	-30.56	9.06
89	667.68	336.92	620.73	--	--	--	0.00	111.79	-40.99	-40.70	0.29
90	667.68	417.55	619.51	--	--	--	0.00	113.66	-42.86	-53.55	-10.69
94	667.68	679.52	628.65	--	--	--	0.00	117.89	-47.09	-37.14	9.95
95	667.68	806.24	625.60	--	--	--	0.00	119.37	-48.57	-39.66	8.91
96	667.68	864.60	622.55	--	--	--	0.00	119.98	-49.18	-55.79	-6.61
97	667.68	902.53	619.81	--	--	--	0.00	120.35	-49.55	-61.26	-11.71
98	667.68	936.26	620.12	830.93	625.14	105.33	-29.92	120.67	-79.79	-71.54	8.25
99	667.68	960.22	621.94	--	--	--	0.00	120.89	-50.09	-44.00	6.09
101	667.68	975.77	633.53	--	--	--	0.00	121.03	-50.23	-46.26	3.97
104	667.68	835.18	632.31	--	--	--	0.00	119.68	-48.88	-43.72	5.16
106	667.68	750.64	628.65	--	--	--	0.00	118.75	-47.95	-40.63	7.32
107	667.68	658.58	626.82	--	--	--	0.00	117.61	-46.81	-35.93	10.88
109	667.68	612.82	618.59	553.90	624.54	58.93	-33.81	116.99	-80.00	-72.41	7.59

B.3a 902 MHz: single blockage, without Fresnel zones and with interpolation.

Receiver Location Number	Tower Height (m)	Path Length (m)	Receiver Height (m)	D1 (m)	Blockage Height (m)	D2 (m)	Diffraction Gain (dB)	Path Loss (dBm)	Predicted Received Power (dBm)	Measured Received Power (dBm)	Difference (dB)
1	667.68	125.38	632.31	--	--	--	0.00	73.52	-41.74	-50.80	-9.06
2	667.68	178.00	632.31	--	--	--	0.00	76.56	-44.78	-65.00	-20.22
4	667.68	316.75	625.91	201.00	644.35	115.75	-27.41	81.57	-77.19	-76.80	0.39
5	667.68	456.55	621.94	233.00	650.44	223.55	-29.27	84.74	-82.24	-82.50	-0.26
6	667.68	557.16	625.60	--	--	--	0.00	86.47	-54.69	-74.50	-19.81
7	667.68	531.60	624.38	--	--	--	0.00	86.06	-54.28	-68.70	-14.42
8	667.68	518.61	626.82	274.00	646.24	244.61	-25.40	85.85	-79.47	-85.60	-6.13
9	667.68	444.91	627.13	262.00	646.79	182.91	-26.30	84.52	-79.04	-79.10	-0.06
10	667.68	439.31	626.21	267.00	646.79	172.31	-26.82	84.41	-79.44	-74.80	4.64
11	667.68	407.95	624.08	263.00	646.59	144.95	-28.09	83.76	-80.08	-73.15	6.93
12	667.68	416.37	623.16	--	--	--	0.00	83.94	-52.16	-63.58	-11.42
14	667.68	395.00	622.55	210.00	650.44	185.00	-29.73	83.48	-81.44	-82.18	-0.74
15	667.68	407.40	621.94	224.00	644.35	183.40	-27.72	83.75	-79.69	-82.72	-3.03
16	667.68	420.04	621.03	--	--	--	0.00	84.02	-52.24	-86.75	-34.51
17	667.68	444.44	620.12	220.00	645.26	224.44	-28.30	84.51	-81.03	-93.08	-12.05
18	667.68	501.11	621.03	--	--	--	0.00	85.55	-53.77	-79.44	-25.67
19	667.68	503.93	622.55	--	--	--	0.00	85.60	-53.82	-88.90	-35.08
20	667.68	496.44	622.86	209.00	650.44	287.44	-28.74	85.47	-82.42	-85.83	-3.41
22	667.68	482.01	623.77	--	--	--	0.00	85.21	-53.43	-67.10	-13.67
23	667.68	493.32	624.38	262.00	645.13	231.32	-26.20	85.41	-79.83	-72.41	7.42
24	667.68	506.84	626.21	272.00	646.36	234.84	-25.83	85.65	-79.70	-72.69	7.01
26	667.68	611.38	624.38	534.00	638.86	77.38	-25.67	87.28	-81.16	-98.00	-16.84
28	667.68	576.68	624.38	542.00	638.54	34.68	-28.64	86.77	-83.63	-95.50	-11.87
30	667.68	646.93	625.30	541.00	638.66	105.93	-23.79	87.77	-79.78	-86.60	-6.82
31	667.68	645.06	625.91	--	--	--	0.00	87.74	-55.96	-71.90	-15.94
32	667.68	658.21	632.31	559.00	649.22	99.21	-26.06	87.92	-82.20	-77.31	4.89
34	667.68	750.24	628.65	555.00	638.86	195.24	-19.85	89.06	-77.13	-102.51	-25.38
36	667.68	749.97	628.35	608.00	637.31	141.97	-19.69	89.05	-76.96	-95.99	-19.03
37	667.68	814.92	631.39	714.00	640.01	100.92	-20.64	89.77	-78.63	-85.78	-7.15
38	667.68	702.97	633.53	--	--	--	0.00	88.49	-56.71	-72.78	-16.07
39	667.68	725.82	633.83	565.00	649.22	160.82	-23.52	88.77	-80.51	-92.51	-12.00
40	667.68	725.89	633.83	541.00	649.22	184.89	-23.10	88.77	-80.09	-81.42	-1.33
41	667.68	736.20	634.14	542.00	649.22	194.20	-22.77	88.89	-79.88	-89.11	-9.23
44	667.68	698.20	633.22	615.00	660.84	83.20	-30.92	88.43	-87.58	-89.13	-1.55

45	667.68	801.68	638.71	748.00	648.61	53.68	-23.67	89.63	-81.52	-83.55	-2.03
46	667.68	856.64	642.06	722.00	648.61	134.64	-16.88	90.21	-75.31	-98.70	-23.39
49	667.68	964.43	643.28	754.00	648.61	210.43	-14.10	91.24	-73.56	-86.92	-13.36
50	667.68	958.40	643.28	749.00	648.61	209.40	-14.12	91.18	-73.52	-100.98	-27.46
51	667.68	941.05	642.98	795.00	656.23	146.05	-22.29	91.02	-81.53	-90.13	-8.60
53	667.68	864.88	637.79	551.00	649.22	313.88	-19.35	90.29	-77.86	-85.26	-7.40
54	667.68	844.35	636.27	616.00	649.22	228.35	-20.78	90.08	-79.08	-77.89	1.19
55	667.68	813.49	660.65	--	--	--	0.00	89.76	-57.98	-73.96	-15.98
56	667.68	780.70	634.75	568.00	649.22	212.70	-22.07	89.40	-79.69	-88.85	-9.16
58	667.68	1002.58	641.45	732.00	648.61	270.58	-15.44	91.57	-75.24	-98.73	-23.49
59	667.68	1016.16	640.23	899.00	660.50	117.16	-26.73	91.69	-86.64	-98.18	-11.54
60	667.68	1033.42	638.40	607.00	662.64	426.42	-24.45	91.84	-84.51	-98.67	-14.16
61	667.68	1054.76	636.57	929.00	651.36	125.76	-23.70	92.01	-83.94	-84.42	-0.48
63	667.68	1052.07	636.27	--	--	--	0.00	91.99	-60.21	-82.69	-22.48
64	667.68	1007.46	635.36	783.00	649.76	224.46	-21.51	91.62	-81.34	-83.22	-1.88
65	667.68	977.35	636.27	861.00	651.36	116.35	-24.22	91.35	-83.79	-81.80	1.99
66	667.68	972.20	637.79	--	--	--	0.00	91.31	-59.53	-83.26	-23.73
67	667.68	914.25	637.18	--	--	--	0.00	90.77	-58.99	-87.51	-28.52
68	667.68	835.14	637.49	579.00	646.79	256.14	-17.95	89.99	-76.16	-78.12	-1.96
69	667.68	879.28	642.67	754.00	648.61	125.28	-16.32	90.43	-74.97	-92.60	-17.63
70	667.68	853.70	642.67	822.00	655.71	31.70	-28.21	90.18	-86.60	-92.05	-5.45
71	667.68	805.38	635.05	566.00	649.22	239.38	-21.52	89.67	-79.41	-93.53	-14.12
73	667.68	779.85	634.75	572.00	649.22	207.85	-22.13	89.39	-79.75	-83.16	-3.41
74	667.68	797.47	634.75	545.00	649.22	252.47	-21.60	89.59	-79.40	-88.31	-8.91
75	667.68	811.71	635.05	543.00	649.22	268.71	-21.23	89.74	-79.19	-92.87	-13.68
76	667.68	808.19	635.05	562.00	649.22	246.19	-21.44	89.70	-79.37	-80.57	-1.20
77	667.68	805.96	635.36	675.00	641.30	130.96	-16.24	89.68	-74.14	-77.42	-3.28
78	667.68	847.19	635.66	--	--	--	0.00	90.11	-58.33	-83.43	-25.10
79	667.68	895.79	637.79	813.00	658.01	82.79	-28.11	90.60	-86.92	-91.84	-4.92
83	667.68	71.85	624.38	--	--	--	0.00	68.68	-36.90	-80.45	-43.55
84	667.68	74.22	627.43	--	--	--	0.00	68.96	-37.18	-50.26	-13.08
85	667.68	106.20	627.74	--	--	--	0.00	72.07	-40.29	-55.79	-15.50
87	667.68	209.18	623.47	--	--	--	0.00	77.96	-46.18	-59.50	-13.32
88	667.68	287.64	622.86	--	--	--	0.00	80.73	-48.95	-65.65	-16.70
89	667.68	336.92	620.73	--	--	--	0.00	82.10	-50.32	-57.91	-7.59
90	667.68	417.55	619.51	--	--	--	0.00	83.97	-52.19	-66.30	-14.11
94	667.68	679.52	628.65	--	--	--	0.00	88.20	-56.42	-67.09	-10.67
95	667.68	806.24	625.60	--	--	--	0.00	89.68	-57.90	-71.02	-13.12
96	667.68	864.60	622.55	--	--	--	0.00	90.29	-58.51	-78.51	-20.00
97	667.68	902.53	619.81	--	--	--	0.00	90.66	-58.88	-86.56	-27.68

98	667.68	936.26	620.12	834.00	625.31	102.26	-15.93	90.98	-75.13	-95.84	-20.71
99	667.68	960.22	621.94	--	--	--	0.00	91.20	-59.42	-80.10	-20.68
101	667.68	975.77	633.53	--	--	--	0.00	91.34	-59.56	-72.58	-13.02
104	667.68	835.18	632.31	--	--	--	0.00	89.99	-58.21	-70.85	-12.64
106	667.68	750.64	628.65	--	--	--	0.00	89.06	-57.28	-65.63	-8.35
107	667.68	658.58	626.82	--	--	--	0.00	87.92	-56.14	-67.07	-10.93
109	667.68	612.82	618.59	562.00	624.50	50.82	-20.04	87.30	-75.56	-78.25	-2.69

B.3b 2.4 GHz: single blockage, without Fresnel zones and with interpolation.

Receiver Location Number	Tower Height (m)	Path Length (m)	Receiver Height (m)	D1 (m)	Blockage Height (m)	D2 (m)	Diffraction Gain (dB)	Path Loss (dBm)	Predicted Received Power (dBm)	Measured Received Power (dBm)	Difference (dB)
1	667.31	57.15	623.32	4.00	664.36	53.15	-51.56	75.19	-88.75	-47.66	41.09
2	667.31	196.74	623.62	--	--	--	0.00	85.93	-47.93	-63.80	-15.87
3	667.31	307.10	622.71	--	--	--	0.00	89.80	-51.80	-55.63	-3.83
4	667.31	329.40	626.06	--	--	--	0.00	90.41	-52.41	-70.42	-18.01
5	667.31	339.46	628.80	--	--	--	0.00	90.67	-52.67	-54.19	-1.52
6	667.31	348.59	631.24	--	--	--	0.00	90.90	-52.90	-62.55	-9.65
7	667.31	386.19	636.42	--	--	--	0.00	91.79	-53.79	-69.95	-16.16
8	667.31	381.52	637.34	--	--	--	0.00	91.68	-53.68	-61.05	-7.37
9	667.31	460.90	638.56	--	--	--	0.00	93.32	-55.32	-64.53	-9.21
10	667.31	456.55	636.42	--	--	--	0.00	93.24	-55.24	-58.17	-2.93
11	667.31	514.73	635.20	--	--	--	0.00	94.28	-56.28	-64.73	-8.45
12	667.31	550.23	633.07	--	--	--	0.00	94.86	-56.86	-74.22	-17.36
13	667.31	510.00	632.76	--	--	--	0.00	94.20	-56.20	-60.70	-4.50
14	667.31	481.50	627.28	--	--	--	0.00	93.70	-55.70	-57.72	-2.02
15	667.31	453.34	627.28	--	--	--	0.00	93.18	-55.18	-69.44	-14.26
16	667.31	118.42	624.54	15.00	665.07	103.42	-45.99	81.52	-89.51	-71.18	18.33
17	667.31	124.37	624.54	9.00	665.07	115.37	-47.94	81.95	-91.89	-69.11	22.78
18	667.31	128.78	624.84	9.00	665.07	119.78	-47.86	82.25	-92.11	-84.32	7.79
19	667.31	145.90	624.54	23.00	665.07	122.90	-44.29	83.33	-89.62	-77.79	11.83
20	667.31	179.62	623.93	24.00	665.07	155.62	-44.11	85.14	-91.25	-85.31	5.94
21	667.31	169.65	624.23	13.00	665.07	156.65	-46.43	84.64	-93.07	-80.72	12.35
22	667.31	155.54	625.14	10.00	665.07	145.54	-47.31	83.89	-93.20	-77.74	15.46
23	667.31	179.20	625.75	10.00	665.07	169.20	-47.14	85.12	-94.26	-72.74	21.52

24	667.31	189.35	624.54	10.00	665.07	179.35	-47.39	85.60	-94.99	-65.12	29.87
25	667.31	199.34	623.93	11.00	665.07	188.34	-47.12	86.04	-95.16	-76.23	18.93
26	667.31	229.97	623.93	19.00	665.07	210.97	-44.87	87.29	-94.16	-75.34	18.82
27	667.31	257.48	624.84	19.00	665.07	238.48	-44.64	88.27	-94.90	-79.12	15.78
28	667.31	217.58	624.54	19.00	665.07	198.58	-44.77	86.80	-93.57	-72.95	20.62
29	667.31	200.02	627.28	12.00	665.07	188.02	-46.03	86.07	-94.10	-78.53	15.57
30	667.31	196.25	627.28	--	--	--	0.00	85.91	-47.91	-57.74	-9.83
31	667.31	249.64	630.63	--	--	--	0.00	88.00	-50.00	-55.06	-5.06
32	667.31	263.24	631.85	--	--	--	0.00	88.46	-50.46	-59.07	-8.61
33	667.31	275.16	631.85	--	--	--	0.00	88.84	-50.84	-57.29	-6.45
34	667.31	237.22	629.11	--	--	--	0.00	87.56	-49.56	-52.32	-2.76
35	667.31	216.60	628.80	--	--	--	0.00	86.77	-48.77	-51.47	-2.70
36	667.31	209.74	628.50	--	--	--	0.00	86.49	-48.49	-48.02	0.47
37	667.31	207.07	627.89	19.00	665.07	188.07	-44.04	86.37	-92.41	-89.56	2.85
38	667.31	214.18	630.63	61.00	665.07	153.18	-39.34	86.67	-88.01	-77.60	10.41
39	667.31	221.94	632.16	62.00	664.29	159.94	-38.64	86.98	-87.62	-56.37	31.25
40	667.31	226.62	633.37	--	--	--	0.00	87.16	-49.16	-54.63	-5.47
41	667.31	231.19	634.29	--	--	--	0.00	87.33	-49.33	-62.69	-13.36
42	667.31	237.73	634.59	--	--	--	0.00	87.57	-49.57	-55.67	-6.10
43	667.31	317.68	635.51	236.00	658.98	81.68	-34.58	90.09	-86.67	-101.01	-14.34
44	667.31	259.36	634.90	218.00	640.08	41.36	-23.88	88.33	-74.21	-84.96	-10.75
45	667.31	250.07	633.07	--	--	--	0.00	88.01	-50.01	-97.13	-47.12
46	667.31	232.23	631.85	165.00	647.09	67.23	-31.87	87.37	-81.24	-91.86	-10.62
47	667.31	223.83	630.63	208.00	643.02	15.83	-35.19	87.05	-84.24	-63.81	20.43
48	667.31	151.81	630.02	74.00	649.53	77.81	-35.01	83.68	-80.69	-68.13	12.56
49	667.31	142.89	628.50	85.00	649.53	57.89	-36.09	83.15	-81.24	-83.90	-2.66
50	667.31	128.13	631.24	69.00	649.53	59.13	-35.21	82.21	-79.42	-75.01	4.41
51	667.31	204.66	628.80	175.00	638.92	29.66	-31.06	86.27	-79.34	-95.17	-15.83
52	667.31	40.45	627.58	26.00	643.82	14.45	-39.53	72.19	-73.72	-47.05	26.67
53	667.31	323.89	627.28	164.00	647.09	159.89	-31.86	90.26	-84.12	-95.87	-11.75
54	667.31	363.61	623.62	271.00	646.71	92.61	-33.88	91.26	-87.14	-84.27	2.87
55	667.31	428.04	622.40	--	--	--	0.00	92.68	-54.68	-73.86	-19.18
56	667.31	510.48	623.01	--	--	--	0.00	94.21	-56.21	-72.33	-16.12
57	667.31	501.79	622.71	--	--	--	0.00	94.06	-56.06	-84.38	-28.32
58	667.31	304.96	625.45	--	--	--	0.00	89.74	-51.74	-65.36	-13.62
59	667.31	303.98	626.06	227.00	650.44	76.98	-35.15	89.71	-86.86	-88.31	-1.45
60	667.31	323.97	625.14	177.00	644.35	146.97	-31.62	90.26	-83.88	-86.40	-2.52
61	667.31	352.86	623.93	222.00	645.26	130.86	-32.43	91.00	-85.43	-99.79	-14.36
62	667.31	400.19	620.57	295.00	638.63	105.19	-31.24	92.10	-85.34	-96.65	-11.31
63	667.31	498.44	620.27	--	--	--	0.00	94.00	-56.00	-90.13	-34.13

B.3c 24.12 GHz: single blockage, without Fresnel zones and with interpolation.

Receiver Location Number	Tower Height (m)	Path Length (m)	Receiver Height (m)	D1 (m)	Blockage Height (m)	D2 (m)	Diffraction Gain (dB)	Path Loss (dBm)	Predicted Received Power (dBm)	Measured Received Power (dBm)	Difference (dB)
3	666.07	207.64	630.63	61.00	665.07	146.64	-49.42	106.44	-110.86	-98	12.86
10	666.07	240.35	635.20	--	--	--	0.00	107.71	-62.71	-92	-29.29
11	666.07	215.08	635.51	147.00	645.26	68.08	-38.13	106.75	-99.88	-89	10.88
14	666.07	381.85	640.38	226.00	658.98	155.85	-40.76	111.73	-107.49	-94	13.49
16	666.07	469.49	639.47	--	--	--	0.00	113.53	-68.53	-94	-25.47
22	666.07	75.82	646.18	--	--	--	0.00	97.69	-52.69	-58	-5.31
23	666.07	344.92	628.50	--	--	--	0.00	110.85	-65.85	-87	-21.15
24	666.07	413.01	629.72	--	--	--	0.00	112.41	-67.41	-90	-22.59
25	666.07	490.30	629.41	--	--	--	0.00	113.90	-68.90	-93	-24.10
26	666.07	453.69	627.58	277.00	646.73	176.69	-40.34	113.23	-108.57	-97	11.57
27	666.07	495.19	624.23	270.00	646.45	225.19	-41.07	113.99	-110.06	-94	16.06
31	666.07	434.89	622.71	192.00	646.93	242.89	-42.40	112.86	-110.27	-84	26.27
32	666.07	391.98	622.40	--	--	--	0.00	111.96	-66.96	-81	-14.04
33	666.07	391.49	623.32	259.00	646.79	132.49	-43.00	111.95	-109.95	-99	10.95
34	666.07	332.85	623.93	157.00	647.09	175.85	-43.13	110.54	-108.67	-87	21.67
36	666.07	261.41	633.68	218.00	648.00	43.41	-42.56	108.44	-106.00	-102	4.00
37	666.07	156.05	634.29	103.00	645.26	53.05	-40.39	103.96	-99.35	-84	15.35
38	666.07	115.33	632.76	68.00	646.48	47.33	-43.31	101.33	-99.64	-89	10.64
39	666.07	167.31	634.29	121.00	645.26	46.31	-40.58	104.57	-100.14	-101	-0.86
40	666.07	169.30	631.55	100.00	646.48	69.30	-42.39	104.67	-102.05	-84	18.05
41	666.07	252.00	630.33	180.00	644.35	72.00	-40.85	108.12	-103.97	-100	3.97
42	666.07	283.64	626.97	204.00	644.35	79.64	-42.24	109.15	-106.39	-101	5.39
44	666.07	447.91	620.88	216.00	650.44	231.91	-43.95	113.12	-112.07	-101	11.07
45	666.07	554.65	650.14	--	--	--	0.00	114.98	-69.98	-96	-26.02
46	666.07	518.02	623.93	225.00	650.44	293.02	-42.45	114.38	-111.83	-104	7.83
47	666.07	561.28	625.14	--	--	--	0.00	115.08	-70.08	-97	-26.92
48	666.07	545.51	636.73	--	--	--	0.00	114.83	-69.83	-96	-26.17
49	666.07	463.79	619.05	219.00	645.26	244.79	-42.76	113.42	-111.19	-101	10.19
50	666.07	469.31	619.05	223.00	645.26	246.31	-42.71	113.52	-111.23	-101	10.23
51	666.07	492.00	620.27	--	--	--	0.00	113.93	-68.93	-97	-28.07
52	666.07	399.61	620.57	296.00	639.81	103.61	-41.86	112.13	-108.98	-97	11.98
53	666.07	322.03	625.14	174.00	644.35	148.03	-41.66	110.25	-106.91	-96	10.91
54	666.07	343.85	626.06	189.00	645.26	154.85	-41.39	110.82	-107.21	-100	7.21

B.3d 27.525 GHz: single blockage, without Fresnel zones and with interpolation.

Receiver Location Number	Tower Height (m)	Path Length (m)	Receiver Height (m)	D1 (m)	Blockage Height (m)	D2 (m)	Diffraction Gain (dB)	Path Loss (dBm)	Predicted Received Power (dBm)	Measured Received Power (dBm)	Difference (dB)
1	667.68	125.38	632.31	--	--	--	0.00	103.21	-32.41	-26.66	5.75
2	667.68	178.00	632.31	--	--	--	0.00	106.25	-35.45	-48.50	-13.05
4	667.68	316.75	625.91	201.00	644.35	115.75	-42.25	111.26	-82.71	-71.50	11.21
5	667.68	456.55	621.94	233.00	650.44	223.55	-44.12	114.43	-87.75	-77.20	10.55
6	667.68	557.16	625.60	--	--	--	0.00	116.16	-45.36	-80.00	-34.64
7	667.68	531.60	624.38	--	--	--	0.00	115.75	-44.95	-38.60	6.35
8	667.68	518.61	626.82	274.00	646.24	244.61	-40.24	115.54	-84.98	-66.20	18.78
9	667.68	444.91	627.13	262.00	646.79	182.91	-41.14	114.21	-84.55	-75.90	8.65
10	667.68	439.31	626.21	267.00	646.79	172.31	-41.66	114.10	-84.96	-59.90	25.06
11	667.68	407.95	624.08	263.00	646.59	144.95	-42.94	113.45	-85.59	-61.88	23.71
12	667.68	416.37	623.16	--	--	--	0.00	113.63	-42.83	-56.98	-14.15
14	667.68	395.00	622.55	210.00	650.44	185.00	-44.58	113.17	-86.95	-66.91	20.04
15	667.68	407.40	621.94	224.00	644.35	183.40	-42.57	113.44	-85.21	-74.17	11.04
16	667.68	420.04	621.03	--	--	--	0.00	113.71	-42.91	-70.00	-27.09
17	667.68	444.44	620.12	220.00	645.26	224.44	-43.15	114.20	-86.55	-86.94	-0.39
18	667.68	501.11	621.03	--	--	--	0.00	115.24	-44.44	-65.68	-21.24
19	667.68	503.93	622.55	--	--	--	0.00	115.29	-44.49	-72.62	-28.13
20	667.68	496.44	622.86	209.00	650.44	287.44	-43.58	115.16	-87.94	-60.45	27.49
22	667.68	482.01	623.77	--	--	--	0.00	114.90	-44.10	-32.74	11.36
23	667.68	493.32	624.38	262.00	645.13	231.32	-41.04	115.10	-85.35	-59.00	26.35
24	667.68	506.84	626.21	272.00	646.36	234.84	-40.67	115.34	-85.21	-69.58	15.63
26	667.68	611.38	624.38	534.00	638.86	77.38	-40.51	116.97	-86.68	-82.39	4.29
28	667.68	576.68	624.38	542.00	638.54	34.68	-43.48	116.46	-89.15	-87.14	2.01
30	667.68	646.93	625.30	541.00	638.66	105.93	-38.64	117.46	-85.30	-57.40	27.90
31	667.68	645.06	625.91	--	--	--	0.00	117.43	-46.63	-32.62	14.01
32	667.68	658.21	632.31	559.00	649.22	99.21	-40.91	117.61	-87.72	-40.43	47.29
34	667.68	750.24	628.65	555.00	638.86	195.24	-34.18	118.75	-82.13	-76.36	5.77
36	667.68	749.97	628.35	608.00	637.31	141.97	-34.04	118.74	-81.98	-101.86	-19.88
38	667.68	702.97	633.53	--	--	--	0.00	118.18	-47.38	-40.17	7.21
39	667.68	725.82	633.83	565.00	649.22	160.82	-38.37	118.46	-86.03	-66.25	19.78
40	667.68	725.89	633.83	541.00	649.22	184.89	-37.95	118.46	-85.61	-67.00	18.61
41	667.68	736.20	634.14	542.00	649.22	194.20	-37.62	118.58	-85.40	-83.00	2.40
44	667.68	698.20	633.22	615.00	660.84	83.20	-45.77	118.12	-93.09	-81.18	11.91
45	667.68	801.68	638.71	748.00	648.61	53.68	-38.52	119.32	-87.04	-80.62	6.42

46	667.68	856.64	642.06	722.00	648.61	134.64	-31.38	119.90	-80.47	-83.11	-2.64
49	667.68	964.43	643.28	754.00	648.61	210.43	-27.97	120.93	-78.10	-89.54	-11.44
50	667.68	958.40	643.28	749.00	648.61	209.40	-28.00	120.87	-78.07	-90.13	-12.06
51	667.68	941.05	642.98	795.00	656.23	146.05	-37.13	120.71	-87.05	-90.39	-3.34
53	667.68	864.88	637.79	551.00	649.22	313.88	-33.75	119.98	-82.93	-76.36	6.57
54	667.68	844.35	636.27	616.00	649.22	228.35	-35.63	119.77	-84.60	-64.15	20.45
55	667.68	813.49	660.65	--	--	--	0.00	119.45	-48.65	-45.81	2.84
56	667.68	780.70	634.75	568.00	649.22	212.70	-36.91	119.09	-85.21	-82.51	2.70
58	667.68	1002.58	641.45	732.00	648.61	270.58	-29.74	121.26	-80.21	-71.77	8.44
59	667.68	1016.16	640.23	899.00	660.50	117.16	-41.58	121.38	-92.16	-89.23	2.93
60	667.68	1033.42	638.40	607.00	662.64	426.42	-39.30	121.53	-90.02	-77.61	12.41
61	667.68	1054.76	636.57	929.00	651.36	125.76	-38.55	121.71	-89.45	-84.41	5.04
63	667.68	1052.07	636.27	--	--	--	0.00	121.68	-50.88	-79.56	-28.68
64	667.68	1007.46	635.36	783.00	649.76	224.46	-36.35	121.31	-86.86	-73.05	13.81
65	667.68	977.35	636.27	861.00	651.36	116.35	-39.06	121.04	-89.30	-79.65	9.65
66	667.68	972.20	637.79	--	--	--	0.00	121.00	-50.20	-68.57	-18.37
67	667.68	914.25	637.18	--	--	--	0.00	120.46	-49.66	-79.77	-30.11
68	667.68	835.14	637.49	579.00	646.79	256.14	-32.47	119.68	-81.35	-69.72	11.63
69	667.68	879.28	642.67	754.00	648.61	125.28	-30.77	120.12	-80.09	-74.94	5.15
70	667.68	853.70	642.67	822.00	655.71	31.70	-43.05	119.87	-92.12	-92.93	-0.81
71	667.68	805.38	635.05	566.00	649.22	239.38	-36.37	119.36	-84.93	-82.66	2.27
73	667.68	779.85	634.75	572.00	649.22	207.85	-36.98	119.08	-85.26	-79.05	6.21
74	667.68	797.47	634.75	545.00	649.22	252.47	-36.44	119.28	-84.92	-79.91	5.01
75	667.68	811.71	635.05	543.00	649.22	268.71	-36.08	119.43	-84.71	-73.79	10.92
76	667.68	808.19	635.05	562.00	649.22	246.19	-36.29	119.39	-84.88	-76.52	8.36
77	667.68	805.96	635.36	675.00	641.30	130.96	-30.68	119.37	-79.24	-64.30	14.94
78	667.68	847.19	635.66	--	--	--	0.00	119.80	-49.00	-77.70	-28.70
79	667.68	895.79	637.79	813.00	658.01	82.79	-42.95	120.29	-92.44	-79.47	12.97
83	667.68	71.85	624.38	--	--	--	0.00	98.37	-27.57	-53.13	-25.56
84	667.68	74.22	627.43	--	--	--	0.00	98.65	-27.85	-21.34	6.51
85	667.68	106.20	627.74	--	--	--	0.00	101.76	-30.96	-38.73	-7.77
87	667.68	209.18	623.47	--	--	--	0.00	107.65	-36.85	-25.16	11.69
88	667.68	287.64	622.86	--	--	--	0.00	110.42	-39.62	-30.56	9.06
89	667.68	336.92	620.73	--	--	--	0.00	111.79	-40.99	-40.70	0.29
90	667.68	417.55	619.51	--	--	--	0.00	113.66	-42.86	-53.55	-10.69
94	667.68	679.52	628.65	--	--	--	0.00	117.89	-47.09	-37.14	9.95
95	667.68	806.24	625.60	--	--	--	0.00	119.37	-48.57	-39.66	8.91
96	667.68	864.60	622.55	--	--	--	0.00	119.98	-49.18	-55.79	-6.61
97	667.68	902.53	619.81	--	--	--	0.00	120.35	-49.55	-61.26	-11.71
98	667.68	936.26	620.12	834.00	625.31	102.26	-30.32	120.67	-80.19	-71.54	8.65

99	667.68	960.22	621.94	--	--	--	0.00	120.89	-50.09	-44.00	6.09
101	667.68	975.77	633.53	--	--	--	0.00	121.03	-50.23	-46.26	3.97
104	667.68	835.18	632.31	--	--	--	0.00	119.68	-48.88	-43.72	5.16
106	667.68	750.64	628.65	--	--	--	0.00	118.75	-47.95	-40.63	7.32
107	667.68	658.58	626.82	--	--	--	0.00	117.61	-46.81	-35.93	10.88
109	667.68	612.82	618.59	562.00	624.50	50.82	-34.34	116.99	-80.53	-72.41	8.12

B.4a 902 MHz: single blockage, with Fresnel zones and with interpolation.

Receiver Location Number	Tower Height (m)	Path Length (m)	Receiver Height (m)	D1 (m)	Blockage Height (m)	D2 (m)	Diffraction Gain (dB)	Path Loss (dBm)	Predicted Received Power (dBm)	Measured Received Power (dBm)	Difference (dB)
1	667.68	125.38	632.31	--	--	--	0.00	73.52	-41.74	-50.80	-9.06
2	667.68	178.00	632.31	--	--	--	0.00	76.56	-44.78	-65.00	-20.22
4	667.68	316.75	625.91	201.00	644.35	115.75	-27.41	81.57	-77.19	-76.80	0.39
5	667.68	456.55	621.94	233.00	650.44	223.55	-28.05	84.74	-81.01	-82.50	-1.49
6	667.68	557.16	625.60	--	--	--	0.00	86.47	-54.69	-74.50	-19.81
7	667.68	531.60	624.38	--	--	--	0.00	86.06	-54.28	-68.70	-14.42
8	667.68	518.61	626.82	274.00	646.24	244.61	-25.28	85.85	-79.34	-85.60	-6.26
9	667.68	444.91	627.13	262.00	646.79	182.91	-26.30	84.52	-79.04	-79.10	-0.06
10	667.68	439.31	626.21	267.00	646.79	172.31	-26.82	84.41	-79.44	-74.80	4.64
11	667.68	407.95	624.08	263.00	646.59	144.95	-28.09	83.76	-80.08	-73.15	6.93
12	667.68	416.37	623.16	--	--	--	0.00	83.94	-52.16	-63.58	-11.42
14	667.68	395.00	622.55	210.00	650.44	185.00	-27.57	83.48	-79.28	-82.18	-2.90
15	667.68	407.40	621.94	224.00	644.35	183.40	-27.68	83.75	-79.65	-82.72	-3.07
16	667.68	420.04	621.03	--	--	--	0.00	84.02	-52.24	-86.75	-34.51
17	667.68	444.44	620.12	220.00	645.26	224.44	-28.32	84.51	-81.05	-93.08	-12.03
18	667.68	501.11	621.03	--	--	--	0.00	85.55	-53.77	-79.44	-25.67
19	667.68	503.93	622.55	--	--	--	0.00	85.60	-53.82	-88.90	-35.08
20	667.68	496.44	622.86	209.00	650.44	287.44	-28.74	85.47	-82.42	-85.83	-3.41
22	667.68	482.01	623.77	--	--	--	0.00	85.21	-53.43	-67.10	-13.67
23	667.68	493.32	624.38	262.00	645.13	231.32	-25.98	85.41	-79.61	-72.41	7.20
24	667.68	506.84	626.21	272.00	646.36	234.84	-25.41	85.65	-79.28	-72.69	6.59
26	667.68	611.38	624.38	534.00	638.86	77.38	-25.67	87.28	-81.16	-98.00	-16.84
28	667.68	576.68	624.38	542.00	638.54	34.68	-28.64	86.77	-83.63	-95.50	-11.87
30	667.68	646.93	625.30	541.00	638.66	105.93	-23.79	87.77	-79.78	-86.60	-6.82
31	667.68	645.06	625.91	--	--	--	0.00	87.74	-55.96	-71.90	-15.94
32	667.68	658.21	632.31	559.00	649.22	99.21	-26.06	87.92	-82.20	-77.31	4.89

34	667.68	750.24	628.65	555.00	638.86	195.24	-19.82	89.06	-77.09	-102.51	-25.42
36	667.68	749.97	628.35	608.00	637.31	141.97	-17.90	89.05	-75.17	-95.99	-20.82
37	667.68	814.92	631.39	714.00	640.01	100.92	-20.64	89.77	-78.63	-85.78	-7.15
38	667.68	702.97	633.53	--	--	--	0.00	88.49	-56.71	-72.78	-16.07
39	667.68	725.82	633.83	565.00	649.22	160.82	-23.52	88.77	-80.51	-92.51	-12.00
40	667.68	725.89	633.83	541.00	649.22	184.89	-23.10	88.77	-80.09	-81.42	-1.33
41	667.68	736.20	634.14	542.00	649.22	194.20	-22.77	88.89	-79.88	-89.11	-9.23
44	667.68	698.20	633.22	615.00	660.84	83.20	-15.53	88.43	-72.18	-89.13	-16.95
45	667.68	801.68	638.71	748.00	648.61	53.68	-23.67	89.63	-81.52	-83.55	-2.03
46	667.68	856.64	642.06	722.00	648.61	134.64	-16.88	90.21	-75.31	-98.70	-23.39
49	667.68	964.43	643.28	741.00	648.61	223.43	-14.26	91.24	-73.72	-86.92	-13.20
50	667.68	958.40	643.28	748.00	648.61	210.40	-14.11	91.18	-73.51	-100.98	-27.47
51	667.68	941.05	642.98	795.00	656.23	146.05	-22.29	91.02	-81.53	-90.13	-8.60
53	667.68	864.88	637.79	551.00	649.22	313.88	-19.35	90.29	-77.86	-85.26	-7.40
54	667.68	844.35	636.27	616.00	649.22	228.35	-20.78	90.08	-79.08	-77.89	1.19
55	667.68	813.49	660.65	--	--	--	0.00	89.76	-57.98	-73.96	-15.98
56	667.68	780.70	634.75	568.00	649.22	212.70	-22.07	89.40	-79.69	-88.85	-9.16
58	667.68	1002.58	641.45	732.00	648.61	270.58	-15.41	91.57	-75.21	-98.73	-23.52
59	667.68	1016.16	640.23	899.00	660.50	117.16	-26.73	91.69	-86.64	-98.18	-11.54
60	667.68	1033.42	638.40	607.00	662.64	426.42	-24.45	91.84	-84.51	-98.67	-14.16
61	667.68	1054.76	636.57	929.00	651.36	125.76	-23.70	92.01	-83.94	-84.42	-0.48
63	667.68	1052.07	636.27	--	--	--	0.00	91.99	-60.21	-82.69	-22.48
64	667.68	1007.46	635.36	783.00	649.76	224.46	-21.51	91.62	-81.34	-83.22	-1.88
65	667.68	977.35	636.27	861.00	651.36	116.35	-24.22	91.35	-83.79	-81.80	1.99
66	667.68	972.20	637.79	--	--	--	0.00	91.31	-59.53	-83.26	-23.73
67	667.68	914.25	637.18	--	--	--	0.00	90.77	-58.99	-87.51	-28.52
68	667.68	835.14	637.49	578.00	646.79	257.14	-17.94	89.99	-76.15	-78.12	-1.97
69	667.68	879.28	642.67	754.00	648.61	125.28	-16.32	90.43	-74.97	-92.60	-17.63
70	667.68	853.70	642.67	822.00	655.71	31.70	-28.21	90.18	-86.60	-92.05	-5.45
71	667.68	805.38	635.05	566.00	649.22	239.38	-21.52	89.67	-79.41	-93.53	-14.12
73	667.68	779.85	634.75	572.00	649.22	207.85	-22.13	89.39	-79.75	-83.16	-3.41
74	667.68	797.47	634.75	545.00	649.22	252.47	-21.60	89.59	-79.40	-88.31	-8.91
75	667.68	811.71	635.05	543.00	649.22	268.71	-21.23	89.74	-79.19	-92.87	-13.68
76	667.68	808.19	635.05	562.00	649.22	246.19	-19.44	89.70	-77.36	-80.57	-3.21
77	667.68	805.96	635.36	675.00	641.30	130.96	-15.86	89.68	-73.75	-77.42	-3.67
78	667.68	847.19	635.66	--	--	--	0.00	90.11	-58.33	-83.43	-25.10
79	667.68	895.79	637.79	813.00	658.01	82.79	-12.69	90.60	-71.51	-91.84	-20.33
83	667.68	71.85	624.38	--	--	--	0.00	68.68	-36.90	-80.45	-43.55
84	667.68	74.22	627.43	--	--	--	0.00	68.96	-37.18	-50.26	-13.08
85	667.68	106.20	627.74	--	--	--	0.00	72.07	-40.29	-55.79	-15.50

87	667.68	209.18	623.47	--	--	--	0.00	77.96	-46.18	-59.50	-13.32
88	667.68	287.64	622.86	--	--	--	0.00	80.73	-48.95	-65.65	-16.70
89	667.68	336.92	620.73	--	--	--	0.00	82.10	-50.32	-57.91	-7.59
90	667.68	417.55	619.51	--	--	--	0.00	83.97	-52.19	-66.30	-14.11
94	667.68	679.52	628.65	--	--	--	0.00	88.20	-56.42	-67.09	-10.67
95	667.68	806.24	625.60	--	--	--	0.00	89.68	-57.90	-71.02	-13.12
96	667.68	864.60	622.55	--	--	--	0.00	90.29	-58.51	-78.51	-20.00
97	667.68	902.53	619.81	--	--	--	0.00	90.66	-58.88	-86.56	-27.68
98	667.68	936.26	620.12	799.00	626.62	137.26	-16.69	90.98	-75.89	-95.84	-19.95
99	667.68	960.22	621.94	--	--	--	0.00	91.20	-59.42	-80.10	-20.68
101	667.68	975.77	633.53	--	--	--	0.00	91.34	-59.56	-72.58	-13.02
104	667.68	835.18	632.31	--	--	--	0.00	89.99	-58.21	-70.85	-12.64
106	667.68	750.64	628.65	--	--	--	0.00	89.06	-57.28	-65.63	-8.35
107	667.68	658.58	626.82	--	--	--	0.00	87.92	-56.14	-67.07	-10.93
109	667.68	612.82	618.59	562.00	624.50	50.82	-20.04	87.30	-75.56	-78.25	-2.69

B.4b 2.4 GHz: single blockage, with Fresnel zones and with interpolation.

Receiver Location Number	Tower Height (m)	Path Length (m)	Receiver Height (m)	D1 (m)	Blockage Height (m)	D2 (m)	Diffraction Gain (dB)	Path Loss (dBm)	Predicted Received Power (dBm)	Measured Received Power (dBm)	Difference (dB)
1	667.31	57.15	623.32	4.00	664.36	53.15	-51.56	75.19	-88.75	-47.66	41.09
2	667.31	196.74	623.62	--	--	--	0.00	85.93	-47.93	-63.80	-15.87
3	667.31	307.10	622.71	--	--	--	0.00	89.80	-51.80	-55.63	-3.83
4	667.31	329.40	626.06	--	--	--	0.00	90.41	-52.41	-70.42	-18.01
5	667.31	339.46	628.80	--	--	--	0.00	90.67	-52.67	-54.19	-1.52
6	667.31	348.59	631.24	--	--	--	0.00	90.90	-52.90	-62.55	-9.65
7	667.31	386.19	636.42	--	--	--	0.00	91.79	-53.79	-69.95	-16.16
8	667.31	381.52	637.34	--	--	--	0.00	91.68	-53.68	-61.05	-7.37
9	667.31	460.90	638.56	--	--	--	0.00	93.32	-55.32	-64.53	-9.21
10	667.31	456.55	636.42	--	--	--	0.00	93.24	-55.24	-58.17	-2.93
11	667.31	514.73	635.20	--	--	--	0.00	94.28	-56.28	-64.73	-8.45
12	667.31	550.23	633.07	--	--	--	0.00	94.86	-56.86	-74.22	-17.36
13	667.31	510.00	632.76	--	--	--	0.00	94.20	-56.20	-60.70	-4.50
14	667.31	481.50	627.28	--	--	--	0.00	93.70	-55.70	-57.72	-2.02
15	667.31	453.34	627.28	--	--	--	0.00	93.18	-55.18	-69.44	-14.26
16	667.31	118.42	624.54	15.00	665.07	103.42	-45.99	81.52	-89.51	-71.18	18.33
17	667.31	124.37	624.54	9.00	665.07	115.37	-47.94	81.95	-91.89	-69.11	22.78

18	667.31	128.78	624.84	9.00	665.07	119.78	-47.86	82.25	-92.11	-84.32	7.79
19	667.31	145.90	624.54	23.00	665.07	122.90	-44.29	83.33	-89.62	-77.79	11.83
20	667.31	179.62	623.93	24.00	665.07	155.62	-47.97	85.14	-95.11	-85.31	9.80
21	667.31	169.65	624.23	13.00	665.07	156.65	-46.43	84.64	-93.07	-80.72	12.35
22	667.31	155.54	625.14	8.00	665.07	147.54	-48.22	83.89	-94.11	-77.74	16.37
23	667.31	179.20	625.75	10.00	665.07	169.20	-47.14	85.12	-94.26	-72.74	21.52
24	667.31	189.35	624.54	10.00	665.07	179.35	-47.39	85.60	-94.99	-65.12	29.87
25	667.31	199.34	623.93	10.00	665.07	189.34	-47.51	86.04	-95.56	-76.23	19.33
26	667.31	229.97	623.93	19.00	665.07	210.97	-44.87	87.29	-94.16	-75.34	18.82
27	667.31	257.48	624.84	19.00	665.07	238.48	-46.18	88.27	-96.44	-79.12	17.32
28	667.31	217.58	624.54	19.00	665.07	198.58	-46.97	86.80	-95.77	-72.95	22.82
29	667.31	200.02	627.28	11.00	665.07	189.02	-46.38	86.07	-94.45	-78.53	15.92
30	667.31	196.25	627.28	--	--	--	0.00	85.91	-47.91	-57.74	-9.83
31	667.31	249.64	630.63	--	--	--	0.00	88.00	-50.00	-55.06	-5.06
32	667.31	263.24	631.85	--	--	--	0.00	88.46	-50.46	-59.07	-8.61
33	667.31	275.16	631.85	--	--	--	0.00	88.84	-50.84	-57.29	-6.45
34	667.31	237.22	629.11	--	--	--	0.00	87.56	-49.56	-52.32	-2.76
35	667.31	216.60	628.80	--	--	--	0.00	86.77	-48.77	-51.47	-2.70
36	667.31	209.74	628.50	--	--	--	0.00	86.49	-48.49	-48.02	0.47
37	667.31	207.07	627.89	19.00	665.07	188.07	-44.04	86.37	-92.41	-89.56	2.85
38	667.31	214.18	630.63	61.00	665.07	153.18	-39.34	86.67	-88.01	-77.60	10.41
39	667.31	221.94	632.16	62.00	664.29	159.94	-38.64	86.98	-87.62	-56.37	31.25
40	667.31	226.62	633.37	--	--	--	0.00	87.16	-49.16	-54.63	-5.47
41	667.31	231.19	634.29	--	--	--	0.00	87.33	-49.33	-62.69	-13.36
42	667.31	237.73	634.59	--	--	--	0.00	87.57	-49.57	-55.67	-6.10
43	667.31	317.68	635.51	236.00	658.98	81.68	-34.58	90.09	-86.67	-101.01	-14.34
44	667.31	259.36	634.90	217.00	640.08	42.36	-23.79	88.33	-74.12	-84.96	-10.84
45	667.31	250.07	633.07	--	--	--	0.00	88.01	-50.01	-97.13	-47.12
46	667.31	232.23	631.85	165.00	647.09	67.23	-31.87	87.37	-81.24	-91.86	-10.62
47	667.31	223.83	630.63	208.00	643.02	15.83	-35.19	87.05	-84.24	-63.81	20.43
48	667.31	151.81	630.02	72.00	649.53	79.81	-35.02	83.68	-80.70	-68.13	12.57
49	667.31	142.89	628.50	85.00	649.53	57.89	-35.96	83.15	-81.12	-83.90	-2.78
50	667.31	128.13	631.24	69.00	649.53	59.13	-35.19	82.21	-79.39	-75.01	4.38
51	667.31	204.66	628.80	175.00	638.92	29.66	-31.06	86.27	-79.34	-95.17	-15.83
52	667.31	40.45	627.58	26.00	643.82	14.45	-39.53	72.19	-73.72	-47.05	26.67
53	667.31	323.89	627.28	163.00	647.09	160.89	-31.86	90.26	-84.12	-95.87	-11.75
54	667.31	363.61	623.62	271.00	646.71	92.61	-33.88	91.26	-87.14	-84.27	2.87
55	667.31	428.04	622.40	193.00	646.97	235.04	-32.56	92.68	-87.24	-73.86	13.38
56	667.31	510.48	623.01	--	--	--	0.00	94.21	-56.21	-72.33	-16.12
57	667.31	501.79	622.71	--	--	--	0.00	94.06	-56.06	-84.38	-28.32

58	667.31	304.96	625.45	--	--	--	0.00	89.74	-51.74	-65.36	-13.62
59	667.31	303.98	626.06	227.00	650.44	76.98	-31.49	89.71	-83.20	-88.31	-5.11
60	667.31	323.97	625.14	177.00	644.35	146.97	-31.62	90.26	-83.88	-86.40	-2.52
61	667.31	352.86	623.93	222.00	645.26	130.86	-32.43	91.00	-85.43	-99.79	-14.36
62	667.31	400.19	620.57	295.00	638.63	105.19	-27.90	92.10	-82.00	-96.65	-14.65
63	667.31	498.44	620.27	--	--	--	0.00	94.00	-56.00	-90.13	-34.13

B.4c 24.12 GHz: single blockage, with Fresnel zones and with interpolation.

Receiver Location Number	Tower Height (m)	Path Length (m)	Receiver Height (m)	D1 (m)	Blockage Height (m)	D2 (m)	Diffraction Gain (dB)	Path Loss (dBm)	Predicted Received Power (dBm)	Measured Received Power (dBm)	Difference (dB)
3	666.07	207.64	630.63	49.00	665.07	158.64	-50.03	106.44	-111.47	-98	13.47
10	666.07	240.35	635.20	--	--	--	0.00	107.71	-62.71	-92	-29.29
11	666.07	215.08	635.51	147.00	645.26	68.08	-38.13	106.75	-99.88	-89	10.88
14	666.07	381.85	640.38	226.00	658.98	155.85	-40.76	111.73	-107.49	-94	13.49
16	666.07	469.49	639.47	--	--	--	0.00	113.53	-68.53	-94	-25.47
22	666.07	75.82	646.18	--	--	--	0.00	97.69	-52.69	-58	-5.31
23	666.07	344.92	628.50	--	--	--	0.00	110.85	-65.85	-87	-21.15
24	666.07	413.01	629.72	--	--	--	0.00	112.41	-67.41	-90	-22.59
25	666.07	490.30	629.41	--	--	--	0.00	113.90	-68.90	-93	-24.10
26	666.07	453.69	627.58	277.00	646.73	176.69	-40.34	113.23	-108.57	-97	11.57
27	666.07	495.19	624.23	270.00	646.45	225.19	-41.07	113.99	-110.06	-94	16.06
31	666.07	434.89	622.71	192.00	646.93	242.89	-42.40	112.86	-110.27	-84	26.27
32	666.07	391.98	622.40	--	--	--	0.00	111.96	-66.96	-81	-14.04
33	666.07	391.49	623.32	259.00	646.79	132.49	-43.00	111.95	-109.95	-99	10.95
34	666.07	332.85	623.93	157.00	647.09	175.85	-43.13	110.54	-108.67	-87	21.67
36	666.07	261.41	633.68	218.00	648.00	43.41	-42.56	108.44	-106.00	-102	4.00
37	666.07	156.05	634.29	102.00	645.26	54.05	-40.35	103.96	-99.31	-84	15.31
38	666.07	115.33	632.76	68.00	646.48	47.33	-43.31	101.33	-99.64	-89	10.64
39	666.07	167.31	634.29	121.00	645.26	46.31	-40.58	104.57	-100.14	-101	-0.86
40	666.07	169.30	631.55	100.00	646.48	69.30	-42.32	104.67	-101.99	-84	17.99
41	666.07	252.00	630.33	180.00	644.35	72.00	-40.85	108.12	-103.97	-100	3.97
42	666.07	283.64	626.97	204.00	644.35	79.64	-42.24	109.15	-106.39	-101	5.39
44	666.07	447.91	620.88	216.00	650.44	231.91	-43.95	113.12	-112.07	-101	11.07
45	666.07	554.65	650.14	--	--	--	0.00	114.98	-69.98	-96	-26.02
46	666.07	518.02	623.93	225.00	650.44	293.02	-42.45	114.38	-111.83	-104	7.83
47	666.07	561.28	625.14	--	--	--	0.00	115.08	-70.08	-97	-26.92

48	666.07	545.51	636.73	--	--	--	0.00	114.83	-69.83	-96	-26.17
49	666.07	463.79	619.05	219.00	645.26	244.79	-42.81	113.42	-111.23	-101	10.23
50	666.07	469.31	619.05	223.00	645.26	246.31	-42.71	113.52	-111.23	-101	10.23
51	666.07	492.00	620.27	--	--	--	0.00	113.93	-68.93	-97	-28.07
52	666.07	399.61	620.57	296.00	639.81	103.61	-41.86	112.13	-108.98	-97	11.98
53	666.07	322.03	625.14	174.00	644.35	148.03	-41.66	110.25	-106.91	-96	10.91
54	666.07	343.85	626.06	189.00	645.26	154.85	-41.39	110.82	-107.21	-100	7.21

B.4d 27.525 GHz: single blockage, with Fresnel zones and with interpolation.

Receiver Location Number	Tower Height (m)	Path Length (m)	Receiver Height (m)	D1 (m)	Blockage Height (m)	D2 (m)	Diffraction Gain (dB)	Path Loss (dBm)	Predicted Received Power (dBm)	Measured Received Power (dBm)	Difference (dB)
1	667.68	125.38	632.31	--	--	--	0.00	103.21	-32.41	-26.66	5.75
2	667.68	178.00	632.31	--	--	--	0.00	106.25	-35.45	-48.50	-13.05
4	667.68	316.75	625.91	201.00	644.35	115.75	-42.25	111.26	-82.71	-71.50	11.21
5	667.68	456.55	621.94	233.00	650.44	223.55	-44.12	114.43	-87.75	-77.20	10.55
6	667.68	557.16	625.60	--	--	--	0.00	116.16	-45.36	-80.00	-34.64
7	667.68	531.60	624.38	--	--	--	0.00	115.75	-44.95	-38.60	6.35
8	667.68	518.61	626.82	274.00	646.24	244.61	-40.24	115.54	-84.98	-66.20	18.78
9	667.68	444.91	627.13	262.00	646.79	182.91	-41.14	114.21	-84.55	-75.90	8.65
10	667.68	439.31	626.21	267.00	646.79	172.31	-41.66	114.10	-84.96	-59.90	25.06
11	667.68	407.95	624.08	263.00	646.59	144.95	-42.94	113.45	-85.59	-61.88	23.71
12	667.68	416.37	623.16	--	--	--	0.00	113.63	-42.83	-56.98	-14.15
14	667.68	395.00	622.55	210.00	650.44	185.00	-44.58	113.17	-86.95	-66.91	20.04
15	667.68	407.40	621.94	224.00	644.35	183.40	-42.57	113.44	-85.21	-74.17	11.04
16	667.68	420.04	621.03	--	--	--	0.00	113.71	-42.91	-70.00	-27.09
17	667.68	444.44	620.12	220.00	645.26	224.44	-43.16	114.20	-86.56	-86.94	-0.38
18	667.68	501.11	621.03	--	--	--	0.00	115.24	-44.44	-65.68	-21.24
19	667.68	503.93	622.55	--	--	--	0.00	115.29	-44.49	-72.62	-28.13
20	667.68	496.44	622.86	209.00	650.44	287.44	-43.58	115.16	-87.94	-60.45	27.49
22	667.68	482.01	623.77	--	--	--	0.00	114.90	-44.10	-32.74	11.36
23	667.68	493.32	624.38	262.00	645.13	231.32	-41.04	115.10	-85.35	-59.00	26.35
24	667.68	506.84	626.21	272.00	646.36	234.84	-40.67	115.34	-85.21	-69.58	15.63
26	667.68	611.38	624.38	534.00	638.86	77.38	-40.51	116.97	-86.68	-82.39	4.29
28	667.68	576.68	624.38	542.00	638.54	34.68	-43.48	116.46	-89.15	-87.14	2.01
30	667.68	646.93	625.30	541.00	638.66	105.93	-38.64	117.46	-85.30	-57.40	27.90
31	667.68	645.06	625.91	--	--	--	0.00	117.43	-46.63	-32.62	14.01

32	667.68	658.21	632.31	559.00	649.22	99.21	-40.91	117.61	-87.72	-40.43	47.29
34	667.68	750.24	628.65	555.00	638.86	195.24	-34.15	118.75	-82.10	-76.36	5.74
36	667.68	749.97	628.35	608.00	637.31	141.97	-34.04	118.74	-81.98	-101.86	-19.88
38	667.68	702.97	633.53	--	--	--	0.00	118.18	-47.38	-40.17	7.21
39	667.68	725.82	633.83	565.00	649.22	160.82	-38.37	118.46	-86.03	-66.25	19.78
40	667.68	725.89	633.83	541.00	649.22	184.89	-37.95	118.46	-85.61	-67.00	18.61
41	667.68	736.20	634.14	542.00	649.22	194.20	-37.62	118.58	-85.40	-83.00	2.40
44	667.68	698.20	633.22	615.00	660.84	83.20	-29.84	118.12	-77.16	-81.18	-4.02
45	667.68	801.68	638.71	748.00	648.61	53.68	-38.52	119.32	-87.04	-80.62	6.42
46	667.68	856.64	642.06	722.00	648.61	134.64	-31.38	119.90	-80.47	-83.11	-2.64
49	667.68	964.43	643.28	754.00	648.61	210.43	-27.96	120.93	-78.09	-89.54	-11.45
50	667.68	958.40	643.28	748.00	648.61	210.40	-27.98	120.87	-78.06	-90.13	-12.07
51	667.68	941.05	642.98	795.00	656.23	146.05	-37.13	120.71	-87.05	-90.39	-3.34
53	667.68	864.88	637.79	551.00	649.22	313.88	-33.75	119.98	-82.93	-76.36	6.57
54	667.68	844.35	636.27	616.00	649.22	228.35	-35.63	119.77	-84.60	-64.15	20.45
55	667.68	813.49	660.65	--	--	--	0.00	119.45	-48.65	-45.81	2.84
56	667.68	780.70	634.75	568.00	649.22	212.70	-36.91	119.09	-85.21	-82.51	2.70
58	667.68	1002.58	641.45	732.00	648.61	270.58	-29.70	121.26	-80.17	-71.77	8.40
59	667.68	1016.16	640.23	899.00	660.50	117.16	-41.58	121.38	-92.16	-89.23	2.93
60	667.68	1033.42	638.40	607.00	662.64	426.42	-39.30	121.53	-90.02	-77.61	12.41
61	667.68	1054.76	636.57	929.00	651.36	125.76	-38.55	121.71	-89.45	-84.41	5.04
63	667.68	1052.07	636.27	--	--	--	0.00	121.68	-50.88	-79.56	-28.68
64	667.68	1007.46	635.36	783.00	649.76	224.46	-36.35	121.31	-86.86	-73.05	13.81
65	667.68	977.35	636.27	861.00	651.36	116.35	-39.06	121.04	-89.30	-79.65	9.65
66	667.68	972.20	637.79	--	--	--	0.00	121.00	-50.20	-68.57	-18.37
67	667.68	914.25	637.18	--	--	--	0.00	120.46	-49.66	-79.77	-30.11
68	667.68	835.14	637.49	578.00	646.79	257.14	-32.46	119.68	-81.34	-69.72	11.62
69	667.68	879.28	642.67	754.00	648.61	125.28	-30.77	120.12	-80.09	-74.94	5.15
70	667.68	853.70	642.67	822.00	655.71	31.70	-43.05	119.87	-92.12	-92.93	-0.81
71	667.68	805.38	635.05	566.00	649.22	239.38	-36.37	119.36	-84.93	-82.66	2.27
73	667.68	779.85	634.75	572.00	649.22	207.85	-36.98	119.08	-85.26	-79.05	6.21
74	667.68	797.47	634.75	545.00	649.22	252.47	-36.44	119.28	-84.92	-79.91	5.01
75	667.68	811.71	635.05	543.00	649.22	268.71	-36.08	119.43	-84.71	-73.79	10.92
76	667.68	808.19	635.05	562.00	649.22	246.19	-33.83	119.39	-82.42	-76.52	5.90
77	667.68	805.96	635.36	675.00	641.30	130.96	-30.23	119.37	-78.80	-64.30	14.50
78	667.68	847.19	635.66	--	--	--	0.00	119.80	-49.00	-77.70	-28.70
79	667.68	895.79	637.79	813.00	658.01	82.79	-42.95	120.29	-92.44	-79.47	12.97
83	667.68	71.85	624.38	--	--	--	0.00	98.37	-27.57	-53.13	-25.56
84	667.68	74.22	627.43	--	--	--	0.00	98.65	-27.85	-21.34	6.51
85	667.68	106.20	627.74	--	--	--	0.00	101.76	-30.96	-38.73	-7.77

87	667.68	209.18	623.47	--	--	--	0.00	107.65	-36.85	-25.16	11.69
88	667.68	287.64	622.86	--	--	--	0.00	110.42	-39.62	-30.56	9.06
89	667.68	336.92	620.73	--	--	--	0.00	111.79	-40.99	-40.70	0.29
90	667.68	417.55	619.51	--	--	--	0.00	113.66	-42.86	-53.55	-10.69
94	667.68	679.52	628.65	--	--	--	0.00	117.89	-47.09	-37.14	9.95
95	667.68	806.24	625.60	--	--	--	0.00	119.37	-48.57	-39.66	8.91
96	667.68	864.60	622.55	--	--	--	0.00	119.98	-49.18	-55.79	-6.61
97	667.68	902.53	619.81	--	--	--	0.00	120.35	-49.55	-61.26	-11.71
98	667.68	936.26	620.12	832.00	625.36	104.26	-30.33	120.67	-80.20	-71.54	8.66
99	667.68	960.22	621.94	--	--	--	0.00	120.89	-50.09	-44.00	6.09
101	667.68	975.77	633.53	--	--	--	0.00	121.03	-50.23	-46.26	3.97
104	667.68	835.18	632.31	--	--	--	0.00	119.68	-48.88	-43.72	5.16
106	667.68	750.64	628.65	--	--	--	0.00	118.75	-47.95	-40.63	7.32
107	667.68	658.58	626.82	--	--	--	0.00	117.61	-46.81	-35.93	10.88
109	667.68	612.82	618.59	562.00	624.50	50.82	-34.34	116.99	-80.53	-72.41	8.12

B.5a 902 MHz: double blockage, without Fresnel zones and without interpolation, tower height: 667.68 meters.

Receiver Location Number	Path Length (m)	Receiver Height (m)	D1 (m)	Blockage Height (m)	D2 (m)	2nd D1 (m)	2nd Blockage Height (m)	Virtual D1 (m)	Virtual Blockage Height (m)	Virtual D2 (m)	Diffraction Gain (dB)	Path Loss (dBm)	Predicted Received Power (dBm)	Measured Received Power (dBm)	Difference (dB)
1	125.38	632.31	--	--	--	--	--	--	--	--	0.00	73.52	-41.74	-50.80	-9.06
2	178.00	632.31	--	--	--	--	--	--	--	--	0.00	76.56	-44.78	-65.00	-20.22
4	316.75	625.91	190.05	644.35	126.70	200.61	644.35	--	--	--	-27.26	81.57	-77.04	-76.80	0.24
5	456.55	621.94	213.06	650.44	243.49	223.20	650.44	--	--	--	-29.29	84.74	-82.25	-82.50	-0.25
6	557.16	625.60	--	--	--	--	--	--	--	--	0.00	86.47	-54.69	-74.50	-19.81
7	531.60	624.38	--	--	--	--	--	--	--	--	0.00	86.06	-54.28	-68.70	-14.42
8	518.61	626.82	270.11	646.79	248.50	--	--	--	--	--	-25.64	85.85	-79.70	-85.60	-5.90
9	444.91	627.13	264.83	646.79	180.08	275.42	646.79	--	--	--	-26.32	84.52	-79.06	-79.10	-0.04
10	439.31	626.21	267.87	646.79	171.44	278.59	646.79	--	--	--	-26.82	84.41	-79.45	-74.80	4.65
11	407.95	624.08	259.60	646.79	148.34	--	--	--	--	--	-28.12	83.76	-80.11	-73.15	6.96
12	416.37	623.16	--	--	--	--	--	--	--	--	0.00	83.94	-52.16	-63.58	-11.42
14	395.00	622.55	212.69	650.44	182.31	222.82	650.44	--	--	--	-29.74	83.48	-81.44	-82.18	-0.74
15	407.40	621.94	208.44	644.35	198.96	217.91	644.35	--	--	--	-27.68	83.75	-79.65	-82.72	-3.07
16	420.04	621.03	--	--	--	--	--	--	--	--	0.00	84.02	-52.24	-86.75	-34.51
17	444.44	620.12	208.61	645.26	235.82	217.68	645.26	--	--	--	-28.32	84.51	-81.05	-93.08	-12.03
18	501.11	621.03	--	--	--	--	--	--	--	--	0.00	85.55	-53.77	-79.44	-25.67
19	503.93	622.55	--	--	--	--	--	--	--	--	0.00	85.60	-53.82	-88.90	-35.08

20	496.44	622.86	212.76	650.44	283.68	222.89	650.44	--	--	--	-28.72	85.47	-82.40	-85.83	-3.43
22	482.01	623.77	--	--	--	--	--	--	--	--	0.00	85.21	-53.43	-67.10	-13.67
23	493.32	624.38	264.71	646.79	228.61	--	--	--	--	--	-26.87	85.41	-80.50	-72.41	8.09
24	506.84	626.21	270.31	646.79	236.53	--	--	--	--	--	-26.01	85.65	-79.88	-72.69	7.19
26	611.38	624.38	530.63	638.86	80.75	542.17	638.86	--	--	--	-25.51	87.28	-81.01	-98.00	-16.99
28	576.68	624.38	529.61	638.86	47.08	--	--	--	--	--	-27.61	86.77	-82.60	-95.50	-12.90
30	646.93	625.30	534.96	638.86	111.97	--	--	--	--	--	-23.73	87.77	-79.72	-86.60	-6.88
31	645.06	625.91	--	--	--	--	--	--	--	--	0.00	87.74	-55.96	-71.90	-15.94
32	658.21	632.31	554.28	649.22	103.93	565.83	649.22	--	--	--	-25.90	87.92	-82.03	-77.31	4.72
34	750.24	628.65	548.68	638.86	201.56	559.88	638.86	--	--	--	-19.75	89.06	-77.02	-102.51	-25.49
36	749.97	628.35	602.09	638.56	147.88	--	--	--	--	--	-20.88	89.05	-78.15	-95.99	-17.84
37	814.92	631.39	706.26	641.30	108.66	738.86	641.30	--	--	--	-20.93	89.77	-78.92	-85.78	-6.86
38	702.97	633.53	--	--	--	--	--	--	--	--	0.00	88.49	-56.71	-72.78	-16.07
39	725.82	633.83	533.03	649.22	192.80	555.71	649.22	--	--	--	-22.99	88.77	-79.97	-92.51	-12.54
40	725.89	633.83	544.42	649.22	181.47	555.76	649.22	--	--	--	-23.16	88.77	-80.15	-81.42	-1.27
41	736.20	634.14	538.41	649.22	197.78	549.40	649.22	--	--	--	-22.72	88.89	-79.83	-89.11	-9.28
44	698.20	633.22	603.85	662.64	94.35	--	--	--	--	--	-31.00	88.43	-87.66	-89.13	-1.47
45	801.68	638.71	734.07	648.61	67.61	743.73	648.61	--	--	--	-22.75	89.63	-80.60	-83.55	-2.95
46	856.64	642.06	717.19	648.61	139.45	727.15	648.61	--	--	--	-16.76	90.21	-75.19	-98.70	-23.51
49	964.43	643.28	755.64	648.61	208.79	--	--	--	--	--	-14.12	91.24	-73.58	-86.92	-13.34
50	958.40	643.28	744.29	648.61	214.11	754.48	648.61	--	--	--	-14.07	91.18	-73.47	-100.98	-27.51
51	941.05	642.98	793.02	656.23	148.03	803.59	656.23	--	--	--	-22.24	91.02	-81.48	-90.13	-8.65
53	864.88	637.79	547.39	649.22	317.49	558.34	649.22	--	--	--	-19.32	90.29	-77.83	-85.26	-7.43
54	844.35	636.27	609.81	649.22	234.54	621.53	649.22	--	--	--	-20.71	90.08	-79.01	-77.89	1.12
55	813.49	660.65	--	--	--	--	--	--	--	--	0.00	89.76	-57.98	-73.96	-15.98
56	780.70	634.75	543.09	649.22	237.60	554.41	649.22	--	--	--	-21.78	89.40	-79.40	-88.85	-9.45
58	1002.58	641.45	724.63	648.61	277.94	734.56	648.61	--	--	--	-15.39	91.57	-75.18	-98.73	-23.55
59	1016.16	640.23	890.35	660.50	125.81	900.02	660.50	--	--	--	-26.46	91.69	-86.38	-98.18	-11.80
60	1033.42	638.40	602.83	662.64	430.59	612.40	662.64	--	--	--	-24.44	91.84	-84.50	-98.67	-14.17
61	1054.76	636.57	922.91	651.36	131.84	932.33	651.36	--	--	--	-23.52	92.01	-83.76	-84.42	-0.66
63	1052.07	636.27	--	--	--	--	--	--	--	--	0.00	91.99	-60.21	-82.69	-22.48
64	1007.46	635.36	776.39	649.83	231.07	--	--	--	--	--	-21.46	91.62	-81.30	-83.22	-1.92
65	977.35	636.27	856.34	651.36	121.01	865.65	651.36	--	--	--	-24.07	91.35	-83.64	-81.80	1.84
66	972.20	637.79	--	--	--	--	--	--	--	--	0.00	91.31	-59.53	-83.26	-23.73
67	914.25	637.18	--	--	--	--	--	--	--	--	0.00	90.77	-58.99	-87.51	-28.52
68	835.14	637.49	578.91	646.79	256.24	--	--	--	--	--	-17.95	89.99	-76.16	-78.12	-1.96
69	879.28	642.67	717.57	648.61	161.71	727.68	648.61	--	--	--	-15.55	90.43	-74.21	-92.60	-18.39
70	853.70	642.67	812.56	656.23	41.14	--	--	--	--	--	-27.47	90.18	-85.87	-92.05	-6.18
71	805.38	635.05	544.18	649.22	261.21	555.06	649.22	--	--	--	-21.31	89.67	-79.20	-93.53	-14.33
73	779.85	634.75	566.20	649.22	213.66	576.88	649.22	--	--	--	-22.06	89.39	-79.67	-83.16	-3.49

74	797.47	634.75	546.21	649.22	251.26	557.14	649.22	--	--	--	-21.61	89.59	-79.41	-88.31	-8.90
75	811.71	635.05	544.85	649.22	266.86	555.97	649.22	--	--	--	-21.25	89.74	-79.21	-92.87	-13.66
76	808.19	635.05	535.00	649.22	273.19	557.76	649.22	--	--	--	-21.21	89.70	-79.13	-80.57	-1.44
77	805.96	635.36	654.84	641.30	151.12	667.44	641.30	--	--	--	-15.81	89.68	-73.71	-77.42	-3.71
78	847.19	635.66	--	--	--	--	--	--	--	--	0.00	90.11	-58.33	-83.43	-25.10
79	895.79	637.79	809.90	658.67	85.90	--	--	--	--	--	-28.24	90.60	-87.06	-91.84	-4.78
83	71.85	624.38	--	--	--	--	--	--	--	--	0.00	68.68	-36.90	-80.45	-43.55
84	74.22	627.43	--	--	--	--	--	--	--	--	0.00	68.96	-37.18	-50.26	-13.08
85	106.20	627.74	--	--	--	--	--	--	--	--	0.00	72.07	-40.29	-55.79	-15.50
87	209.18	623.47	--	--	--	--	--	--	--	--	0.00	77.96	-46.18	-59.50	-13.32
88	287.64	622.86	--	--	--	--	--	--	--	--	0.00	80.73	-48.95	-65.65	-16.70
89	336.92	620.73	--	--	--	--	--	--	--	--	0.00	82.10	-50.32	-57.91	-7.59
90	417.55	619.51	--	--	--	--	--	--	--	--	0.00	83.97	-52.19	-66.30	-14.11
94	679.52	628.65	--	--	--	--	--	--	--	--	0.00	88.20	-56.42	-67.09	-10.67
95	806.24	625.60	--	--	--	--	--	--	--	--	0.00	89.68	-57.90	-71.02	-13.12
96	864.60	622.55	--	--	--	--	--	--	--	--	0.00	90.29	-58.51	-78.51	-20.00
97	902.53	619.81	--	--	--	--	--	--	--	--	0.00	90.66	-58.88	-86.56	-27.68
98	936.26	620.12	830.93	625.14	105.33	--	--	--	--	--	-15.59	90.98	-74.79	-95.84	-21.05
99	960.22	621.94	--	--	--	--	--	--	--	--	0.00	91.20	-59.42	-80.10	-20.68
101	975.77	633.53	--	--	--	--	--	--	--	--	0.00	91.34	-59.56	-72.58	-13.02
104	835.18	632.31	--	--	--	--	--	--	--	--	0.00	89.99	-58.21	-70.85	-12.64
106	750.64	628.65	--	--	--	--	--	--	--	--	0.00	89.06	-57.28	-65.63	-8.35
107	658.58	626.82	--	--	--	--	--	--	--	--	0.00	87.92	-56.14	-67.07	-10.93
109	612.82	618.59	553.90	624.54	58.93	--	--	--	--	--	-19.42	87.30	-74.94	-78.25	-3.31

B.5b 2.4 GHz: double blockage, without Fresnel zones, without interpolation and tower height: 667.31 meters.

Receiver Location Number	Path Length (m)	Receiver Height (m)	D1 (m)	Blockage Height (m)	D2 (m)	2nd D1 (m)	2nd Blockage Height (m)	Virtual D1 (m)	Virtual Blockage Height (m)	Virtual D2 (m)	Diffraction Gain (dB)	Path Loss (dBm)	Predicted Received Power (dBm)	Measured Received Power (dBm)	Difference (dB)
1	57.15	623.32	--	--	--	--	--	--	--	--	0.00	75.19	-37.19	-47.66	-10.47
2	196.74	623.62	--	--	--	--	--	--	--	--	0.00	85.93	-47.93	-63.80	-15.87
3	307.10	622.71	--	--	--	--	--	--	--	--	0.00	89.80	-51.80	-55.63	-3.83
4	329.40	626.06	--	--	--	--	--	--	--	--	0.00	90.41	-52.41	-70.42	-18.01
5	339.46	628.80	--	--	--	--	--	--	--	--	0.00	90.67	-52.67	-54.19	-1.52
6	348.59	631.24	--	--	--	--	--	--	--	--	0.00	90.90	-52.90	-62.55	-9.65
7	386.19	636.42	--	--	--	--	--	--	--	--	0.00	91.79	-53.79	-69.95	-16.16
8	381.52	637.34	--	--	--	--	--	--	--	--	0.00	91.68	-53.68	-61.05	-7.37

9	460.90	638.56	--	--	--	--	--	--	--	--	0.00	93.32	-55.32	-64.53	-9.21
10	456.55	636.42	--	--	--	--	--	--	--	--	0.00	93.24	-55.24	-58.17	-2.93
11	514.73	635.20	--	--	--	--	--	--	--	--	0.00	94.28	-56.28	-64.73	-8.45
12	550.23	633.07	--	--	--	--	--	--	--	--	0.00	94.86	-56.86	-74.22	-17.36
13	510.00	632.76	--	--	--	--	--	--	--	--	0.00	94.20	-56.20	-60.70	-4.50
14	481.50	627.28	--	--	--	--	--	--	--	--	0.00	93.70	-55.70	-57.72	-2.02
15	453.34	627.28	--	--	--	--	--	--	--	--	0.00	93.18	-55.18	-69.44	-14.26
16	118.42	624.54	9.11	665.07	109.31	18.22	665.07	--	--	--	-47.91	81.52	-91.43	-71.18	20.25
17	124.37	624.54	11.31	665.07	113.06	22.61	665.07	--	--	--	-47.04	81.95	-90.98	-69.11	21.87
18	128.78	624.84	8.59	665.07	120.19	17.17	665.07	--	--	--	-48.05	82.25	-92.30	-84.32	7.98
19	145.90	624.54	8.58	665.07	137.32	17.16	665.07	--	--	--	-48.09	83.33	-93.42	-77.79	15.63
20	179.62	623.93	17.11	665.07	162.52	25.66	665.07	--	--	--	-45.39	85.14	-92.53	-85.31	7.22
21	169.65	624.23	8.93	665.07	160.72	17.86	665.07	--	--	--	-47.95	84.64	-94.59	-80.72	13.87
22	155.54	625.14	11.11	665.07	144.43	22.22	665.07	--	--	--	-46.89	83.89	-92.78	-77.74	15.04
23	179.20	625.75	11.20	665.07	168.00	22.40	665.07	--	--	--	-46.68	85.12	-93.80	-72.74	21.06
24	189.35	624.54	9.97	665.07	179.38	19.93	665.07	--	--	--	-47.41	85.60	-95.00	-65.12	29.88
25	199.34	623.93	18.12	665.07	181.22	27.18	665.07	--	--	--	-45.12	86.04	-93.16	-76.23	16.93
26	229.97	623.93	17.69	665.07	212.28	26.54	665.07	--	--	--	-45.16	87.29	-94.44	-75.34	19.10
27	257.48	624.84	17.76	665.07	239.72	26.64	665.07	--	--	--	-44.91	88.27	-95.18	-79.12	16.06
28	217.58	624.54	19.78	665.07	197.80	29.67	665.07	--	--	--	-44.61	86.80	-93.41	-72.95	20.46
29	200.02	627.28	11.77	665.07	188.25	23.53	665.07	--	--	--	-46.11	86.07	-94.18	-78.53	15.65
30	196.25	627.28	--	--	--	--	--	--	--	--	0.00	85.91	-47.91	-57.74	-9.83
31	249.64	630.63	--	--	--	--	--	--	--	--	0.00	88.00	-50.00	-55.06	-5.06
32	263.24	631.85	--	--	--	--	--	--	--	--	0.00	88.46	-50.46	-59.07	-8.61
33	275.16	631.85	--	--	--	--	--	--	--	--	0.00	88.84	-50.84	-57.29	-6.45
34	237.22	629.11	--	--	--	--	--	--	--	--	0.00	87.56	-49.56	-52.32	-2.76
35	216.60	628.80	--	--	--	--	--	--	--	--	0.00	86.77	-48.77	-51.47	-2.70
36	209.74	628.50	--	--	--	--	--	--	--	--	0.00	86.49	-48.49	-48.02	0.47
37	207.07	627.89	21.80	665.07	185.27	32.70	665.07	--	--	--	-43.51	86.37	-91.88	-89.56	2.32
38	214.18	630.63	59.49	665.07	154.68	71.39	665.07	--	--	--	-39.41	86.67	-88.08	-77.60	10.48
39	221.94	632.16	63.41	665.07	158.53	--	--	--	--	--	-38.79	86.98	-87.77	-56.37	31.40
40	226.62	633.37	--	--	--	--	--	--	--	--	0.00	87.16	-49.16	-54.63	-5.47
41	231.19	634.29	--	--	--	--	--	--	--	--	0.00	87.33	-49.33	-62.69	-13.36
42	237.73	634.59	--	--	--	--	--	--	--	--	0.00	87.57	-49.57	-55.67	-6.10
43	317.68	635.51	220.61	658.98	97.07	229.44	658.98	--	--	--	-34.12	90.09	-86.22	-101.01	-14.79
44	259.36	634.90	214.64	640.08	44.72	223.59	640.08	--	--	--	-23.61	88.33	-73.94	-84.96	-11.02
45	250.07	633.07	--	--	--	--	--	--	--	--	0.00	88.01	-50.01	-97.13	-47.12
46	232.23	631.85	158.34	647.09	73.89	168.89	647.09	--	--	--	-31.64	87.37	-81.01	-91.86	-10.85
47	223.83	630.63	202.51	644.35	21.32	--	--	--	--	--	-34.89	87.05	-83.94	-63.81	20.13
48	151.81	630.02	71.44	649.53	80.37	80.37	649.53	--	--	--	-35.03	83.68	-80.70	-68.13	12.57

49	142.89	628.50	62.52	649.53	80.38	71.45	649.53	--	--	--	-36.00	83.15	-81.15	-83.90	-2.75
50	128.13	631.24	59.79	649.53	68.34	68.34	649.53	--	--	--	-35.21	82.21	-79.41	-75.01	4.40
51	204.66	628.80	169.06	639.78	35.59	--	--	--	--	--	-31.12	86.27	-79.40	-95.17	-15.77
52	40.45	627.58	24.27	646.48	16.18	--	--	--	--	--	-40.66	72.19	-74.85	-47.05	27.80
53	323.89	627.28	161.95	647.09	161.95	172.07	647.09	--	--	--	-31.86	90.26	-84.12	-95.87	-11.75
54	363.61	623.62	261.34	646.79	102.26	--	--	--	--	--	-33.63	91.26	-86.90	-84.27	2.63
55	428.04	622.40	190.24	647.09	237.80	--	--	--	--	--	-32.61	92.68	-87.29	-73.86	13.43
56	510.48	623.01	--	--	--	--	--	--	--	--	0.00	94.21	-56.21	-72.33	-16.12
57	501.79	622.71	--	--	--	--	--	--	--	--	0.00	94.06	-56.06	-84.38	-28.32
58	304.96	625.45	--	--	--	--	--	--	--	--	0.00	89.74	-51.74	-65.36	-13.62
59	303.98	626.06	222.92	650.44	81.06	233.05	650.44	--	--	--	-35.00	89.71	-86.71	-88.31	-1.60
60	323.97	625.14	171.51	644.35	152.46	181.04	644.35	--	--	--	-31.60	90.26	-83.86	-86.40	-2.54
61	352.86	623.93	217.15	645.26	135.72	226.19	645.26	--	--	--	-32.37	91.00	-85.37	-99.79	-14.42
62	400.19	620.57	291.05	642.82	109.14	--	--	--	--	--	-32.95	92.10	-87.05	-96.65	-9.60
63	498.44	620.27	--	--	--	--	--	--	--	--	0.00	94.00	-56.00	-90.13	-34.13

B.5c 24.12 GHz: double blockage, without Fresnel zones, without interpolation and tower height: 666.07 meters.

Receiver Location Number	Path Length (m)	Receiver Height (m)	D1 (m)	Blockage Height (m)	D2 (m)	2nd D1 (m)	2nd Blockage Height (m)	Virtual D1 (m)	Virtual Blockage Height (m)	Virtual D2 (m)	Diffraction Gain (dB)	Path Loss (dBm)	Predicted Received Power (dBm)	Measured Received Power (dBm)	Difference (dB)
3	207.64	630.63	57.68	665.07	149.96	69.21	665.07	--	--	--	-49.57	106.44	-111.01	-98	13.01
10	240.35	635.20	--	--	--	--	--	--	--	--	0.00	107.71	-62.71	-92	-29.29
11	215.08	635.51	146.25	645.26	68.82	--	--	--	--	--	-38.10	106.75	-99.85	-89	10.85
14	381.85	640.38	222.00	658.98	159.84	230.88	658.98	--	--	--	-40.73	111.73	-107.46	-94	13.46
16	469.49	639.47	--	--	--	--	--	--	--	--	0.00	113.53	-68.53	-94	-25.47
22	75.82	646.18	--	--	--	--	--	--	--	--	0.00	97.69	-52.69	-58	-5.31
23	344.92	628.50	--	--	--	--	--	--	--	--	0.00	110.85	-65.85	-87	-21.15
24	413.01	629.72	220.91	648.00	192.10	--	--	--	--	--	-40.15	112.41	-107.56	-90	17.56
25	490.30	629.41	--	--	--	--	--	--	--	--	0.00	113.90	-68.90	-93	-24.10
26	453.69	627.58	274.33	646.79	179.37	--	--	--	--	--	-40.34	113.23	-108.57	-97	11.57
27	495.19	624.23	264.87	646.79	230.32	--	--	--	--	--	-41.18	113.99	-110.17	-94	16.17
31	434.89	622.71	12.43	665.07	422.47	--	--	--	--	--	-56.75	112.86	-124.61	-84	40.61
32	391.98	622.40	--	--	--	--	--	--	--	--	0.00	111.96	-66.96	-81	-14.04
33	391.49	623.32	257.26	646.79	134.22	268.45	646.79	--	--	--	-42.98	111.95	-109.93	-99	10.93
34	332.85	623.93	12.33	665.07	320.52	147.93	647.09	--	--	--	-56.56	110.54	-122.10	-87	35.10
36	261.41	633.68	214.73	648.00	46.68	224.06	648.00	--	--	--	-42.31	108.44	-105.75	-102	3.75
37	156.05	634.29	100.97	645.26	55.08	--	--	--	--	--	-40.31	103.96	-99.27	-84	15.27

38	115.33	632.76	62.91	646.48	52.42	73.39	646.48	--	--	--	-43.20	101.33	-99.54	-89	10.54
39	167.31	634.29	117.12	645.26	50.19	125.48	645.26	--	--	--	-40.37	104.57	-99.94	-101	-1.06
40	169.30	631.55	95.23	646.48	74.07	105.81	646.48	--	--	--	-42.31	104.67	-101.98	-84	17.98
41	252.00	630.33	158.67	644.35	93.33	168.00	644.35	--	--	--	-40.27	108.12	-103.39	-100	3.39
42	283.64	626.97	189.10	644.35	94.55	199.60	644.35	--	--	--	-41.82	109.15	-105.98	-101	4.98
44	447.91	620.88	218.98	650.44	228.93	228.93	650.44	--	--	--	-43.95	113.12	-112.07	-101	11.07
45	554.65	650.14	--	--	--	--	--	--	--	--	0.00	114.98	-69.98	-96	-26.02
46	518.02	623.93	219.16	650.44	298.86	229.13	650.44	--	--	--	-42.47	114.38	-111.86	-104	7.86
47	561.28	625.14	--	--	--	--	--	--	--	--	0.00	115.08	-70.08	-97	-26.92
48	545.51	636.73	--	--	--	--	--	--	--	--	0.00	114.83	-69.83	-96	-26.17
49	463.79	619.05	205.14	645.26	258.65	214.06	645.26	--	--	--	-42.81	113.42	-111.23	-101	10.23
50	469.31	619.05	216.60	645.26	252.70	225.63	645.26	--	--	--	-42.72	113.52	-111.25	-101	10.25
51	492.00	620.27	--	--	--	--	--	--	--	--	0.00	113.93	-68.93	-97	-28.07
52	399.61	620.57	290.63	642.82	108.99	--	--	--	--	--	-42.98	112.13	-110.11	-97	13.11
53	322.03	625.14	174.81	644.35	147.21	184.02	644.35	--	--	--	-41.66	110.25	-106.92	-96	10.92
54	343.85	626.06	190.02	645.26	153.83	199.07	645.26	--	--	--	-41.39	110.82	-107.22	-100	7.22

B.5d 27.525 GHz: double blockage, without Fresnel zones, without interpolation and tower height: 667.68 meters.

Receiver Location Number	Path Length (m)	Receiver Height (m)	D1 (m)	Blockage Height (m)	D2 (m)	2nd D1 (m)	2nd Blockage Height (m)	Virtual D1 (m)	Virtual Blockage Height (m)	Virtual D2 (m)	Diffraction Gain (dB)	Path Loss (dBm)	Predicted Received Power (dBm)	Measured Received Power (dBm)	Difference (dB)
1	125.38	632.31	--	--	--	--	--	--	--	--	0.00	103.21	-32.41	-26.66	5.75
2	178.00	632.31	--	--	--	--	--	--	--	--	0.00	106.25	-35.45	-48.50	-13.05
4	316.75	625.91	190.05	644.35	126.70	200.61	644.35	--	--	--	-42.10	111.26	-82.56	-71.50	11.06
5	456.55	621.94	213.06	650.44	243.49	223.20	650.44	--	--	--	-44.14	114.43	-87.77	-77.20	10.57
6	557.16	625.60	--	--	--	--	--	--	--	--	0.00	116.16	-45.36	-80.00	-34.64
7	531.60	624.38	--	--	--	--	--	--	--	--	0.00	115.75	-44.95	-38.60	6.35
8	518.61	626.82	270.11	646.79	248.50	--	--	--	--	--	-40.48	115.54	-85.22	-66.20	19.02
9	444.91	627.13	264.83	646.79	180.08	275.42	646.79	--	--	--	-41.17	114.21	-84.57	-75.90	8.67
10	439.31	626.21	267.87	646.79	171.44	278.59	646.79	--	--	--	-41.67	114.10	-84.97	-59.90	25.07
11	407.95	624.08	259.60	646.79	148.34	--	--	--	--	--	-42.97	113.45	-85.62	-61.88	23.74
12	416.37	623.16	--	--	--	--	--	--	--	--	0.00	113.63	-42.83	-56.98	-14.15
14	395.00	622.55	212.69	650.44	182.31	222.82	650.44	--	--	--	-44.58	113.17	-86.96	-66.91	20.05
15	407.40	621.94	208.44	644.35	198.96	217.91	644.35	--	--	--	-42.52	113.44	-85.17	-74.17	11.00
16	420.04	621.03	--	--	--	--	--	--	--	--	0.00	113.71	-42.91	-70.00	-27.09
17	444.44	620.12	208.61	645.26	235.82	217.68	645.26	--	--	--	-43.16	114.20	-86.56	-86.94	-0.38
18	501.11	621.03	--	--	--	--	--	--	--	--	0.00	115.24	-44.44	-65.68	-21.24

19	503.93	622.55	--	--	--	--	--	--	--	--	0.00	115.29	-44.49	-72.62	-28.13
20	496.44	622.86	212.76	650.44	283.68	222.89	650.44	--	--	--	-43.56	115.16	-87.92	-60.45	27.47
22	482.01	623.77	--	--	--	--	--	--	--	--	0.00	114.90	-44.10	-32.74	11.36
23	493.32	624.38	264.71	646.79	228.61	--	--	--	--	--	-41.71	115.10	-86.02	-59.00	27.02
24	506.84	626.21	270.31	646.79	236.53	--	--	--	--	--	-40.85	115.34	-85.39	-69.58	15.81
26	611.38	624.38	530.63	638.86	80.75	542.17	638.86	--	--	--	-40.35	116.97	-86.52	-82.39	4.13
28	576.68	624.38	529.61	638.86	47.08	--	--	--	--	--	-42.45	116.46	-88.11	-87.14	0.97
30	646.93	625.30	534.96	638.86	111.97	--	--	--	--	--	-38.58	117.46	-85.24	-57.40	27.84
31	645.06	625.91	--	--	--	--	--	--	--	--	0.00	117.43	-46.63	-32.62	14.01
32	658.21	632.31	554.28	649.22	103.93	565.83	649.22	--	--	--	-40.74	117.61	-87.55	-40.43	47.12
34	750.24	628.65	548.68	638.86	201.56	559.88	638.86	--	--	--	-34.09	118.75	-82.04	-76.36	5.68
36	749.97	628.35	602.09	638.56	147.88	--	--	--	--	--	-35.03	118.74	-82.97	-101.86	-18.89
38	702.97	633.53	--	--	--	--	--	--	--	--	0.00	118.18	-47.38	-40.17	7.21
39	725.82	633.83	533.03	649.22	192.80	555.71	649.22	--	--	--	-37.83	118.46	-85.49	-66.25	19.24
40	725.89	633.83	544.42	649.22	181.47	555.76	649.22	--	--	--	-38.00	118.46	-85.66	-67.00	18.66
41	736.20	634.14	538.41	649.22	197.78	549.40	649.22	--	--	--	-37.57	118.58	-85.35	-83.00	2.35
44	698.20	633.22	603.85	662.64	94.35	--	--	--	--	--	-45.85	118.12	-93.17	-81.18	11.99
45	801.68	638.71	734.07	648.61	67.61	743.73	648.61	--	--	--	-37.60	119.32	-86.12	-80.62	5.50
46	856.64	642.06	717.19	648.61	139.45	727.15	648.61	--	--	--	-31.25	119.90	-80.35	-83.11	-2.76
49	964.43	643.28	755.64	648.61	208.79	--	--	--	--	--	-28.00	120.93	-78.13	-89.54	-11.41
50	958.40	643.28	744.29	648.61	214.11	754.48	648.61	--	--	--	-27.93	120.87	-78.00	-90.13	-12.13
51	941.05	642.98	793.02	656.23	148.03	803.59	656.23	--	--	--	-37.09	120.71	-87.00	-90.39	-3.39
53	864.88	637.79	547.39	649.22	317.49	558.34	649.22	--	--	--	-33.73	119.98	-82.91	-76.36	6.55
54	844.35	636.27	609.81	649.22	234.54	621.53	649.22	--	--	--	-35.55	119.77	-84.53	-64.15	20.38
55	813.49	660.65	--	--	--	--	--	--	--	--	0.00	119.45	-48.65	-45.81	2.84
56	780.70	634.75	543.09	649.22	237.60	554.41	649.22	--	--	--	-36.63	119.09	-84.92	-82.51	2.41
58	1002.58	641.45	724.63	648.61	277.94	734.56	648.61	--	--	--	-29.67	121.26	-80.13	-71.77	8.36
59	1016.16	640.23	890.35	660.50	125.81	900.02	660.50	--	--	--	-41.31	121.38	-91.89	-89.23	2.66
60	1033.42	638.40	602.83	662.64	430.59	612.40	662.64	--	--	--	-39.28	121.53	-90.01	-77.61	12.40
61	1054.76	636.57	922.91	651.36	131.84	932.33	651.36	--	--	--	-38.37	121.71	-89.28	-84.41	4.87
63	1052.07	636.27	--	--	--	--	--	--	--	--	0.00	121.68	-50.88	-79.56	-28.68
64	1007.46	635.36	776.39	649.83	231.07	--	--	--	--	--	-36.30	121.31	-86.81	-73.05	13.76
65	977.35	636.27	856.34	651.36	121.01	865.65	651.36	--	--	--	-38.91	121.04	-89.16	-79.65	9.51
66	972.20	637.79	--	--	--	--	--	--	--	--	0.00	121.00	-50.20	-68.57	-18.37
67	914.25	637.18	--	--	--	--	--	--	--	--	0.00	120.46	-49.66	-79.77	-30.11
68	835.14	637.49	578.91	646.79	256.24	--	--	--	--	--	-32.47	119.68	-81.34	-69.72	11.62
69	879.28	642.67	717.57	648.61	161.71	727.68	648.61	--	--	--	-29.87	120.12	-79.20	-74.94	4.26
70	853.70	642.67	812.56	656.23	41.14	--	--	--	--	--	-42.31	119.87	-91.38	-92.93	-1.55
71	805.38	635.05	544.18	649.22	261.21	555.06	649.22	--	--	--	-36.16	119.36	-84.72	-82.66	2.06
73	779.85	634.75	566.20	649.22	213.66	576.88	649.22	--	--	--	-36.90	119.08	-85.19	-79.05	6.14

74	797.47	634.75	546.21	649.22	251.26	557.14	649.22	--	--	--	-36.45	119.28	-84.93	-79.91	5.02
75	811.71	635.05	544.85	649.22	266.86	555.97	649.22	--	--	--	-36.09	119.43	-84.72	-73.79	10.93
76	808.19	635.05	535.00	649.22	273.19	557.76	649.22	--	--	--	-36.05	119.39	-84.64	-76.52	8.12
77	805.96	635.36	654.84	641.30	151.12	667.44	641.30	--	--	--	-30.19	119.37	-78.75	-64.30	14.45
78	847.19	635.66	--	--	--	--	--	--	--	--	0.00	119.80	-49.00	-77.70	-28.70
79	895.79	637.79	809.90	658.67	85.90	--	--	--	--	--	-43.09	120.29	-92.57	-79.47	13.10
83	71.85	624.38	--	--	--	--	--	--	--	--	0.00	98.37	-27.57	-53.13	-25.56
84	74.22	627.43	--	--	--	--	--	--	--	--	0.00	98.65	-27.85	-21.34	6.51
85	106.20	627.74	--	--	--	--	--	--	--	--	0.00	101.76	-30.96	-38.73	-7.77
87	209.18	623.47	--	--	--	--	--	--	--	--	0.00	107.65	-36.85	-25.16	11.69
88	287.64	622.86	--	--	--	--	--	--	--	--	0.00	110.42	-39.62	-30.56	9.06
89	336.92	620.73	--	--	--	--	--	--	--	--	0.00	111.79	-40.99	-40.70	0.29
90	417.55	619.51	--	--	--	--	--	--	--	--	0.00	113.66	-42.86	-53.55	-10.69
94	679.52	628.65	--	--	--	--	--	--	--	--	0.00	117.89	-47.09	-37.14	9.95
95	806.24	625.60	--	--	--	--	--	--	--	--	0.00	119.37	-48.57	-39.66	8.91
96	864.60	622.55	--	--	--	--	--	--	--	--	0.00	119.98	-49.18	-55.79	-6.61
97	902.53	619.81	--	--	--	--	--	--	--	--	0.00	120.35	-49.55	-61.26	-11.71
98	936.26	620.12	830.93	625.14	105.33	--	--	--	--	--	-29.92	120.67	-79.79	-71.54	8.25
99	960.22	621.94	--	--	--	--	--	--	--	--	0.00	120.89	-50.09	-44.00	6.09
101	975.77	633.53	--	--	--	--	--	--	--	--	0.00	121.03	-50.23	-46.26	3.97
104	835.18	632.31	--	--	--	--	--	--	--	--	0.00	119.68	-48.88	-43.72	5.16
106	750.64	628.65	--	--	--	--	--	--	--	--	0.00	118.75	-47.95	-40.63	7.32
107	658.58	626.82	--	--	--	--	--	--	--	--	0.00	117.61	-46.81	-35.93	10.88
109	612.82	618.59	553.90	624.54	58.93	--	--	--	--	--	-33.81	116.99	-80.00	-72.41	7.59

B.6a 902 MHz: double blockage, without Fresnel zones, with interpolation and tower height: 667.68 meters.

Receiver Location Number	Path Length (m)	Receiver Height (m)	D1 (m)	Blockage Height (m)	D2 (m)	2nd D1 (m)	2nd Blockage Height (m)	Virtual D1 (m)	Virtual Blockage Height (m)	Virtual D2 (m)	Diffraction Gain (dB)	Path Loss (dBm)	Predicted Received Power (dBm)	Measured Received Power (dBm)	Difference (dB)
1	125.38	632.31	--	--	--	--	--	--	--	--	0.00	73.52	-41.74	-50.80	-9.06
2	178.00	632.31	--	--	--	--	--	--	--	--	0.00	76.56	-44.78	-65.00	-20.22
4	316.75	625.91	201.00	644.35	115.75	210.00	644.35	--	--	--	-27.41	81.57	-77.19	-76.80	0.39
5	456.55	621.94	233.00	650.44	223.55	--	--	--	--	--	-29.27	84.74	-82.24	-82.50	-0.26
6	557.16	625.60	--	--	--	--	--	--	--	--	0.00	86.47	-54.69	-74.50	-19.81
7	531.60	624.38	--	--	--	--	--	--	--	--	0.00	86.06	-54.28	-68.70	-14.42
8	518.61	626.82	274.00	646.24	244.61	--	--	--	--	--	-25.40	85.85	-79.47	-85.60	-6.13
9	444.91	627.13	262.00	646.79	182.91	263.00	646.79	--	--	--	-26.30	84.52	-79.04	-79.10	-0.06

10	439.31	626.21	267.00	646.79	172.31	268.00	646.79	--	--	--	-26.82	84.41	-79.44	-74.80	4.64
11	407.95	624.08	263.00	646.59	144.95	264.00	646.48	263.65	646.53	144.30	-28.08	83.76	-80.06	-73.15	6.91
12	416.37	623.16	--	--	--	--	--	--	--	--	0.00	83.94	-52.16	-63.58	-11.42
14	395.00	622.55	210.00	650.44	185.00	216.00	650.44	--	--	--	-29.73	83.48	-81.44	-82.18	-0.74
15	407.40	621.94	224.00	644.35	183.40	229.00	644.35	--	--	--	-27.72	83.75	-79.69	-82.72	-3.03
16	420.04	621.03	--	--	--	--	--	--	--	--	0.00	84.02	-52.24	-86.75	-34.51
17	444.44	620.12	220.00	645.26	224.44	221.00	645.26	--	--	--	-28.30	84.51	-81.03	-93.08	-12.05
18	501.11	621.03	--	--	--	--	--	--	--	--	0.00	85.55	-53.77	-79.44	-25.67
19	503.93	622.55	--	--	--	--	--	--	--	--	0.00	85.60	-53.82	-88.90	-35.08
20	496.44	622.86	209.00	650.44	287.44	210.00	650.44	--	--	--	-28.74	85.47	-82.42	-85.83	-3.41
22	482.01	623.77	--	--	--	--	--	--	--	--	0.00	85.21	-53.43	-67.10	-13.67
23	493.32	624.38	262.00	645.13	231.32	263.00	645.09	--	--	--	-26.20	85.41	-79.83	-72.41	7.42
24	506.84	626.21	272.00	646.36	234.84	--	--	--	--	--	-25.83	85.65	-79.70	-72.69	7.01
26	611.38	624.38	534.00	638.86	77.38	536.00	638.86	--	--	--	-25.67	87.28	-81.16	-98.00	-16.84
28	576.68	624.38	542.00	638.54	34.68	543.00	638.52	--	--	--	-28.64	86.77	-83.63	-95.50	-11.87
30	646.93	625.30	541.00	638.66	105.93	542.00	638.63	--	--	--	-23.79	87.77	-79.78	-86.60	-6.82
31	645.06	625.91	--	--	--	--	--	--	--	--	0.00	87.74	-55.96	-71.90	-15.94
32	658.21	632.31	559.00	649.22	99.21	561.00	649.22	--	--	--	-26.06	87.92	-82.20	-77.31	4.89
34	750.24	628.65	555.00	638.86	195.24	568.00	638.86	--	--	--	-19.85	89.06	-77.13	-102.51	-25.38
36	749.97	628.35	608.00	637.31	141.97	--	--	--	--	--	-19.69	89.05	-76.96	-95.99	-19.03
37	814.92	631.39	714.00	640.01	100.92	715.00	639.94	714.42	639.99	100.50	-20.64	89.77	-78.63	-85.78	-7.15
38	702.97	633.53	--	--	--	--	--	--	--	--	0.00	88.49	-56.71	-72.78	-16.07
39	725.82	633.83	565.00	649.22	160.82	577.00	649.22	--	--	--	-23.52	88.77	-80.51	-92.51	-12.00
40	725.89	633.83	541.00	649.22	184.89	551.00	649.22	--	--	--	-23.10	88.77	-80.09	-81.42	-1.33
41	736.20	634.14	542.00	649.22	194.20	548.00	649.22	--	--	--	-22.77	88.89	-79.88	-89.11	-9.23
44	698.20	633.22	615.00	660.84	83.20	616.00	660.53	615.05	660.84	83.15	-30.93	88.43	-87.58	-89.13	-1.55
45	801.68	638.71	748.00	648.61	53.68	753.00	648.61	--	--	--	-23.67	89.63	-81.52	-83.55	-2.03
46	856.64	642.06	722.00	648.61	134.64	729.00	648.61	--	--	--	-16.88	90.21	-75.31	-98.70	-23.39
49	964.43	643.28	754.00	648.61	210.43	755.00	648.61	--	--	--	-14.10	91.24	-73.56	-86.92	-13.36
50	958.40	643.28	749.00	648.61	209.40	750.00	648.61	--	--	--	-14.12	91.18	-73.52	-100.98	-27.46
51	941.05	642.98	795.00	656.23	146.05	836.00	656.23	--	--	--	-22.29	91.02	-81.53	-90.13	-8.60
53	864.88	637.79	551.00	649.22	313.88	568.00	649.22	--	--	--	-19.35	90.29	-77.86	-85.26	-7.40
54	844.35	636.27	616.00	649.22	228.35	617.00	649.22	--	--	--	-20.78	90.08	-79.08	-77.89	1.19
55	813.49	660.65	--	--	--	--	--	--	--	--	0.00	89.76	-57.98	-73.96	-15.98
56	780.70	634.75	568.00	649.22	212.70	579.00	649.22	--	--	--	-22.07	89.40	-79.69	-88.85	-9.16
58	1002.58	641.45	732.00	648.61	270.58	733.00	648.61	--	--	--	-15.44	91.57	-75.24	-98.73	-23.49
59	1016.16	640.23	899.00	660.50	117.16	900.00	660.50	--	--	--	-26.73	91.69	-86.64	-98.18	-11.54
60	1033.42	638.40	607.00	662.64	426.42	609.00	662.64	--	--	--	-24.45	91.84	-84.51	-98.67	-14.16
61	1054.76	636.57	929.00	651.36	125.76	930.00	651.36	--	--	--	-23.70	92.01	-83.94	-84.42	-0.48
63	1052.07	636.27	--	--	--	--	--	--	--	--	0.00	91.99	-60.21	-82.69	-22.48

64	1007.46	635.36	783.00	649.76	224.46	784.00	649.75	--	--	--	-21.51	91.62	-81.34	-83.22	-1.88
65	977.35	636.27	861.00	651.36	116.35	910.00	651.36	--	--	--	-24.22	91.35	-83.79	-81.80	1.99
66	972.20	637.79	--	--	--	--	--	--	--	--	0.00	91.31	-59.53	-83.26	-23.73
67	914.25	637.18	--	--	--	--	--	--	--	--	0.00	90.77	-58.99	-87.51	-28.52
68	835.14	637.49	579.00	646.79	256.14	580.00	646.79	--	--	--	-17.95	89.99	-76.16	-78.12	-1.96
69	879.28	642.67	754.00	648.61	125.28	755.00	648.61	--	--	--	-16.32	90.43	-74.97	-92.60	-17.63
70	853.70	642.67	822.00	655.71	31.70	823.00	655.37	822.20	655.70	31.49	-28.23	90.18	-86.63	-92.05	-5.42
71	805.38	635.05	566.00	649.22	239.38	570.00	649.22	--	--	--	-21.52	89.67	-79.41	-93.53	-14.12
73	779.85	634.75	572.00	649.22	207.85	576.00	649.22	--	--	--	-22.13	89.39	-79.75	-83.16	-3.41
74	797.47	634.75	545.00	649.22	252.47	558.00	649.22	--	--	--	-21.60	89.59	-79.40	-88.31	-8.91
75	811.71	635.05	543.00	649.22	268.71	546.00	649.22	--	--	--	-21.23	89.74	-79.19	-92.87	-13.68
76	808.19	635.05	562.00	649.22	246.19	568.00	649.22	--	--	--	-21.44	89.70	-79.37	-80.57	-1.20
77	805.96	635.36	675.00	641.30	130.96	692.00	641.30	--	--	--	-16.24	89.68	-74.14	-77.42	-3.28
78	847.19	635.66	--	--	--	--	--	--	--	--	0.00	90.11	-58.33	-83.43	-25.10
79	895.79	637.79	813.00	658.01	82.79	--	--	--	--	--	-28.11	90.60	-86.92	-91.84	-4.92
83	71.85	624.38	--	--	--	--	--	--	--	--	0.00	68.68	-36.90	-80.45	-43.55
84	74.22	627.43	--	--	--	--	--	--	--	--	0.00	68.96	-37.18	-50.26	-13.08
85	106.20	627.74	--	--	--	--	--	--	--	--	0.00	72.07	-40.29	-55.79	-15.50
87	209.18	623.47	--	--	--	--	--	--	--	--	0.00	77.96	-46.18	-59.50	-13.32
88	287.64	622.86	--	--	--	--	--	--	--	--	0.00	80.73	-48.95	-65.65	-16.70
89	336.92	620.73	--	--	--	--	--	--	--	--	0.00	82.10	-50.32	-57.91	-7.59
90	417.55	619.51	--	--	--	--	--	--	--	--	0.00	83.97	-52.19	-66.30	-14.11
94	679.52	628.65	--	--	--	--	--	--	--	--	0.00	88.20	-56.42	-67.09	-10.67
95	806.24	625.60	--	--	--	--	--	--	--	--	0.00	89.68	-57.90	-71.02	-13.12
96	864.60	622.55	--	--	--	--	--	--	--	--	0.00	90.29	-58.51	-78.51	-20.00
97	902.53	619.81	--	--	--	--	--	--	--	--	0.00	90.66	-58.88	-86.56	-27.68
98	936.26	620.12	834.00	625.31	102.26	840.00	625.06	--	--	--	-15.93	90.98	-75.13	-95.84	-20.71
99	960.22	621.94	--	--	--	--	--	--	--	--	0.00	91.20	-59.42	-80.10	-20.68
101	975.77	633.53	--	--	--	--	--	--	--	--	0.00	91.34	-59.56	-72.58	-13.02
104	835.18	632.31	--	--	--	--	--	--	--	--	0.00	89.99	-58.21	-70.85	-12.64
106	750.64	628.65	--	--	--	--	--	--	--	--	0.00	89.06	-57.28	-65.63	-8.35
107	658.58	626.82	--	--	--	--	--	--	--	--	0.00	87.92	-56.14	-67.07	-10.93
109	612.82	618.59	562.00	624.50	50.82	563.00	624.43	--	--	--	-20.04	87.30	-75.56	-78.25	-2.69

B.6b 2.4 GHz: double blockage, without Fresnel zones, with interpolation and tower height: 667.31 meters.

Receiver Location Number	Path Length (m)	Receiver Height (m)	D1 (m)	Blockage Height (m)	D2 (m)	2nd D1 (m)	2nd Blockage Height (m)	Virtual D1 (m)	Virtual Blockage Height (m)	Virtual D2 (m)	Diffraction Gain (dB)	Path Loss (dBm)	Predicted Received Power (dBm)	Measured Received Power (dBm)	Difference (dB)
1	57.15	623.32	4.00	664.36	53.15	--	--	--	--	--	-51.56	75.19	-88.75	-47.66	41.09
2	196.74	623.62	--	--	--	--	--	--	--	--	0.00	85.93	-47.93	-63.80	-15.87
3	307.10	622.71	--	--	--	--	--	--	--	--	0.00	89.80	-51.80	-55.63	-3.83
4	329.40	626.06	--	--	--	--	--	--	--	--	0.00	90.41	-52.41	-70.42	-18.01
5	339.46	628.80	--	--	--	--	--	--	--	--	0.00	90.67	-52.67	-54.19	-1.52
6	348.59	631.24	--	--	--	--	--	--	--	--	0.00	90.90	-52.90	-62.55	-9.65
7	386.19	636.42	--	--	--	--	--	--	--	--	0.00	91.79	-53.79	-69.95	-16.16
8	381.52	637.34	--	--	--	--	--	--	--	--	0.00	91.68	-53.68	-61.05	-7.37
9	460.90	638.56	--	--	--	--	--	--	--	--	0.00	93.32	-55.32	-64.53	-9.21
10	456.55	636.42	--	--	--	--	--	--	--	--	0.00	93.24	-55.24	-58.17	-2.93
11	514.73	635.20	--	--	--	--	--	--	--	--	0.00	94.28	-56.28	-64.73	-8.45
12	550.23	633.07	--	--	--	--	--	--	--	--	0.00	94.86	-56.86	-74.22	-17.36
13	510.00	632.76	--	--	--	--	--	--	--	--	0.00	94.20	-56.20	-60.70	-4.50
14	481.50	627.28	--	--	--	--	--	--	--	--	0.00	93.70	-55.70	-57.72	-2.02
15	453.34	627.28	--	--	--	--	--	--	--	--	0.00	93.18	-55.18	-69.44	-14.26
16	118.42	624.54	15.00	665.07	103.42	16.00	665.07	--	--	--	-45.99	81.52	-89.51	-71.18	18.33
17	124.37	624.54	9.00	665.07	115.37	13.00	665.07	--	--	--	-47.94	81.95	-91.89	-69.11	22.78
18	128.78	624.84	9.00	665.07	119.78	22.00	665.07	--	--	--	-47.86	82.25	-92.11	-84.32	7.79
19	145.90	624.54	23.00	665.07	122.90	24.00	665.07	--	--	--	-44.29	83.33	-89.62	-77.79	11.83
20	179.62	623.93	24.00	665.07	155.62	27.00	665.07	--	--	--	-44.11	85.14	-91.25	-85.31	5.94
21	169.65	624.23	13.00	665.07	156.65	20.00	665.07	--	--	--	-46.43	84.64	-93.07	-80.72	12.35
22	155.54	625.14	10.00	665.07	145.54	11.00	665.07	--	--	--	-47.31	83.89	-93.20	-77.74	15.46
23	179.20	625.75	10.00	665.07	169.20	11.00	665.07	--	--	--	-47.14	85.12	-94.26	-72.74	21.52
24	189.35	624.54	10.00	665.07	179.35	19.00	665.07	--	--	--	-47.39	85.60	-94.99	-65.12	29.87
25	199.34	623.93	11.00	665.07	188.34	12.00	665.07	--	--	--	-47.12	86.04	-95.16	-76.23	18.93
26	229.97	623.93	19.00	665.07	210.97	21.00	665.07	--	--	--	-44.87	87.29	-94.16	-75.34	18.82
27	257.48	624.84	19.00	665.07	238.48	21.00	665.07	--	--	--	-44.64	88.27	-94.90	-79.12	15.78
28	217.58	624.54	19.00	665.07	198.58	21.00	665.07	--	--	--	-44.77	86.80	-93.57	-72.95	20.62
29	200.02	627.28	12.00	665.07	188.02	13.00	665.07	--	--	--	-46.03	86.07	-94.10	-78.53	15.57
30	196.25	627.28	--	--	--	--	--	--	--	--	0.00	85.91	-47.91	-57.74	-9.83
31	249.64	630.63	--	--	--	--	--	--	--	--	0.00	88.00	-50.00	-55.06	-5.06
32	263.24	631.85	--	--	--	--	--	--	--	--	0.00	88.46	-50.46	-59.07	-8.61
33	275.16	631.85	--	--	--	--	--	--	--	--	0.00	88.84	-50.84	-57.29	-6.45
34	237.22	629.11	--	--	--	--	--	--	--	--	0.00	87.56	-49.56	-52.32	-2.76
35	216.60	628.80	--	--	--	--	--	--	--	--	0.00	86.77	-48.77	-51.47	-2.70

36	209.74	628.50	--	--	--	--	--	--	--	--	0.00	86.49	-48.49	-48.02	0.47
37	207.07	627.89	19.00	665.07	188.07	30.00	665.07	--	--	--	-44.04	86.37	-92.41	-89.56	2.85
38	214.18	630.63	61.00	665.07	153.18	138.00	665.07	--	--	--	-39.34	86.67	-88.01	-77.60	10.41
39	221.94	632.16	62.00	664.29	159.94	63.00	664.09	62.04	664.29	159.91	-38.64	86.98	-87.61	-56.37	31.24
40	226.62	633.37	--	--	--	--	--	--	--	--	0.00	87.16	-49.16	-54.63	-5.47
41	231.19	634.29	--	--	--	--	--	--	--	--	0.00	87.33	-49.33	-62.69	-13.36
42	237.73	634.59	--	--	--	--	--	--	--	--	0.00	87.57	-49.57	-55.67	-6.10
43	317.68	635.51	236.00	658.98	81.68	240.00	658.98	--	--	--	-34.58	90.09	-86.67	-101.01	-14.34
44	259.36	634.90	218.00	640.08	41.36	219.00	640.08	--	--	--	-23.88	88.33	-74.21	-84.96	-10.75
45	250.07	633.07	--	--	--	--	--	--	--	--	0.00	88.01	-50.01	-97.13	-47.12
46	232.23	631.85	165.00	647.09	67.23	166.00	647.09	--	--	--	-31.87	87.37	-81.24	-91.86	-10.62
47	223.83	630.63	208.00	643.02	15.83	209.00	642.96	--	--	--	-35.19	87.05	-84.24	-63.81	20.43
48	151.81	630.02	74.00	649.53	77.81	75.00	649.53	--	--	--	-35.01	83.68	-80.69	-68.13	12.56
49	142.89	628.50	85.00	649.53	57.89	87.00	649.53	--	--	--	-36.09	83.15	-81.24	-83.90	-2.66
50	128.13	631.24	69.00	649.53	59.13	74.00	649.53	--	--	--	-35.21	82.21	-79.42	-75.01	4.41
51	204.66	628.80	175.00	638.92	29.66	176.00	638.78	--	--	--	-31.06	86.27	-79.34	-95.17	-15.83
52	40.45	627.58	26.00	643.82	14.45	27.00	643.70	--	--	--	-39.53	72.19	-73.72	-47.05	26.67
53	323.89	627.28	164.00	647.09	159.89	165.00	647.09	--	--	--	-31.86	90.26	-84.12	-95.87	-11.75
54	363.61	623.62	271.00	646.71	92.61	272.00	646.52	271.31	646.69	92.30	-33.88	91.26	-87.15	-84.27	2.88
55	428.04	622.40	--	--	--	--	--	--	--	--	0.00	92.68	-54.68	-73.86	-19.18
56	510.48	623.01	--	--	--	--	--	--	--	--	0.00	94.21	-56.21	-72.33	-16.12
57	501.79	622.71	--	--	--	--	--	--	--	--	0.00	94.06	-56.06	-84.38	-28.32
58	304.96	625.45	--	--	--	--	--	--	--	--	0.00	89.74	-51.74	-65.36	-13.62
59	303.98	626.06	227.00	650.44	76.98	228.00	650.44	--	--	--	-35.15	89.71	-86.86	-88.31	-1.45
60	323.97	625.14	177.00	644.35	146.97	184.00	644.35	--	--	--	-31.62	90.26	-83.88	-86.40	-2.52
61	352.86	623.93	222.00	645.26	130.86	223.00	645.26	--	--	--	-32.43	91.00	-85.43	-99.79	-14.36
62	400.19	620.57	295.00	638.63	105.19	296.00	638.50	295.60	638.57	104.59	-31.23	92.10	-85.32	-96.65	-11.33
63	498.44	620.27	--	--	--	--	--	--	--	--	0.00	94.00	-56.00	-90.13	-34.13

B.6c 24.12 GHz: double blockage, without Fresnel zones, with interpolation and tower height: 666.07 meters.

Receiver Location Number	Path Length (m)	Receiver Height (m)	D1 (m)	Blockage Height (m)	D2 (m)	2nd D1 (m)	2nd Blockage Height (m)	Virtual D1 (m)	Virtual Blockage Height (m)	Virtual D2 (m)	Diffraction Gain (dB)	Path Loss (dBm)	Predicted Received Power (dBm)	Measured Received Power (dBm)	Difference (dB)
3	207.64	630.63	49.00	665.07	158.64	50.00	665.07	--	--	--	-50.03	106.44	-111.47	-98	13.47
10	240.35	635.20	--	--	--	--	--	--	--	--	0.00	107.71	-62.71	-92	-29.29
11	215.08	635.51	147.00	645.26	68.08	--	--	--	--	--	-38.13	106.75	-99.88	-89	10.88
14	381.85	640.38	226.00	658.98	155.85	227.00	658.98	--	--	--	-40.76	111.73	-107.49	-94	13.49

16	469.49	639.47	--	--	--	--	--	--	--	--	0.00	113.53	-68.53	-94	-25.47
22	75.82	646.18	--	--	--	--	--	--	--	--	0.00	97.69	-52.69	-58	-5.31
23	344.92	628.50	--	--	--	--	--	--	--	--	0.00	110.85	-65.85	-87	-21.15
24	413.01	629.72	--	--	--	--	--	--	--	--	0.00	112.41	-67.41	-90	-22.59
25	490.30	629.41	--	--	--	--	--	--	--	--	0.00	113.90	-68.90	-93	-24.10
26	453.69	627.58	277.00	646.73	176.69	--	--	--	--	--	-40.34	113.23	-108.57	-97	11.57
27	495.19	624.23	270.00	646.45	225.19	271.00	646.40	--	--	--	-41.07	113.99	-110.06	-94	16.06
31	434.89	622.71	192.00	646.93	242.89	--	--	--	--	--	-42.40	112.86	-110.27	-84	26.27
32	391.98	622.40	--	--	--	--	--	--	--	--	0.00	111.96	-66.96	-81	-14.04
33	391.49	623.32	259.00	646.79	132.49	261.00	646.79	--	--	--	-43.00	111.95	-109.95	-99	10.95
34	332.85	623.93	157.00	647.09	175.85	173.00	647.09	--	--	--	-43.13	110.54	-108.67	-87	21.67
36	261.41	633.68	218.00	648.00	43.41	222.00	648.00	--	--	--	-42.56	108.44	-106.00	-102	4.00
37	156.05	634.29	103.00	645.26	53.05	107.00	645.01	--	--	--	-40.39	103.96	-99.35	-84	15.35
38	115.33	632.76	68.00	646.48	47.33	70.00	646.48	--	--	--	-43.31	101.33	-99.64	-89	10.64
39	167.31	634.29	121.00	645.26	46.31	126.00	645.26	--	--	--	-40.58	104.57	-100.14	-101	-0.86
40	169.30	631.55	100.00	646.48	69.30	101.00	646.48	--	--	--	-42.39	104.67	-102.05	-84	18.05
41	252.00	630.33	180.00	644.35	72.00	182.00	644.35	--	--	--	-40.85	108.12	-103.97	-100	3.97
42	283.64	626.97	204.00	644.35	79.64	209.00	644.35	--	--	--	-42.24	109.15	-106.39	-101	5.39
44	447.91	620.88	216.00	650.44	231.91	217.00	650.44	--	--	--	-43.95	113.12	-112.07	-101	11.07
45	554.65	650.14	--	--	--	--	--	--	--	--	0.00	114.98	-69.98	-96	-26.02
46	518.02	623.93	225.00	650.44	293.02	227.00	650.44	--	--	--	-42.45	114.38	-111.83	-104	7.83
47	561.28	625.14	--	--	--	--	--	--	--	--	0.00	115.08	-70.08	-97	-26.92
48	545.51	636.73	--	--	--	--	--	--	--	--	0.00	114.83	-69.83	-96	-26.17
49	463.79	619.05	219.00	645.26	244.79	229.00	645.26	--	--	--	-42.76	113.42	-111.19	-101	10.19
50	469.31	619.05	223.00	645.26	246.31	225.00	645.26	--	--	--	-42.71	113.52	-111.23	-101	10.23
51	492.00	620.27	--	--	--	--	--	--	--	--	0.00	113.93	-68.93	-97	-28.07
52	399.61	620.57	296.00	639.81	103.61	297.00	639.72	--	--	--	-41.86	112.13	-108.98	-97	11.98
53	322.03	625.14	174.00	644.35	148.03	176.00	644.35	--	--	--	-41.66	110.25	-106.91	-96	10.91
54	343.85	626.06	189.00	645.26	154.85	198.00	645.26	--	--	--	-41.39	110.82	-107.21	-100	7.21

B.6d 27.525 GHz: double blockage, without Fresnel zones, with interpolation and tower height: 667.68 meters.

Receiver Location Number	Path Length (m)	Receiver Height (m)	D1 (m)	Blockage Height (m)	D2 (m)	2nd D1 (m)	2nd Blockage Height (m)	Virtual D1 (m)	Virtual Blockage Height (m)	Virtual D2 (m)	Diffraction Gain (dB)	Path Loss (dBm)	Predicted Received Power (dBm)	Measured Received Power (dBm)	Difference (dB)
1	125.38	632.31	--	--	--	--	--	--	--	--	0.00	103.21	-32.41	-26.66	5.75
2	178.00	632.31	--	--	--	--	--	--	--	--	0.00	106.25	-35.45	-48.50	-13.05
4	316.75	625.91	201.00	644.35	115.75	210.00	644.35	--	--	--	-42.25	111.26	-82.71	-71.50	11.21

5	456.55	621.94	233.00	650.44	223.55	--	--	--	--	--	-44.12	114.43	-87.75	-77.20	10.55
6	557.16	625.60	--	--	--	--	--	--	--	--	0.00	116.16	-45.36	-80.00	-34.64
7	531.60	624.38	--	--	--	--	--	--	--	--	0.00	115.75	-44.95	-38.60	6.35
8	518.61	626.82	274.00	646.24	244.61	--	--	--	--	--	-40.24	115.54	-84.98	-66.20	18.78
9	444.91	627.13	262.00	646.79	182.91	263.00	646.79	--	--	--	-41.14	114.21	-84.55	-75.90	8.65
10	439.31	626.21	267.00	646.79	172.31	268.00	646.79	--	--	--	-41.66	114.10	-84.96	-59.90	25.06
11	407.95	624.08	263.00	646.59	144.95	264.00	646.48	263.65	646.53	144.30	-42.93	113.45	-85.58	-61.88	23.70
12	416.37	623.16	--	--	--	--	--	--	--	--	0.00	113.63	-42.83	-56.98	-14.15
14	395.00	622.55	210.00	650.44	185.00	216.00	650.44	--	--	--	-44.58	113.17	-86.95	-66.91	20.04
15	407.40	621.94	224.00	644.35	183.40	229.00	644.35	--	--	--	-42.57	113.44	-85.21	-74.17	11.04
16	420.04	621.03	--	--	--	--	--	--	--	--	0.00	113.71	-42.91	-70.00	-27.09
17	444.44	620.12	220.00	645.26	224.44	221.00	645.26	--	--	--	-43.15	114.20	-86.55	-86.94	-0.39
18	501.11	621.03	--	--	--	--	--	--	--	--	0.00	115.24	-44.44	-65.68	-21.24
19	503.93	622.55	--	--	--	--	--	--	--	--	0.00	115.29	-44.49	-72.62	-28.13
20	496.44	622.86	209.00	650.44	287.44	210.00	650.44	--	--	--	-43.58	115.16	-87.94	-60.45	27.49
22	482.01	623.77	--	--	--	--	--	--	--	--	0.00	114.90	-44.10	-32.74	11.36
23	493.32	624.38	262.00	645.13	231.32	263.00	645.09	--	--	--	-41.04	115.10	-85.35	-59.00	26.35
24	506.84	626.21	272.00	646.36	234.84	--	--	--	--	--	-40.67	115.34	-85.21	-69.58	15.63
26	611.38	624.38	534.00	638.86	77.38	536.00	638.86	--	--	--	-40.51	116.97	-86.68	-82.39	4.29
28	576.68	624.38	542.00	638.54	34.68	543.00	638.52	--	--	--	-43.48	116.46	-89.15	-87.14	2.01
30	646.93	625.30	541.00	638.66	105.93	542.00	638.63	--	--	--	-38.64	117.46	-85.30	-57.40	27.90
31	645.06	625.91	--	--	--	--	--	--	--	--	0.00	117.43	-46.63	-32.62	14.01
32	658.21	632.31	559.00	649.22	99.21	561.00	649.22	--	--	--	-40.91	117.61	-87.72	-40.43	47.29
34	750.24	628.65	555.00	638.86	195.24	568.00	638.86	--	--	--	-34.18	118.75	-82.13	-76.36	5.77
36	749.97	628.35	608.00	637.31	141.97	--	--	--	--	--	-34.04	118.74	-81.98	-101.86	-19.88
38	702.97	633.53	--	--	--	--	--	--	--	--	0.00	118.18	-47.38	-40.17	7.21
39	725.82	633.83	565.00	649.22	160.82	577.00	649.22	--	--	--	-38.37	118.46	-86.03	-66.25	19.78
40	725.89	633.83	541.00	649.22	184.89	551.00	649.22	--	--	--	-37.95	118.46	-85.61	-67.00	18.61
41	736.20	634.14	542.00	649.22	194.20	548.00	649.22	--	--	--	-37.62	118.58	-85.40	-83.00	2.40
44	698.20	633.22	615.00	660.84	83.20	616.00	660.53	615	661	83	-45.77	118.12	-93.09	-81.18	11.91
45	801.68	638.71	748.00	648.61	53.68	753.00	648.61	--	--	--	-38.52	119.32	-87.04	-80.62	6.42
46	856.64	642.06	722.00	648.61	134.64	729.00	648.61	--	--	--	-31.38	119.90	-80.47	-83.11	-2.64
49	964.43	643.28	754.00	648.61	210.43	755.00	648.61	--	--	--	-27.97	120.93	-78.10	-89.54	-11.44
50	958.40	643.28	749.00	648.61	209.40	750.00	648.61	--	--	--	-28.00	120.87	-78.07	-90.13	-12.06
51	941.05	642.98	795.00	656.23	146.05	836.00	656.23	--	--	--	-37.13	120.71	-87.05	-90.39	-3.34
53	864.88	637.79	551.00	649.22	313.88	568.00	649.22	--	--	--	-33.75	119.98	-82.93	-76.36	6.57
54	844.35	636.27	616.00	649.22	228.35	617.00	649.22	--	--	--	-35.63	119.77	-84.60	-64.15	20.45
55	813.49	660.65	--	--	--	--	--	--	--	--	0.00	119.45	-48.65	-45.81	2.84
56	780.70	634.75	568.00	649.22	212.70	579.00	649.22	--	--	--	-36.91	119.09	-85.21	-82.51	2.70
58	1002.58	641.45	732.00	648.61	270.58	733.00	648.61	--	--	--	-29.74	121.26	-80.21	-71.77	8.44

59	1016.16	640.23	899.00	660.50	117.16	900.00	660.50	--	--	--	-41.58	121.38	-92.16	-89.23	2.93
60	1033.42	638.40	607.00	662.64	426.42	609.00	662.64	--	--	--	-39.30	121.53	-90.02	-77.61	12.41
61	1054.76	636.57	929.00	651.36	125.76	930.00	651.36	--	--	--	-38.55	121.71	-89.45	-84.41	5.04
63	1052.07	636.27	--	--	--	--	--	--	--	--	0.00	121.68	-50.88	-79.56	-28.68
64	1007.46	635.36	783.00	649.76	224.46	784.00	649.75	--	--	--	-36.35	121.31	-86.86	-73.05	13.81
65	977.35	636.27	861.00	651.36	116.35	910.00	651.36	--	--	--	-39.06	121.04	-89.30	-79.65	9.65
66	972.20	637.79	--	--	--	--	--	--	--	--	0.00	121.00	-50.20	-68.57	-18.37
67	914.25	637.18	--	--	--	--	--	--	--	--	0.00	120.46	-49.66	-79.77	-30.11
68	835.14	637.49	579.00	646.79	256.14	580.00	646.79	--	--	--	-32.47	119.68	-81.35	-69.72	11.63
69	879.28	642.67	754.00	648.61	125.28	755.00	648.61	--	--	--	-30.77	120.12	-80.09	-74.94	5.15
70	853.70	642.67	822.00	655.71	31.70	823.00	655.37	822	656	31	-43.08	119.87	-92.15	-92.93	-0.78
71	805.38	635.05	566.00	649.22	239.38	570.00	649.22	--	--	--	-36.37	119.36	-84.93	-82.66	2.27
73	779.85	634.75	572.00	649.22	207.85	576.00	649.22	--	--	--	-36.98	119.08	-85.26	-79.05	6.21
74	797.47	634.75	545.00	649.22	252.47	558.00	649.22	--	--	--	-36.44	119.28	-84.92	-79.91	5.01
75	811.71	635.05	543.00	649.22	268.71	546.00	649.22	--	--	--	-36.08	119.43	-84.71	-73.79	10.92
76	808.19	635.05	562.00	649.22	246.19	568.00	649.22	--	--	--	-36.29	119.39	-84.88	-76.52	8.36
77	805.96	635.36	675.00	641.30	130.96	692.00	641.30	--	--	--	-30.68	119.37	-79.24	-64.30	14.94
78	847.19	635.66	--	--	--	--	--	--	--	--	0.00	119.80	-49.00	-77.70	-28.70
79	895.79	637.79	813.00	658.01	82.79	--	--	--	--	--	-42.95	120.29	-92.44	-79.47	12.97
83	71.85	624.38	--	--	--	--	--	--	--	--	0.00	98.37	-27.57	-53.13	-25.56
84	74.22	627.43	--	--	--	--	--	--	--	--	0.00	98.65	-27.85	-21.34	6.51
85	106.20	627.74	--	--	--	--	--	--	--	--	0.00	101.76	-30.96	-38.73	-7.77
87	209.18	623.47	--	--	--	--	--	--	--	--	0.00	107.65	-36.85	-25.16	11.69
88	287.64	622.86	--	--	--	--	--	--	--	--	0.00	110.42	-39.62	-30.56	9.06
89	336.92	620.73	--	--	--	--	--	--	--	--	0.00	111.79	-40.99	-40.70	0.29
90	417.55	619.51	--	--	--	--	--	--	--	--	0.00	113.66	-42.86	-53.55	-10.69
94	679.52	628.65	--	--	--	--	--	--	--	--	0.00	117.89	-47.09	-37.14	9.95
95	806.24	625.60	--	--	--	--	--	--	--	--	0.00	119.37	-48.57	-39.66	8.91
96	864.60	622.55	--	--	--	--	--	--	--	--	0.00	119.98	-49.18	-55.79	-6.61
97	902.53	619.81	--	--	--	--	--	--	--	--	0.00	120.35	-49.55	-61.26	-11.71
98	936.26	620.12	834.00	625.31	102.26	840.00	625.06	--	--	--	-30.32	120.67	-80.19	-71.54	8.65
99	960.22	621.94	--	--	--	--	--	--	--	--	0.00	120.89	-50.09	-44.00	6.09
101	975.77	633.53	--	--	--	--	--	--	--	--	0.00	121.03	-50.23	-46.26	3.97
104	835.18	632.31	--	--	--	--	--	--	--	--	0.00	119.68	-48.88	-43.72	5.16
106	750.64	628.65	--	--	--	--	--	--	--	--	0.00	118.75	-47.95	-40.63	7.32
107	658.58	626.82	--	--	--	--	--	--	--	--	0.00	117.61	-46.81	-35.93	10.88
109	612.82	618.59	562.00	624.50	50.82	563.00	624.43	--	--	--	-34.34	116.99	-80.53	-72.41	8.12

Appendix C: Apparent GPS coordinates and error for receiver locations collected in this study.

Receiver Location Number	X Coordinate (decimal degrees)	Y Coordinate (decimal degrees)	Coordinate Error (ft)
1	37.2308	80.4254	12.4
2	37.2300	80.4267	19.4
3	37.2291	80.4275	11.2
4	37.2295	80.4280	11.5
5	37.2298	80.4283	16.7
6	37.2301	80.4285	11.2
7	37.2309	80.4291	12.4
8	37.2314	80.4289	13.6
9	37.2312	80.4299	21.7
10	37.2308	80.4298	15.8
11	37.2308	80.4305	12.9
12	37.2308	80.4309	13.0
13	37.2303	80.4305	13.0
14	37.2298	80.4300	12.8
15	37.2293	80.4295	13.1
16	37.2317	80.4253	22.7
17	37.2315	80.4257	17.6
18	37.2318	80.4251	22.1
19	37.2320	80.4248	14.3
20	37.2324	80.4244	15.6
21	37.2322	80.4254	15.9
22	37.2318	80.4259	16.0
23	37.2319	80.4261	16.0
24	37.2322	80.4258	16.1
25	37.2324	80.4255	20.4
26	37.2328	80.4250	15.9
27	37.2330	80.4253	15.7
28	37.2324	80.4260	14.8
29	37.2320	80.4263	13.8
30	37.2318	80.4265	17.6
31	37.2322	80.4268	13.2
32	37.2319	80.4273	14.2
33	37.2317	80.4276	13.5
34	37.2314	80.4273	12.2
35	37.2316	80.4269	12.1
36	37.2317	80.4267	13.2
37	37.2322	80.4234	15.6
38	37.2321	80.4230	12.4
39	37.2320	80.4227	12.4
40	37.2318	80.4225	14.9
41	37.2317	80.4223	15.1
42	37.2315	80.4222	19.4
43	37.2304	80.4212	29.0
44	37.2302	80.4218	19.4
45	37.2298	80.4222	16.2

46	37.2296	80.4225	16.1
47	37.2291	80.4232	23.2
48	37.2294	80.4243	29.1
49	37.2295	80.4246	15.0
50	37.2296	80.4244	14.8
51	37.2291	80.4244	28.3
52	37.2304	80.4248	21.5
53	37.2292	80.4216	22.9
54	37.2287	80.4216	20.4
55	37.2279	80.4215	13.3
56	37.2273	80.4209	13.0
57	37.2270	80.4215	12.5
58	37.2287	80.4225	16.4
59	37.2284	80.4230	13.4
60	37.2280	80.4234	19.4
61	37.2276	80.4240	17.4
62	37.2273	80.4237	10.8
63	37.2265	80.4231	24.7

Appendix D: Apparent transformed coordinates, corrected coordinates based on detailed field notes and distance moved for each receiver location in this study.

Receiver Location Number	Longitude (ft)	Latitude (ft)	Corrected Longitude (ft)	Corrected Latitude (ft)	Distance Moved (ft)
1	10922409.30	3613306.68	10922425.29	3613287.12	25.27
2	10922024.97	3613023.19	10922019.85	3613021.41	5.42
3	10921785.42	3612700.33	10921797.51	3612684.68	19.78
4	10921642.85	3612848.91	10921627.24	3612833.04	22.26
5	10921557.76	3612959.90	10921551.38	3612938.97	21.88
6	10921501.78	3613070.29	10921489.37	3613061.46	15.23
7	10921333.08	3613365.08	10921346.54	3613328.50	38.97
8	10921395.02	3613545.90	10921387.63	3613534.63	13.47
9	10921102.46	3613479.04	10921112.96	3613471.65	12.84
10	10921128.59	3613332.84	10921115.86	3613337.19	13.45
11	10920924.84	3613337.01	10920924.84	3613337.01	0.00
12	10920808.41	3613339.39	10920808.41	3613339.39	0.00
13	10920921.12	3613155.00	10920940.83	3613205.65	54.35
14	10921062.93	3612970.01	10921062.93	3612970.01	0.00
15	10921204.75	3612785.03	10921213.37	3612772.59	15.13
16	10922445.09	3613633.71	10922437.95	3613624.13	11.95
17	10922327.18	3613563.28	10922348.30	3613587.98	32.50
18	10922504.05	3613668.92	10922504.83	3613685.58	16.68
19	10922592.85	3613739.95	10922579.69	3613754.60	19.70
20	10922712.25	3613883.18	10922694.59	3613860.62	28.65
21	10922419.70	3613816.31	10922427.00	3613801.81	16.24
22	10922271.20	3613673.67	10922274.38	3613659.24	14.78
23	10922213.72	3613711.26	10922221.83	3613716.37	9.58
24	10922303.27	3613818.69	10922314.83	3613822.29	12.11
25	10922392.08	3613889.71	10922389.38	3613891.81	3.42
26	10922540.58	3614032.35	10922527.97	3614026.79	13.78
27	10922454.75	3614106.93	10922454.75	3614106.93	0.00
28	10922246.54	3613892.68	10922260.86	3613898.26	15.37
29	10922156.25	3613748.85	10922162.16	3613754.33	8.06
30	10922096.55	3613677.24	10922114.26	3613684.83	19.27
31	10922012.21	3613824.63	10922005.74	3613827.16	6.94
32	10921864.44	3613718.39	10921868.24	3613715.16	4.99
33	10921775.64	3613647.37	10921786.04	3613640.20	12.64
34	10921860.73	3613536.38	10921878.02	3613534.41	17.41
35	10921978.64	3613606.81	10921978.36	3613597.67	9.14
36	10922037.60	3613642.02	10922034.08	3613649.75	8.49
37	10923001.83	3613804.44	10923022.49	3613818.78	25.15
38	10923117.52	3613765.67	10923117.52	3613765.67	0.00
39	10923204.10	3613727.49	10923200.44	3613706.69	21.12
40	10923260.83	3613653.50	10923255.34	3613650.69	6.16
41	10923318.30	3613615.91	10923299.75	3613598.06	25.74
42	10923345.92	3613542.51	10923347.89	3613537.03	5.83
43	10923628.84	3613136.17	10923648.57	3613163.20	33.47
44	10923452.72	3613066.92	10923437.75	3613069.49	15.18

45	10923333.32	3612923.68	10923350.16	3612917.84	17.82
46	10923244.52	3612852.66	10923240.54	3612845.64	8.06
47	10923037.05	3612674.80	10923029.34	3612672.46	8.06
48	10922719.09	3612790.53	10922719.09	3612790.53	0.00
49	10922632.51	3612828.71	10922640.46	3612809.07	21.19
50	10922691.47	3612863.93	10922700.09	3612865.89	8.84
51	10922687.76	3612681.92	10922679.57	3612608.96	73.42
52	10922580.98	3613157.52	10922573.26	3613150.27	10.59
53	10923503.52	3612701.71	10923520.59	3612725.10	28.95
54	10923499.81	3612519.71	10923521.55	3612504.52	26.51
55	10923522.99	3612227.90	10923524.38	3612209.02	18.93
56	10923693.20	3612005.93	10923711.97	3612013.64	20.29
57	10923516.32	3611900.28	10923525.51	3611907.10	11.44
58	10923237.84	3612525.04	10923243.17	3612500.29	25.32
59	10923090.08	3612418.80	10923101.89	3612408.06	15.96
60	10922970.68	3612275.56	10922991.86	3612284.15	22.86
61	10922793.06	3612133.52	10922793.06	3612133.52	0.00
62	10922878.16	3612022.53	10922875.63	3611990.71	31.92
63	10923046.88	3611727.76	10923046.16	3611700.28	27.49

VITA

Paige Marie Baldassaro was born on November 12, 1971 in New Orleans, LA. In 1989, she began attending Louisiana State University where she obtained a B.S. in Geology in 1994. She pursed a master's degree in Geology at Virginia Polytechnic Institute and State University from 1994-2000. Her research topic was examining low temperature phase relations of NaCl-$FeCl_2$-H_2O fluids trapped in synthetic fluid inclusions. During that time, she worked in the summer of 1997 at Exxon Production Research Company analyzing petroleum biomarkers in fluid inclusions.

In the spring of 2000, she entered the Master's program in the Department of Geography to learn GIS modeling techniques and their application to Engineering problems. She obtained her second M.S. in August 2001. She is currently working for the Institute for Software Research in Fairmont, WV examining methods to model remotely sensed high-resolution data in a virtual environment.